UNIVERSITY OF CALIFORNIA
RIVERSIDE

A Phylogenetic Synthesis for Oceanic Dolphins: Total Evidence, Cytonuclear Discordance, and Possible Introgressive Hybridization

A Thesis submitted in partial satisfaction
of the requirements for the degree of

Master of Science

in

Ecology, Evolution, and Organismal Biology

by

David Charles Haisten

June 2016

Thesis Committee:
Dr. John Gatesy, Chairperson
Dr. Nigel Hughes
Dr. Joel Sachs

The Thesis of David Charles Haisten is approved:

_____

_____

_____

Committee Chairperson

University of California, Riverside

AKNOWLEDGEMENTS

I would like to thank the members of Gatesy and Hayashi labs for their assistance in this endeavor. Without the help of my lab mates as well as my major professor, John Gatesy, this work would not have been possible. I am grateful for the excellent faculty within the department of Biology at the University of California Riverside; they have made my years at Riverside a learning experience.

Table of Contents

LIST OF TABLES

LIST OF FIGURES

INTRODUCTION

Introgression and hybridization have long been recognized as important contributing factors to adaptation and speciation within plants (Anderson and Hubricht, 1938; Anderson and Stebbins, Jr., 1954). Interspecific gene flow between animal taxa, however, was traditionally regarded as either inconsequential due to fitness effects and selection against hybrids, or problematic for the maintenance of species integrity (e.g., Allendorf et al., 2001; Dobzhansky, 1940; Mayr, 1942; Rhymer and Simberloff, 1996). It is now recognized that in many animals species integrity is maintained despite gene flow, and certain alleles can be readily introgressed (Cahill et al., 2015; Heliconius Genome Consortium, 2012; McGuire et al., 2007; Nadeau et al., 2012; Song et al., 2011; Sullivan et al., 2014). Introgression can be defined as interspecific gene flow resulting from the backcrossing of a hybrid with one of its parental taxa (Anderson and Hubricht, 1938; Anderson, 1949). In a handful of proposed cases, reticulating lineages remain distinct while interbreeding to form a novel hybrid lineage of identical ploidy (i.e., homoploid hybrid speciation; Abbott et al., 2013; Arnold, 1992; Buerkle et al., 2000; Mallet, 2007; Mavárez and Linares, 2008)

Examples of homoploid hybrid speciation in animal taxa have been suggested primarily for insects, fish, and birds (Brelsford et al., 2011; Hermansen et al., 2011; Mavárez and Linares, 2008; Nice et al., 2013); however, introgressive hybridization, let

alone hybrid speciation, historically was considered to be rare in mammals (e.g., Mallet, 2007; Shurtliff, 2013). Post-zygotic isolating mechanisms such as in utero effects and genomic imprinting, as well as frequent chromosomal rearrangements, are believed to be intrinsic physiological characteristics for a majority of therian mammals (Shurtliff, 2013; Vrana, 2007; Zeh and Zeh, 2008). Nevertheless, increasing evidence suggests that hybridization and introgression is more prevalent within mammals than previously thought (Arnold and Meyer, 2006; Cahill et al., 2015; Hailer et al., 2012; Mallet, 2005; Sullivan et al., 2014), although not necessarily between grossly divergent taxa (Fitzpatrick, 2004; Zeh and Zeh, 2000). Recent examples of mammalian taxa of putative hybrid origin include the bat *Artibeus schwartzi* (Larsen et al., 2010), and the oceanic dolphin *Stenella clymene* (Amaral et al., 2014; but see Schumer et al., 2014).

Cetaceans may be pre-disposed for the capacity to hybridize. Most cetaceans examined to date share striking karyological uniformity (Arnason and Benirschke, 1973; Arnason, 1980; Bonifácio et al., 2012; Heinzelmann et al., 2009; Kulemzina et al., 2009; Pause et al., 2006). Furthermore, cetaceans are characterized by an extremely slow rate of molecular evolution in comparison to other mammals (Bininda-Emonds, 2007; Jackson et al., 2009; Nabholz et al., 2008). Many cetaceans are sympatric throughout their range and can form mixed species groups that differ from mere aggregations that are concentrated on resources (Fig. 1A; Acevedo-Gutiérrez et al., 2005; Frantzis and Herzing, 2002; Herzing and Johnson, 1997; Psarakos et al., 2003; Stensland et al., 2003). In some

instances, mixed-species interactions result in interspecific copulation (e.g., Herzing and Elliser, 2013; Psarakos et al., 2003). Additionally, accounts of viable hybrid progeny have been documented for closely related as well as more distantly related cetacean taxa, both in captivity and in the wild (Fig. 1B; see Bérubé, 2002; Amaral et al., 2014; Caballero and Baker, 2010; Glover et al., 2013; Miralles et al., 2013; Willis et al., 2004). However, the majority of naturally occurring hybridization events reported to date have occurred within oceanic dolphins, family Delphinidae (Fig. 2A; Amaral et al., 2014; Bérubé, 2002; Brown et al., 2014; Kingston et al., 2009; Miralles et al., 2013).

Diversification of Delphinidae into the most speciose family of extant cetaceans (~36 species) commenced during the mid to late Miocene (~10-13 Ma), and is a prime example of an explosive radiation (McGowen, 2011; McGowen et al., 2009; Steeman et al., 2009). Despite the increasing resolution of Delphinidae into three monophyletic sub-families (Delphininae, Globicephalinae, and Lissodelphininae) with the few remaining species irregularly placed in various hypotheses (Caballero et al., 2008; Cunha et al., 2011; Koito et al., 2010; LeDuc et al., 1999; May-Collado and Agnarsson, 2006; McGowen, 2011; McGowen et al., 2009; Vilstrup et al., 2011); many relationships either fail to resolve with strong support (e.g. Delphininae; Amaral et al., 2012; Kingston et al., 2009; McGowen, 2011; Perrin et al., 2013), or are conflicting depending upon the choice of phylogenetic markers and mode of analysis. For example, Kingston et al. (2009) attempted to resolve delphinine relationships with a combination of mitochondrial control

regions and AFLPs. Contrary to previous cytochrome *b* analyses (e.g., Agnarsson and May-Collado, 2008; LeDuc et al., 1999), the spotted dolphins, *Stenella frontalis* and *Stenella attenuata*, were found to be sister taxa and at least four *Stenella frontalis* x *Stenella attenuata* hybrids, as well as possible parental backcrosses, were identified.

The analyses of Kingston et al. (2009) also found the Clymene dolphin, *Stenella clymene*, as sister to the spinner dolphin, *Stenella longirostris*. Based upon external appearance and behavior, and prior to cladistic analyses, *Stenella clymene* was thought to be sister to *Stenella longirostris* (spinner dolphin) (Perrin et al., 1981). Both *Stenella clymene* and *Stenella longirostris* are the only delphinids that exhibit aerial "spinning" displays, but *Stenella longirostris* is the more acrobatic of the two (Fish et al., 2006; Perrin et al., 1981). In contrast, the seminal cytochrome *b* study of LeDuc et al. (1999) had shown *S. clymene* to be sister to the striped dolphin, *Stenella coeruleoalba*. Cranially, *Stenella clymene* resembles a smaller version of *Stenella coeruleoalba* (Perrin et al., 1981). Because of discordance between morphology, behavior, and mitochondrial descent, Le Duc et al. (1999) reasoned that *Stenella clymene* might be a hybrid lineage. Recently, Amaral et al. (2014) indicated that *Stenella clymene* was indeed of hybrid origin based upon nuclear markers and cytochrome *b*. This hypothesis of homoploid hybrid speciation has met with some criticism (see Schumer et al., 2014).

Other conflicting relationships exist within family Delphinidae. The rough-toothed dolphin, *Steno bredanensis*, according to pre-cladistic systematics, was

associated with *Sousa chinensis* (Indo-Pacific humpback dolphin) and *Sotalia* sp. (see LeDuc et al. 1999), and this grouping was closely allied with bottle-nosed-like dolphins (i.e., delphinines). *Steno* is the only long-beaked dolphin with a smoothly sloped melon devoid of an upper crease where it meets the beak (Jefferson, 2002). In reconstructions based on single mitochondrial genes (e.g., cytochrome *b*; LeDuc et al. 1999; May-Collado and Agnarsson, 2006), *Sousa chinensis* grouped with Delphininae, while *Steno* formed a monophyletic clade only with *Sotalia* sp. (subfamily Stenoninae; LeDuc et al. 1999). However, the multilocus analyses of Caballero et al. (2008), revealed conflicting mitochondrial and nuclear trees with respect to *Steno*, and combined analyses of their genetic data supported a novel placement of *Steno* nested within the "blackfish", sub-family Globicephalinae (Caballero et al. 2008). A similar placement of *Steno* with the globicephalines (pilot whales, etc.), as well as conflicting mitochondrial and nuclear gene trees, was independently supported by subsequent phylogenetic studies that were based on many more loci (McGowen, 2011; McGowen et al., 2008, 2009). The multilocus analyses conducted by Steeman et al. (2009), grouped *Steno* with *Sotalia* sp., sister to Delphininae, identical to single locus mitochondrial analyses (Steeman et al. 2009), but only very little of the available published nuclear DNA evidence was considered in this synthesis. Recent mitogenome analyses incorporating subsets of delphinid taxa, likewise group *Steno* with *Sotalia* sp. and Delphininae (Cunha et al. 2011; Vilstrup et al. 2011).

Phylogenetic incongruence is also present at the base of the delphinid radiation. Molecular hypotheses place the killer whale, *Orcinus orca*, either as a basal delphinid allied with the white-beaked dolphin, *Lagenorhynchus albirostris*, and the Atlantic white-sided dolphin, *Leucopleurus actus* (multilocus analyses; McGowen et al., 2009; McGowen et al. 2011), as the basalmost delphinid (McGowen et al., 2009; Steeman et al., 2009), as a member of Globicephalinae (mitogenomes; Vilstrup et al., 2011; but see Cunha et al., 2011), or allied with *Orcaella* sp. (Irrawaddy dolphin, Australian snubfin dolphin) in the clade Orcininae (*MT-CYB*; Agnarsson and May-Collado, 2008; LeDuc et al., 1999). Furthermore, a recent cladistic analysis incorporating extinct as well as extant delphinids found *Orcinus* to be either a basal delphinid closely allied with globicephalines (morphological characters only), or as a basal delphinid allied with *Lagenorhynchus albirostris* and *Leucopleurus acutus* (molecular constraint tree; Murakami et al., 2014a). Because of uncertainty regarding the interrelationships of *Orcinus*, *Lagenorhynchus albirostris*, and *Leucopleurus. acutus*, Banguera-Hinestroza et al. (2014) excluded *Orcinus* from portions of their investigation of the genus *Lagenorhynchu*s. As a result, *Lagenorhynchus albirostris* and *Leucopleurus acutus* were found to be monophyletic with varying degrees of support. Inclusion of *Orcinus* disrupted this relationship.

Based upon analyses conducted thus far, conflicting phylogenetic hypotheses for some delphinids appear to be largely influenced by mitochondrial markers (e.g., Cunha et

al. 2011; Le Duc et al. 1999; Steeman et al. 2009; Vilstrup et al. 2011). The mitochondrial genome seems well suited for resolving recent divergences due to a greater mutation rate and a smaller effective population size in comparison to the nuclear genome (Brown et al., 1982; Cunha et al., 2011; Moore, 1995; Vilstrup et al., 2011). Thus, phylogenetic inference utilizing a large number of mitochondrial markers or entire mitochondrial genomes should be less prone to the effects of lineage sorting (Cummings et al., 1995; Moore, 1995). In spite of these purported benefits, because the mitochondrial genome is often considered a single non-recombining locus (Harrison, 1989; Moore, 1995), phylogenetic inference based on mitochondrial markers alone fails when introgressive hybridization contributes to the evolutionary history of a taxon (Ballard and Whitlock, 2004; Funk and Omland, 2003; Harrison, 1989; Moore, 1995). The incorporation of nuclear markers can result in conflicting patterns for mitochondrial and nuclear gene trees arising from past and present hybridization (e.g., Hailer et al., 2012; Kutschera et al., 2014; McGuire et al., 2007; Sullivan et al., 2014). However, sources of mitochondrial and nuclear incongruence can include both incomplete lineage sorting (ILS) of allelic variation (i.e., deep coalescence) and introgressive hybridization (Funk and Omland, 2003; Maddison, 1997; Rubinoff and Holland, 2005; Toews and Brelsford, 2012).

In the following synthesis I utilized a combination of methodologies to arrive at a novel phylogenetic hypothesis for crown Delphinidae. To this end, I assembled the

largest dataset for the analyses of delphinid relationships to date. My character sets consisted of entire mitochondrial genomes, partial mitochondrial genomes, individual mitochondrial genes, 48 nuclear loci, and 282 osteological characters from Murakami et al. (2014a) scored for 62 extant and extinct members of infraorder Delphinida. These character sets have never before been combined into a single comprehensive analysis. The morphological dataset compiled by Murakami et al. (2014a) consisted of the most extensive taxonomic sampling within Delphinidae for any cladistic analysis. However, their paleontological investigation utilized a modified molecular scaffold derived from McGowen et al. (2009). Here I instead have followed the approach of Kluge (1989) and Nixon and Carpenter (1996), and combined all available evidence for 62 members of Delphinida and executed simultaneous analysis, thus allowing secondary signals in the combined dataset to emerge. The importance of fossils for character polarization and resolution of contemporary relationships has long been recognized (Donoghue et al., 1989; Gauthier et al., 1988). At the same time, I explored the influence of mitochondrial data upon competing hypotheses for difficult to place taxa such as *Orcinus*, I re-examined competing hypothesis for taxa that have exhibited strong cytonuclear discordance in previous analyses, such as *Steno*, and examined possible instances of cytonuclear incongruence for all delphinids represented in my datasets. I sought to quantify the amount of support and conflict for contrasting hypotheses of delphinid relationships by analyzing individual data partitions: nuclear loci, mitochondrial sequences, and

morphology. Because of the possibility of introgressive hybridization within oceanic dolphins, I did not expect that the evolutionary pattern for some delphinids to be in agreement for all data partitions. However, as mentioned above, ILS is an equally plausible factor responsible for taxonomic incongruence between individual genetic loci (Maddison et al., 1997). Therefore, I executed analyses explicitly accounting for ILS via the multi-species coalescent (Hudson, 1990; Rannala and Yang, 2003). I also executed concordance analyses that account for gene tree incongruence but do not assume the sources of genetic discordance a priori. Additionally, I employed phylogenetic super networks (Huson and Bryant, 2006), to explore conflicting patterns in molecular datasets that might be the result of hybridization, ILS, or both. Finally, to add credence to the possibility that difficult to resolve nodes and instances of cytonuclear discordance within Delphinidae are due to interspecific genetic exchange, I surveyed the primary and secondary literature for all known instances of hybridization within Cetacea, and reported the results of my literature survey here.

METHODS

Character sets

To estimate phylogenetic relationships within crown Delphinidae, I combined the molecular supermatrix of McGowen (2011), the morphology matrix of Murakami et al (2014a), nuclear alignments from Caballero et al. (2008; *IFNA1*, Y chromosomal introns: *DBY7*, *DBY8*, *SMCY7*, *UBE1Y7*), nuclear alignments from Amaral et al. (2012; nine anonymous loci: *Del2*, *Del4*, *Del5*, *Del8*, *Del10*, *Del11*, *Del12*, *Del15*, *Del17*; *PLP1* intron), the nuclear *TBX4* (Onbe et al., 2007) alignment of McGowen et al. (2009), olfactory receptor psuedogenes of McGowen et al. (2008), mitogenomes from Arnason et al. (2004), Cunha et al. (2011), Hassanin et al. (2012), (Vilstrup et al. (2011), Xiong et al. (2009), and partial mitogenomes of Alexander et al. (2013) into 39 datasets. Four additional mitogenomes, one additional nuclear marker (*RBP3*, formerly known as *IRBP*) from Stanhope et al., (1996), three nuclear loci from Banguera-Hinestroza et al. (2014; *CAMK2A*, *HEXB*, and *VWF*), one nuclear locus from Harlin-Cognato and Honeycutt (*RAG2*; 2006), and nuclear and mitochondrial loci for taxa with either missing data or partial sequences (obtainable from GenBank as of December 2014) were added to the 39 datasets. One sequence from each locus, as available, was sampled for each species. As per McGowen (2011), the Irrawaddy dolphin, *Orcaella brevirostris*, and snubfin dolphin,

Orcaella heinsohni, were collapsed into the single operational taxonomic unit *Orcaella*. Additionally, sequenced genomes are currently available on NCBI for two delphinids, the bottlenose dolphin (*Tursiops truncatus*; taxid 9739) and the killer whale (*Orcinus orca*; taxid 9733), as well as the now extinct Chinese river dolphin (*Lipotes vexillifer*; taxid 118797). All missing nuclear loci for the above datasets, from these three taxa, were acquired from whole genome shotgun sequences (WGS), with the exception of Y chromosomal introns for *Lipotes* because the only currently sequenced *Lipotes* genome is that of a female individual. Overall taxonomic coverage for the various genetic loci is illustrated in Figure 3.

I used the alignments of Caballero et al. (2008), and McGowen (2011) to incorporate recently published nuclear sequences for taxa with previously missing data. I also updated partial nuclear sequences with longer sequences for *ACTA2*, *LALBA* and *OPN1SW*. Olfactory receptor (OR) genes, and *RBP3* sequences, were aligned with Clustal W2 on the EMBL-BI webserver (Goujon et al., 2010; Larkin et al., 2007) using the "slow" setting with a gap opening penalty of 10 and gap extension penalty of one. Alignments were then adjusted by eye using SE-AL v2.0a11 (A. Rambaut, University of Oxford). For the *RBP3* dataset, a contiguous 28 bp region, terminating at the 3' end of the published *RBP3* sequence for *Steno* (U48713), was determined to be non-orthologous to other delphinids upon alignment; this region was excluded from further analyses. A 99 base pair region, likely a SINE insertion, was difficult to align and was subsequently

excluded from the *HEXB* dataset. For the *ACTA2* dataset, a 64 bp contiguous region, beginning with a poly-A "motif" at the 5' end of a new *ACTA2* sequence (HQ699816) for the common dolphin, *Delphinus delphis*, was not orthologous to the genomes of both *Tursiops truncatus* and *Orcinus.* This region was excluded from the *ACTA2* alignment.

The utility of the OR gene family for phylogenetic reconstructions within Cetartiodactyla has been previously demonstrated (McGowen et al., 2008). However, the inclusion of additional OR sequences, acquired from the genomes of *Tursiops truncatus*, *Orcinus* and *Lipotes*, into OR datasets required screening for paralogs. To this end, I aligned all newly acquired *Tursiops truncatus*, *Orcinus* and *Lipotes* sequences to their respective OR genes and constructed equally weighted parsimony phylograms using an exhaustive (exact) search with PAUP* 4a138 (Swofford, 2002). Potential paralogs were eliminated, and orthology established, for new OR sequences by topological comparisons with known OR sequences. Briefly, branch lengths of new sequences were examined for an excessive number of changes relative to existing sequences and topologies were inspected for unlikely taxonomic alliances.

For mitochondrial datasets, I excluded D-loop regions from both full and partial mitogenomes, and sequence alignment was as described above using CLUSTAL. Mitochondrial protein coding regions, RNAs, and short intergenic regions were delimited using the annotations of *Tursiops truncatus* (EU557093) and *Orcinus* (KF418393). From this initial annotated mitogenome alignment of 32 taxa, four additional mitochondrial

alignments were assembled. One alignment consisted of all 40 taxa present in the nuclear dataset. Thirty-two of these 40 taxa were represented with full and partial mitogenomes, the remaining eight with some or most of the following mitochondrial sequences: *MT-RNR1* (*12s* RNA), *MT-RNR2* (*16s* RNA), *MT-ND3*, MT-*CO1*, *MT-CO2*, and *MT-CYB*. An alternate mitochondrial (mt) alignment consisted of 36 taxa from the morphological dataset, including three species with little to no available nuclear (nu) sequences: the porpoises *Phocoena dioptrica*, *Phocoena sinus*, and *Phocoena spinipinnis* (Fig. 3). This mt alignment was merged with all nu datasets and 282 osteological characters for 35 extant and 27 extinct taxa. Extinct taxa, with the exception of *Lipotes*, were coded as "?" for all molecular characters. Two additional mt alignments, for 32 and 40 taxa respectively, were constructed for data partitioning (see below). This required exclusion of overlapping regions for *MT-ATP8/MT-ATP6*, *MT-ATP6/MT-CO3*, *MT-ND4L/MT-ND4*, and *MT-ND5/MT-ND6*. Unlike some previous studies (e.g., Vilstrup et al., 2011; Xiong et al., 2009), I did not exclude *MT-ND6*, which is encoded on the light strand opposite from the other 12 protein coding genes.

In total, 54 matrices were assembled: 31 for individual nu loci with representative sequence for *Steno* (Y chromosome introns were analyzed as a single locus in gene tree reconstructions), 15 matrices for individual mt protein-coding genes and mt rRNAs, one concatenated matrix consisting entirely of mt tRNAs and adjacent intergenic regions, one concatenated matrix for all nu data (22,354 characters), two matrices for unpartitioned mt

data (as above; full and partial mitogenomes for 32 taxa vs. mitogenomes + additional mitochondrial loci for 40 taxa;15,533 characters), two partitioned mt matrices (as above; 15,521 characters), one concatenated supermatrix consisting of all molecular data combined (37,887 characters), one matrix comprised of concatenated nu and morphological data (22,637 characters), one matrix combining mt sequences with morphology (15,814 characters), and a total-evidence supermatrix consisting of all molecular and morphological data combined (50,795 characters). Thirty-two extant taxa, representative of all major lineages of oceanic dolphins, and eight species sampled from Lipotidae (*Lipotes*), Inioidea (*Inia geoffrensis*, *Pontoporia blainvillei*), and Monodontoidae (*Phocoena phocoena*, *Phocoenoides dalli*, *Neophocoena phocaenoides*, *Delphinapterus leucas*, *Monodon monoceros*), that are well established as delphinid outgroups (e.g., Cassens et al., 2000; Geisler et al., 2011; May-Collado and Agnarsson, 2006; McGowen, 2011; McGowen et al., 2009; Messenger and McGuire, 1998; Xiong et al., 2009; Yan et al., 2005), were represented in the nu, mt, and combined (nu+mt) molecular supermatrices.

Twenty-five extant delphinids and five extinct delphinids, including the re-assigned basal delphinid *Eodelphinus kabatensis* (*Eodelphis kabatensis*, Murakami et al., 2014a; see Murakami et al., 2014b), were represented in supermatrices merging molecules with morphology and fossils. Outgroup taxon sampling for these matrices consisted of 10 extant and 22 extinct species from Lipotidae, Inioidea, Kentriodontidae,

Albireonidae, Odobenocetopsidae, and Monodontoidae. In sum total, 62 OTUs of infraorder Delphinida (sensu Muizon, 1984; Geisler et al., 2011; Gibson and Geisler, 2009) were represented in morphological datasets.

Parsimony analyses

Parsimony analyses of individual genes and supermatrices were conducted with equally weighted characters in PAUP* 4.0a138 (Swofford, 2002). Heuristic searches with 100 random addition steps (RAS) and tree-bisection and reconnection (TBR) branch swapping were used to generate minimum length trees; internal branches were collapsed during search replicates if the minimum length of an internode was zero ("amb-" option in PAUP*). When necessary, strict consensus trees were used to summarize relationships supported by equally parsimonious trees. Nodal support was evaluated with 500 non-parametric bootstrap psuedoreplicates (Felsenstein, 1985), each consisting of 10 RAS and TBR branch swapping, with the maximum number of trees held at each step set to 1000. Nodal support for optimal trees (supermatrix analyses and morphology dataset only) was also assessed with branch support (BS) indices (Bremer, 1994) calculated via PAUP* and TreeRot v.3 (Sorenson and Franzosa, 2007). Random search additions were set to 100.

To quantify support contained within individual genetic loci for alternative phylogenetic placements of *Steno*, a total of eight different constrained searches were executed in PAUP* for each of the following datasets: 31 nu DNA loci, and 16 mt DNA

loci (includes concatenated tRNAs). Four alternative constraint searches were employed to test the following hypotheses: monophyly of *Steno* with *Sotalia* sp. (Cunha et al., 2011; LeDuc et al., 1999; May-Collado and Agnarsson, 2006; Steeman et al., 2009; Vilstrup et al., 2011), monophyly of *Steno* with Globicephalinae (Caballero et al., 2008; McGowen, 2011; McGowen et al., 2009, 2008), monophyly of *Steno* and *Orcaella* with Globicephalinae, and monophyly of *Steno*, *Sotalia* sp., and *Sousa chinensis* with *Delphininae*. For each constrained search, a second search implementing the converse constraint was executed ("anti-constraint" option in PAUP*). Differences in the lengths of shortest trees obtained via searches enforcing a constraint, and the corresponding converse constraint, were used to quantify character support/conflict in individual datasets for alternative placements of *Steno*. These values could be either positive, negative, or zero, depending upon the dataset. All parsimony searches were executed as above.

For parsimony analyses of morphology+fossils alone as well as datasets that combined molecules with morphology+fossils, characters supporting alternative placements of *Steno* were optimized onto consensus cladograms using the "list of apomorphies" and "show reconstructions" commands of PAUP*. When possible (i.e., the number of equally parsimonious trees was not prohibitive), characters were optimized on individual minimum length trees obtained from parsimony searches with "amb-"

disabled. The resultant individual character optimizations were compared to character optimizations on strict consensus trees.

Model and partition selection

I used PartitionFinder v.1.1.1 (Lanfear et al., 2012) to select models of sequence evolution and optimal partitioning schemes for concatenated datasets. PartitionFinder uses maximum likelihood and information theoretic metrics to select best-fit data partitioning schemes from an initial user-defined set of data blocks (i.e., set of sites in an alignment; also termed subsets; Lanfear et al., 2012). Depending upon the initial number of pre-defined subsets, two different algorithms were employed to search for optimal partitioning schemes: the exact algorithm (≤ 12 subsets) and the greedy heuristic algorithm (≤ 100 subsets).

For nuclear data partitioning, nu subsets were defined by gene with the exception of the Y chromosomal introns that were separated into data blocks consisting of individual introns. Sub-division of nu datasets into smaller data blocks (e.g., different codon positions in protein-coding genes) was excluded from consideration because of very low sequence variation for some subsets of characters and the resulting potential for model misspecification. I varied the choice of models tested for different partitioning schemes depending upon the phylogenetic software I would be using. Two different runs were executed for concatenated nuclear datasets: (1) data partitioning via the greedy

heuristic algorithm ("--raxml" option) and GTR + Γ model of sequence evolution, and (2) data partitioning via the greedy heuristic algorithm and 56 different GTR sub-family models.

For mt alignments, pre-defined subsets consisted of first, second, and third codon positions of protein coding genes, 12 discrete blocks of tRNAs concatenated with adjacent short intergenic regions, and two discrete blocks for ribosomal RNAs. Based upon searches for optimal partitioning schemes with nu datasets, sub-division of tRNA subsets into smaller data blocks (< 100 bp) was excluded from consideration because of low sequence variation and thereby the potential for model misspecification. Moreover, eight of 22 tRNAs are encoded on the light strand; attempting to further partition these tRNA would result in analyzing the same regions of DNA twice. Model selection for mt partitioning schemes was identical to nu datasets, with the following exceptions: (1) models specifying equal base frequencies (e.g., Jukes-Cantor) were excluded from PartitionFinder analyses to reduce computational burden, (2) individual mt loci were evaluated using the exact algorithm, and (3) partitioning schemes were obtained for the set of GTR sub-models available in Mr. Bayes v.3.2.4 (Ronquist et al., 2012).

Models of sequence evolution for unpartitioned concatenated datasets and individual nu genes were obtained via JModelTest2 (Darriba et al., 2012) on the Cyberinfrastructure for Phylogenetic Research server (CIPRES) (Miller et al., 2010). The sample-size corrected Aikake Information Criterion (AICc; Sugiura, 1978) was employed

for both model selection and estimation of best-fit data partitioning in all instances. Data partitioning schemes and substitution models are described in Appendix A.

Maximum likelihood analyses

Likelihood inferences were executed with RAxML v.8.1.16 (Stamatakis, 2014), and GARLI v.2.1 (Zwickl, 2006). For RAxML inferences, I used an identical search routine for both single gene and supermatrix analyses. Briefly, 10 independent searches with 10 unique parsimony seeds ("-p") were executed for each dataset. The 10 independent searches consisted of: (1) three different searches starting with 1000 randomized parsimony trees ("-d" option; "-N" set to 1000), (2) four different searches consisting of 1000 rapid bootstrap replicates (unique seed specified) followed by 200 searches for the best tree ("-f a" option), and (3) three different searches starting with 1000 randomized stepwise addition parsimony trees. Optimization precision was set to 0.0001 log likelihood units ("-e" option) and GTRGAMMA was specified for all searches. Likelihood scores of the best trees found in each of the 10 runs were then compared. If trees obtained from different runs had either (1) identical likelihood scores, or (2) equivalent likelihood scores to 0.0001 significant figures, symmetric tree difference distances were calculated in PAUP* to confirm that the same topology had been found in independent runs. I then chose the tree with the greatest likelihood as the best estimate of phylogeny. In the event that trees with identical likelihood scores but

different topologies were found, which can occur because RAxML does not collapse effectively zero length internal branches during tree searches, I used SumTrees v.3.3.1 from the DendroPy v.3.12.0 (Sukumaran and Holder, 2010) software package to generate strict consensus trees. Nodal support for optimal and strict consensus topologies was evaluated with 1000 standard non-parametric bootstrap replicates ("-b" option).

For likelihood inferences using GARLI v.2.1, single gene analyses consisted of four different runs, each comprised of 100 GARLI replicates. GARLI replicates are independent; a pseudorandom seed is generated for each replicate (with "-1" specified in the configuration file), and starting trees for each replicate can be user defined, fast maximum likelihood (ML) step-wise addition trees, or completely random trees. For the four different runs, two runs consisted of fast ML step-wise addition starting trees, and two runs consisted of completely random starting trees. The genetic threshold for topological termination (genthreshfortopoterm) was specified at 20,000 generations, and effectively zero length internal branches were collapsed during search replicates (collapsebranches=1). All other settings were configured at default specifications as per the online GARLI manual (https://molevol.mbl.edu/index.php/Garli_wiki). As above, symmetric tree difference distances were calculated with PAUP* to confirm that at least two identical topologies had been found in independent search runs and that one of these topologies had the greatest likelihood of all four runs. Nodal support was generated with

1000 non-parametric bootstrap psuedoreplicates. The majority consensuses of bootstrap replicates were mapped onto the most likely trees using SumTrees v.3.3.1.

GARLI inferences of larger datasets were executed on the GARLI web service (molecularevolution.org; Bazinet et al., 2014; Zwickl, 2006) using an adaptive tree search with the default settings mentioned above. The adaptive tree search initiates with 10 replicates. Topologies obtained from these 10 replicates are compared with symmetric difference metrics (Robinson and Foulds, 1981), and the number of replicates required to obtain the "best feasible" topology with 95% confidence are estimated following the methods of Regier et al. (2009). From this estimation, search replicates are continually adjusted upwards as needed, to a maximum of 100 replicates, or the adaptive search terminates at 10 replicates. I implemented the same search strategy as single gene analyses: two independent runs utilizing fast ML step-wise addition starting trees for each replicate, and two independent runs utilizing completely random starting trees for each replicate. Topologies and likelihood scores of the best tree obtained from each of the four runs were compared as above. Nodal support was generated with 1000 bootstrap replicates on the GARLI server. I used the models of nucleotide substitution and best-fit data partitioning schemes obtained from PartitionFinder.

Gene-tree based analyses

To explicitly account for the possible effects of ILS and subsequent gene tree discordance upon phylogenetic inference, I used ASTRAL v.4.7.6 (Mirarab et al., 2014) to generate coalescent based species-tree hypotheses of delphinid relationships. Unlike other shortcut-coalescent methods, ASTRAL accepts unrooted and partially unresolved gene trees as input data (Mirarab et al., 2015). The best ML gene trees obtained from GARLI were employed for ASTRAL analyses. I initially input only nu gene trees (30 loci + Y introns gene tree) for 40 taxa. One thousand ASTRAL bootstrap replicates were executed for nodal support of the resultant nu topology. Mitochondrial data was then incorporated into species-tree inference; the best mt topology obtained for the 40-taxon dataset was input as an additional locus. Nodal support was evaluated for the resultant species-tree with 1000 ASTRAL bootstrap replicates. I then tested the potential effects of missing data on coalescent-based phylogenetic hypotheses by conducting an identical set of analyses with a set of reduced taxon input trees (14 gene trees; 28 taxa) without any missing data.

I used the program Bayesian Untangling of Concordance Knots, BUCKy v.1.4.3 (Ané et al., 2007; Larget et al., 2010), to infer primary concordance topologies as well as concordance factors. Concordance factors estimate the proportion of loci that support different clades, whereas primary concordance trees are comprised only of clades with

the greatest concordance (Ané et al., 2007). Unlike coalescent-based species-tree inferences, this method of phylogenetic reconstruction does not attempt to explicitly model sources of genealogical discordance a priori. BUCKy implements a two-stage process for Bayesian concordance analysis; step one requires summarizing posterior distributions obtained from Bayesian analyses of individual loci. Step two implements a Dirichlet process prior, which is dependent upon the discordance parameter "α", and estimates concordance among gene trees from the posterior distribution of gene-to-tree maps (Ané et al., 2007). Parameter values for α range from 0, which specifies a single cluster of underlying gene trees with identical topologies, to ∞, which specifies absolute discordance between all gene tree topologies. BUCKy only estimates concordance factors for taxa that are present in all datasets. Accordingly, I analyzed the 28 taxon dataset with all 14 loci sampled for each taxon.

For the concordance analyses, samples from the posterior distributions of individual loci were obtained with Mr.Bayes 3.2.4 (Ronquist et al., 2012). The optimal models of sequence evolution and partitioning schemes, as estimated above, were applied to all analyses. I unlinked priors for mt data and set all partitions to "variable", allowing site-specific rates of evolution to vary across partitions (Marshall et al., 2006). Each analysis consisted of two concurrent runs with default temperatures for chain heating, and four Metropolis-coupled Markov chain Monte Carlo chains (MCMC). For nu loci, I ran analyses for 14 million generations, sampling every 1000 generations. Mitochondrial

datasets were run for 50 million generations and sampled every 2500 generations. Convergence was assessed with the diagnostics available from the "*sump*" command in Mr.Bayes 3.2.4 (e.g., average standard deviation of split frequencies, effective sample sizes, and potential scale reduction factors) and with the "compare" and "cumulative" plot functions available in the online version of Are We There Yet? (AWTY; Nylander et al., 2008; Wilgenbusch et al., 2004). The first 50% of sampled topologies were discarded as burn-in.

Primary concordance trees were estimated at four different levels of a priori discordance. I used the custom R script available from http://ane-www.cs.wisc.edu to visualize the prior distribution on the number of distinct gene trees for α=0.1, α=1, α=2, α=15, and α=30, given my chosen number of taxa and genetic loci. My choices of the α prior parameter placed high prior density for one shared tree at α=0.1, three to four distinct gene trees at α=2, and approximately 13 distinct gene topologies for α=30. I first input posterior samples into BUCKy from nu loci, and then nu loci and mt (single locus) data combined. Each BUCKy analysis consisted of two concurrent runs with four chains, MCMC sampling for one million generations, default heating temperatures, and 10% relative burnin. Bayesian consensus trees obtained from Mr. Bayes were also input into ASTRAL. Nodal support was generated with 10,000 bootstrap replicates generated from posterior samples of 14,000 trees for each of the 14 loci in the 28-taxon dataset.

I also conducted network analyses with SplitsTree4 v.4.13.1 (Huson and Bryant, 2006) to summarize gene tree incongruence. Phylogenetic supernetworks were constructed with input sets of maximum likelihood gene trees. As above, the best likelihood trees obtained from Garli were used for all analyses. The 14-gene set with complete taxon sampling was used as input for network analyses. A minimum trees filter (Whitfield et al., 2008) was applied to all network reconstructions. Filtering a Z-closure supernetwork allows only those splits that are present in a specified number of gene trees to be constructed in the final network. The resulting filtered supernetwork serves as an exploratory tool for examining conflicting splits in input trees. By varying the minimum trees filter (i.e., number of gene trees that must contain a split) recurrent phylogenetic patterns and incongruence can be observed (Whitfield et al., 2008). I varied the minimum trees filter from three input gene trees to 10 input gene trees for all supernetwork reconstructions.

Literature search

To characterize the amount of known (e.g., molecular evidence) and putative (e.g., morphological accounts) hybridization within Delphinidae, I reviewed the available literature for suspected instances of successful hybridization (viable offspring produced) between cetaceans, and mapped all reported instances of hybridization that were documented with molecular evidence onto a modified Bayesian time tree from McGowen

et al. (2009). Estimated divergence dates between hybridizing taxa were obtained from McGowen et al. (2009) and from Steeman et al. (2009).

RESULTS

Molecular Supermatrices

Individual analyses of nu supermatrices and mt genes + mitogenomes revealed widespread incongruence for concatenated nu loci vs. mt datasets. Partitioned GARLI topologies are presented in figure 4. Delphininae + *Sotalia*, Globicephalinae + *Steno* + *Orcaella*, and Lissodelphininae were recovered with strong support for all nu analyses, irrespective of reconstruction method. However, relationships within the three subfamilies were poorly supported for concatenated nuclear topologies with the exception of some alliances within Globicephalinae, and a clade consisting of *Delphinus* + *Stenella longirostris* + *Lagenodelphis hosei* nested within Delphininae (Fig. 4). The genus *Tursiops* was recovered as monophyletic with marginal support only in ML analyses. *Leucopleurus acutus*, *Lagenorhynchus albirostris*, and *Orcinus* were consistently placed as basal delphinid taxa in all nu topologies.

In contrast, for the mt topology (Fig. 4), a basal delphinine clade consisting of *Stenella attenuata* + *Lagenodelphis hosei* was recovered with moderate bootstrap support (> 70%), *Steno* was allied with *Sotalia* with maximal bootstrap support (100%), and *Orcinus* was closely allied with Lissodelphininae, albeit with moderate support (Fig. 4).

Furthermore, *Stenella longirostris* was not sister to *Delphinus* as in the nuclear topology, but was robustly supported in a more basal position in the mitochondrial hypothesis.

Maximum likelihood analyses of the mitogenome dataset, excluding taxa represented only with individual mitochondrial genes, recovered identical topologies for partitioned and unpartitioned GARLI reconstructions as well as RAxML partitioned analysis. The partitioned GARLI topology is shown in figure 5. Nodal support was > 80% bootstrap support (BS) for all clades within subfamilies except for *Feresa attenuata* + *Peponocephala electra* and *Cephalorhynchus hectori* + *Cephalorhynchus heavisidii*. *Orcinus* was allied with Lissodelphininae with variable support depending upon the method of analysis (e.g., 57% BS PAUP* parsimony vs. 76% RAxML partitioned) and *Steno* was strongly allied with *Sotalia* + Delphininae

Partitioned and unpartitioned ML analyses of the combined nu + mt datasets yielded nearly identical topologies. GARLI and RAxML hypotheses differed at a single marginally supported node within Lissodelphininae (Fig. 6). Maximum parsimony analysis of the concatenated nu + mt dataset (37887 characters; 4924 parsimony informative) yielded a single minimum length tree (19349 steps; CI=0.3883, RI=0.57), which was identical to the RAxML topology. Relationships within the three delphinid subfamilies were generally well supported across analyses, except for most nodes within Delphininae. Both *Tursiops* and *Stenella* were paraphyletic (Fig. 6). *Sotalia* and *Steno* formed a clade sister to Delphininae, while *Orcaell*a was allied with Globicephalinae (>

95% BS support). *Leucopleurus acutus*, *Lagenorhynchus albirostris*, and *Orcinus* were strongly supported as successively branching basal delphinids.

Individual Gene Trees

Maximum likelihood topologies of the 31 individual nu loci with representative sequence for *Steno* were generally incongruent with one another. Higher-level delphinid clades recovered with robust support in simultaneous analysis (e.g., Globicephalinae), if resolved in individual gene trees, were typically recovered with low nodal support. Relationships within higher-level clades were mostly unresolved. However, the following lower-level delphinid clades were recovered in at least two topologies: *Delphinus* + *Stenella longirostris* (*ACTA2*, *MC1R*, *MCPH1*, *OR1I1*), *Globicephala macrorhynchus* + *Globicephala melas* (*OPN1SW*, *PKDREJ,* Yintrons), *Sagmatias obscurus* + *Sagmatias obliquidens* (*LALBA*, *MAS*, *MCPH1*, *MC1R*), and *Tursiops truncatus* + *Tursiops aduncus* (*BTN1A1*, *STAT5A*). *Steno* was allied with Globicephalinae for four nu loci (*LALBA*, *MC1R*, *RAG1*, *OR10J1*), and allied with Delphininae for one nu locus (*CHRNA1*); albeit with < 50% BS. Nuclear topologies as well as bootstrap support trees for individual genetic loci are provided in Appendix B.

Parsimony constraint analyses of 31 individual nu loci, 13 mt protein coding genes, concatenated mt tRNAs + short intergenic regions, and the two mt rRNAs are summarized in Table 1. For the different phylogenetic hypotheses tested, two nu loci

(*OR10J1*, *RAG1*) exhibited positive branch support for *Steno* + Globicephalinae, and two nuclear loci (*LALBA*, *MC1R*) exhibited positive branch support for *Steno* + *Orcaella* + Globicephalinae. Not one nu locus exhibited positive branch support for *Steno* + *Sotalia* or *Steno* + *Sotalia* + Delphininae. In contrast, the majority of mt loci exhibited positive branch support for *Steno* + *Sotalia* and/or *Steno* + *Sotalia* + Delphininae. All mt regions exhibited negative branch support for *Steno* + Globicephalinae and *Steno* + *Orcaella* + Globicephalinae (Table 1).

Combined Analyses of Gene Trees

ASTRAL coalescent analysis of 31 nu loci yielded a topology with poor nodal support for many delphinid relationships (Fig. 7A). Within subfamilies, globicephaline relationships were generally congruent with ML nu supermatrix analyses (Fig. 7A vs. 4A), and a clade consisting of *Steno* + *Orcaella* was allied with Globicephalinae. Relationships within Lissodelphininae were poorly supported, similar to ML nu analyses. Within Delphininae, *Tursiops* was recovered as monophyletic with moderate nodal support (69% BS). Identical to concatenated ML analyses, a clade consisting of *Delphinus delphis* + *Stenella longirostris* + *Delphinus capensis* + *Lagenodelphis hosei* was recovered; however, *Delphinus* was paraphyletic.

Inclusion of one additional locus into ASTRAL analysis, the mt topology, altered the ASTRAL nu hypothesis (Fig. 7B). Nodal support increased for some delphinid

relationships (e.g., within Globicephalinae), but *Steno* was allied with Delphininae rather than Globicephalinae (Fig. 7B). Relationships within Lissodelphininae were congruent with concatenated nu + mt analyses. *Orcinus* was allied with Lissodelphininae rather than positioned as a basal delphinid; albeit with <50% BS. Relationships within Delphininae were altered with incorporation of the mitochondrial genome, and *Tursiops* was rendered paraphyletic.

Topologies obtained via ASTRAL analysis of the 13 nu dataset were largely congruent with topologies obtained with 31 nu genes (Fig. 8A). *Steno* + *Orcaella* was allied with Globicephalinae. Within Delphininae, *Delphinus* was recovered as monophyletic, as was *Tursiops*. Both *Orcinus* and *Leucopleurus acutus* were positioned as basal delphinids. Similar to the 32-gene dataset (31nu + mt), incorporation of mt data increased support for some nodes (Fig. 8A vs. 8D), and decreased support for other nodes. However, *Steno* remained allied with Globicephalinae. Incorporation of the mitochondrial gene tree allied *Orcinus* with Lissodelphininae with low support (Fig. 8D).

Bayesian concordance analysis of the same 13 locus data set recovered *Steno* + *Orcaella* + Globicephalinae (Fig. 8B). Incorporation of the mitochondrial topology disrupted the hypothesis of *Steno* + *Orcaella*, rendering *Steno* basal to Globicephalinae + *Orcaella* (Fig. 8E). Incorporation of mitochondrial data into concordance analysis also generated a clade consisting of *Lagenodelphis hosei* + *Stenella attenuata*, rather than *Lagenodelphis hosei* + *Delphinus* + *Stenella longirostris* (Fig. 8B vs. 8E). For all

concordance analyses, a clade consisting of *Sousa* + *Sotalia fluviatilis* was recovered. Concordance factors were < 50% for all delphinid clades other than *Sagmatias obscurus* + *Sagmatias obliquidens*, regardless of the dataset. Note that concordance factors represent the proportion of a genetic sample for which a clade is true, and are not measures of support (Ané et al., 2007). Similar to ASTRAL ML based coalescent analyses, incorporation of mt data increased the primary concordance factors for some clades present in both nu and nu + mt topologies, while decreasing concordance factors for others (Fig. 8B vs. 8E). Varying the a priori discordance between individual gene trees had negligible effect on all concordance topologies.

ASTRAL analysis of Bayesian consensus nu gene trees generated a topology largely congruent with ML based nu coalescent topologies (Fig. 8C vs. Figs. 8A and 7). Likewise, incorporation of the mt tree disrupted some relationships found only in the nu hypothesis (Fig. 8F vs. 8C).

Filtered super network reconstructions of the 13 nu gene trees recovered three taxon clusters congruent with subfamily clades in ASTRAL and BUCKy topologies. Gene tree incongruence that was present in five or more gene trees, graphically displayed as alternative split(s) for taxa within clusters, is presented in figure 8G. Within the cluster corresponding to Delphininae, there was no incongruence for *Delphinus* + *Stenella longirostris*. Alternative splits were present between all remaining delphinines; *Sousa* was grouped with *Sotalia fluviatilis*, but not unequivocally. Within the cluster

corresponding to Globicephalinae, the branching order among genera was subject to uncertainty. However, both *Steno* and *Orcaella* were clustered with Globicephalinae. Addition of the mt tree increased the number of splits between delphinines (Fig. 8H). Likewise, a split between Globicephalines + *Orcaella* and delphinines + *Sotalia* was visible for the placement of *Steno*.

Morphology and Fossils

Parsimony analyses of the morphology partition generated 56 shortest length trees (734 steps, CI=0.35, RI=0.61) for extant taxa (282 characters, 176 parsimony informative), and 684 shortest length trees (1094 steps, CI=0.27, RI=0.59) for extant and extinct taxa combined (282 characters, 193 parsimony informative). The strict consensus of the 56 minimum length trees obtained from the extant morphology partition was largely unresolved within Delphinidae. Two clades were recovered with marginal bootstrap support: *Sousa* + *Sotalia fluviatilis*, and *Globicephala macrorhynchus* + *Grampus griseus*. *Cephalorhynchus hectori* was recovered as the basalmost delphinid.

Inclusion of fossil taxa resulted in greater resolution of delphinid relationships. The strict consensus of the 684 minimum length trees recovered some delphinine and globicephaline relationships (Fig. 9); however, constituent taxa within Lissodelphininae differed from molecular hypotheses (Figs. 4-8) and not all taxa commonly allied with their respective sub-families were resolved. *Steno* was weakly allied (Bremer Support=1)

with Delphininae. Character optimization for *Steno* + Delphininae recovered three synapomorphies: mandibular tooth count, one periotic character, and one character scored for the tympanic bulla.

Molecules, Morphology, and Fossils

Equally weighted parsimony analysis of the nu + morphology +fossils supermatrix (Nu+foss; 35263 characters, 1038 parsimony informative) yielded six equally parsimonious trees (4305 steps, CI=0.48, RI=0.71). At the base of the delphinid radiation, a clade consisting of *Orcinus* + *Eodelphinus* + *Hemisyntrachelus cortesii* was recovered (Fig. 10). Additionally, the following clades were present in the Nu+Foss consensus: *Lagenorhynchus albirostris* + *Leucopleurus acutus*, *Orcaella* + *Steno* + Globicephalinae, *Feresa attenuata* + *Peponocephala electra*, *Globicephala macrorhynchus* + *Pseuuedorca crassidens*, *Sousa chinensis* + *Sotalia fluviatilis*, *Tursiops. truncatus* + *Tursiops aduncus*, *Tursiops truncatus* + *Tursiops aduncus* + *Stenella coeruleoalba*, *Etruridelphis giullii* + *Tursiops osennae*, *Etruridelphis giulli* + *Tursiops osennae* + *Stenella rayi*, *Stenella frontalis* + *Stenella attenuata*, and *Stenella clymene* + *Lagenodelphis hosei* (Fig. 10). Character optimization for *Steno* + Globicephalinae recovered a single forelimb synapomorphy.

Parsimony analysis of the total evidence supermatrix (50795 characters; 5071 parsimony informative) yielded three minimum length trees of 20212 steps (CI=0.39,

RI=0.54). Strict consensus of these three trees was fully resolved except for relationships within Phocoenidae and at the base of Delphininae (Fig. 11). There was disagreement between minimum length trees for the branching order of *Tursiops osennae*, *Stenella rayi*, *Etruridelphis giullii*, and *Steno* + *Sotalia fluviatilis* at the base of Delphininae. Disagreement between equally parsimonious trees also occurred in a more crownward position within Phocoenidae. The following clades were recovered within Delphinidae with marginal to strong support: Delphininae, Globicephalinae, Lissodelphininae, *Orcaella* + Globicephalinae, *Stenella clymene* + *Stenella coeruleoalba*, *Steno* + *Sotalia fluviatilis*, and *Eodelphinus* + *Hemisyntrachelus cortesii* (Fig. 11). Within Delphininae, the genera *Stenella* and *Tursiops* were paraphyletic. *Leucopleurus actus*, rather than *Eodelphinus*, was found to be the basalmost delphinid.

Literature search

Reports in the literature described at least 59 suggested instances of interspecific hybridization within free-ranging delphinoideans (at least 21 within Delphinidae). Over 30 instances of interspecific hybridization were described for delphinids in captivity. The number of hybrid individuals, method of hybrid detection, and estimated interspecific divergences of free ranging hybridizing taxa are summarized in Table 2. Hybridization that occurred in captivity is summarized in Table 3. All reported instances of interspecific

hybridization to date were documented either by morphological evidence and/or molecular analysis.

Morphological accounts of free-living delphinoid hybridization included one instance of intergeneric hybridization within Monodontidae (*D. leucas* x *M. monoceros*), and multiple accounts of proposed hybridization within Delphinidae (Table 2). For some accounts, proposed hybrid origins of atypical delphinoid cetaceans relied entirely upon photographic evidence. For example, decades-long behavioral studies of sympatric coastal populations of *Tursiops truncatus* and *Stenella frontalis* in the Bahamas documented frequent interspecific sexual encounters as well as the occurrence of a putative hybrid calf of intermediate phenotype (Herzing and Elliser, 2013; Herzing et al., 2003). Additional accounts documented with photographic evidence were reported for two immature delphinid calves believed to be generated from *Stenella longirostris x Stenella attenuata* and *Stenella longirostris x Stenella clymene* pairings (Silva-Jr. et al., 2005). Both putative hybrid offspring were associated with a pod of spinner dolphins, *S. longirostris*, in the Fernando de Noronha National Marine Park, northeast of Brazil. In other cases, morphological examination of stranded individuals or of an anomalous delphinoid skull supported hypotheses of hybrid origins for atypical delphinoids (e.g., Fraser, 1940; Heide-Jorgensen and Reeves, 1993; Reyes, 1996). For instance, Fraser (1940) examined three atypical delphinids stranded in Blacksod Bay, Western Ireland,

and after considering the possibility that these atypical cetaceans were members of a novel species, Fraser (1940) concluded that all three individuals were hybrids generated from *Tursiops truncatus* x *Grampus griseus*. More recently, in coastal waters off of the United Kingdom, Hodgins et al. (2014) described and photographed four possible free-ranging *Tursiops truncatus* x *Grampus griseus*.hybrids (Table 2). Interfertility of *Tursiops truncatus* and *Grampus griseus* has been documented in captivity (Table 3).

Molecular detection of free-ranging hybridization within Delphinoidea has confirmed intergeneric hybridization and introgression between *Phocoena phocoena* and *Phocoenoides dalli*, intergeneric hybridization between *Sousa chinensis* and *Orcaella heinshoni*, intrageneric hybridization between *Stenella frontalis* and *Stenella attenuata*, intrageneric hybridization as well as introgression for *Globicephala melas* and *Globicephala macrorhynchus*, possible hybridization between *Tursiops truncatus* and *Tursiops. aduncus*, and a putative hybrid origin for *Stenella clymene* as the result of ancestral *Stenella longirostris* x *Stenella coeruleoalba* pairings (Fig. 2A; Table 2). The greatest number of detected hybrids, at least 38, as well as post F1 introgressed individuals, was reported for sympatric inshore *Phocoena phocoena* and *Phocoenoides. dalli* in the vicinity of Vancouver Island, British Columbia (see Baird et al., 1998; Crossman et al., 2014; Willis et al., 2004).

Interspecific hybridization in captivity has been limited to family Delphinidae. All instances reported to date have occurred between a bottlenose dolphin, *Tursiops*

truncatus, and another oceanic dolphin (Table 3). For example, the capacity to hybridize within sub-family Delphininae has been demonstrated for *Tursiops truncatus* x *D. capensis* and *Tursiops truncatus x Delphinus delphis* (Table 3); fertility of F_1 hybrids was verified for *Tursiops truncatus* x *Delphinus capensis* (Zornetzer and Duffield, 2003). Hybridization has also occurred between *Tursiops truncatus* and *Sotalia guianensis* (Caballero and Baker, 2010). Additionally, interspecific sexual encounters have been reported for *Tursiops truncatus* and *Sotalia guianensis* in the wild (Acevedo-Gutiérrez et al., 2005). More divergent captive hybridization has occurred between *Tursiops truncatus* and the globicephalines *Grampus griseus*, *Pseudorca crassidens*, and *Globicephala macrorhyncus*, as well as between *Tursiops truncatus* and *Steno* (Table 3). In some instances, interspecific hybridization in captive holding tanks occurred despite the availability of homospecific members of the opposite sex (e.g., Caballero and Baker, 2010; Sylvestre and Tasaka, 1985).

My survey of the literature revealed additional accounts of cetacean hybridization exclusive of Delphinoidea. Within Mysticeti (baleen whales), morphological accounts of putative hybridization between blue whales, *Balaenoptera musculus*, and fin whales, *Balaenoptera physalus*, date to the 19th century (Spillaert et al. 1991; Bérubé and Aguilar, 1998). Molecular evidence confirmed bidirectional hybridization between *Balaenoptera musculus* and *Balaenoptera physalus* (Table 2; Arnason et al., 1991; Bérubé and Aguilar, 1998; Spilliaert et al., 1991), and fertility of a female hybrid (Spillaert et al. 1991).

However, the only two male hybrids that have been examined to date appear to have been sexually immature and/or possibly infertile (Árnason et al. 1991). Bidirectional hybridization as well as backcrossing was also reported between common minke whales, *Balaenoptera acutorostrata*, and Antarctic minke whales, *Balaenoptera bonaerensis* (Fig. 2B; Table 2).

DISCUSSION

Nuclear versus mitochondrial hypotheses

A combination of phylogenetic analyses were applied to datasets sampling the nuclear genome for the majority of extant delphinids. Maximum likelihood supermatrix analyses were largely congruent with one another, differing at only a few weakly supported nodes. For all nuclear topologies, Globicephalinae was sister to Delphininae, and relationships within Globicephalinae were generally well supported (Fig. 4). Congruent with previous analyses (e.g., Caballero et al., 2008; McGowen, 2011; McGowen et al., 2009, 2008), *Steno* and *Orcaella* were strongly allied with the globicephalines. Relationships within Delphininae, however, with the exception of *Delphinus* + *Stenella longirostris* + *Lagenodelphis hosei*, were generally not well supported (Fig. 4). Also consistent with previous investigations, *Stenella*, was not found to be monophyletic (e.g., Amaral et al., 2012; Kingston et al., 2009; McGowen, 2011).

Equally weighted parsimony analysis of the nu supermatrix resulted in a well-resolved topology for strongly supported clades and alliances found in ML topologies, whereas relationships within Lissodelphininae and Delphininae, with the exception of *Delphinus* +*Stenella longirostris* + *Lagenodelphis hosei*, were effectively polytomies. However, with the incorporation of a greater amount of sequence data than previous studies, the genus *Tursiops* was recovered as monophyletic for nu-based ML topologies, exclusive of mt data, for the first time; albeit with marginal support (Fig. 4). *Tursiops* was also recovered as monophyletic for ASTRAL ML based analysis, ASTRAL Bayesian analysis, and for BUCKy concordance analysis, with varying levels of support (Figs. 7A and 8A-C). Considerable phylogenetic conflict between *Tursiops truncatus*, *Tursiops aduncus*, *Stenella frontalis*, and *Stenella coeruleoalba* was apparent in SplitsTree supernetwork reconstructions (Fig 8G). Such incongruence could be the result of ILS, interspecific gene flow, or erroneous gene tree reconstruction (Huson and Bryant, 2006; Whitfield et al., 2008). The monophyly of *Tursiops* has been disputed for over a century, and both *Stenella* and *Tursiops* are junior synonyms for *Delphinus* (Perrin et al., 2013; Xiong et al., 2009).

At the base of the delphinid radiation, *Leucopleurus acutus*, *Lagenorhynchus albirostris*, and *Orcinus* were consistently found to be basal delphinid taxa across nuclear supermatrix analyses, regardless of method and partitioning scheme. However, both nodal support and the branching order of these three taxa varied by analysis.

Unpartitioned GARLI and RAxML analyses grouped *Orcinus* as sister to *Lagenorhynchus albirostris*, which is identical to the nu supermatrix topology and concordance analyses of McGowen (2011). In all partitioned analyses, *Leucopleurus acutus*, *Lagenorhynchus albirostris*, and *Orcinus* were successive branching taxa (Fig. 4). *Leucopleurus acutus*, *Lagenorhynchus albirostris*, and *Orcinus* were also found to be basal delphinids for ASTRAL ML based nu coalescent analyses (Figs. 7A and 8A). But the branching order of these three basal taxa differed between supermatrix analyses and the ASTRAL ML based topology. The ASTRAL ML nu topology presented an alternative hypothesis, that *Lagenorhynchus albirostris* is the basalmost delphinid, rather than *Leucopleurus acutus* as found in all supermatrix analyses irrespective of method. Nodal support, however, was < 50% BS for placement of *Leucopleurus acutus* in the ASTRAL ML based nu topology (Figs. 7A vs. 4). No molecular analyses, irrespective of method, recovered *Lagenorhynchus albirostris* and *Leucopleurus acutus* as sister taxa, as was suggested by Banguera-Hinestroza et al.(2014). Here, *Orcinus* was represented in all datasets.

Consistent across nu analyses was placement of *Steno* and *Orcaella* with Globicephalinae (Figs. 4, 7A, and 8A-C). For both ML and MP topologies, nodal support was > 90% for the position of *Orcaella* as the basalmost globicephaline and *Steno* as sister to the remaining globicephalines. Nodal support was also strong for placement of *Steno* and *Orcaella* with the globicephalines in ASTRAL ML based nu topologies.

However, both ASTRAL ML and ASTRAL Bayesian based analyses for the 31 nu gene and 13 nu gene datasets, as well as Bayesian concordance analysis of the 13 nu gene dataset, recovered *Steno* and *Orcaella* as sister taxa (Figs. 7A and 8A-C), a clade that was not present in any nu gene tree. Likewise, filtered supernetworks clustered *Steno* and *Orcaella* together at the base of Globicephalinae. A sister relationship for *Steno* and *Orcaella* has been suggested previously by Caballero et al. (2008). But, similar to gene tree based analyses here, the hypothesis of *Steno* + *Orcaella* was not well supported in that investigation. Overall, the weight of evidence from the nuclear DNA data robustly groups both *Steno* and *Orcaella* with Globicephalinae to the exclusion of all other extant delphinids, whether the data are analyzed via concatenation or by methods that take conflicts among gene trees into account.

Phylogenetic hypotheses recovered from mitogenome analyses were consistently incongruent with nu topologies for certain alliances. Identical to previous mt results (e.g., Cunha et al., 2011; LeDuc et al., 1999; May-Collado and Agnarsson, 2006; McGowen et al., 2011; Vilstrup et al., 2011), *Steno* was strongly supported as the sister taxon to *Sotalia* in all mt reconstructions (Figs. 4 and 5). Well-supported cytonuclear incongruence was also apparent for placement of *Stenella longirostris* and *Lagenodelphis hosei* within Delphininae, and notable incongruence, although not well supported, was evident for *Orcinus* and *Tursiops* (Fig. 4).

Novel to my investigation, *Orcinus* was recovered as basal to Lissodelphininae in all mt analyses exclusive of morphology, including equally weighted parsimony. Support for this hypothesis ranged from marginal for equally weighted parsimony to > 70% BS support for RAxML partitioned and unpartitioned analyses. Inclusion of additional mitochondrial sequences for taxa with unsequenced mitogenomes did not alter the hypothesis of Lissodelphininae + *Orcinus*. The placement of the charismatic genus *Orcinus* within Delphinidae has been an intransigent problem, with different investigations advancing contradictory evolutionary hypotheses (e.g., Alexander et al., 2013; Cunha et al., 2011; LeDuc et al., 1999; McGowen, 2011; McGowen et al., 2009; Vilstrup et al., 2011). Mitogenome studies alone have suggested that *Orcinus* is allied with Globicephalinae (Vilstrup et al., 2011), sister to *Lagenorhynchus albirostris* (Alexander et al., 2013), or incertae sedis (Cunha et al., 2011). No reported mitogenome analysis to date has recovered *Orcinus* + *Orcaella* (*Orcininae*, LeDuc et al., 1999; May-Collado and Agnarsson, 2006).

The alliance of *Orcinus* with Lissodelphininae was not, however, unique to topologies obtained from mitochondrial datasets. Bayesian concordance analysis and ASTRAL Bayesian analysis of the 13-nu gene dataset grouped *Orcinus* with the lissodelphines for nuclear data with very weak support (<50% bootstrap and <0.13 concordance factors in all cases). Likewise, Splits tree nuclear supernetwork reconstructions unambiguously placed *Orcinus* at the base of the lissodelphine cluster for

the 13-nu gene dataset (filter set to 5). Nevertheless, as mentioned above, *Orcinus* was positioned as basal to Delphinidae for all nuclear analyses employing the full 31-nu gene dataset.

Nuclear and mitochondrial data combined

Topologies obtained by merging nu and mt datasets were virtually identical across supermatrix analyses and differed only at a single marginally supported node within Lissodelphininae. *A priori*, I anticipated that incorporating a mt dataset of this magnitude (15533 characters; 4156 parsimony informative) into simultaneous analyses might overturn hypotheses found only for the nu partition (22354 characters; 768 parsimony informative). This prediction was indeed found to be the case for most taxa that exhibited some degree of cytonuclear incongruence (Fig. 4). In fact, nodal support either decreased for clades with conflicting nu and mt hypotheses, or such clades were eradicated in entirety (Figs. 4 and 6). For example, *Steno* + *Orcaella* + Globicephalinae, *Lagenodelphis hosei* + *Delphinus* + *Stenella longirostris* and *Tursiops truncatus* + *Tursiops aduncus,* all of which were clades consistently recovered in nuclear topologies, were disrupted with the incorporation of the mitogenome. Identical to mitochondrial hypotheses, *Steno* was sister to *Sotalia* and allied with Delphininae; however, for all ML analyses, this hypothesis was recovered with lower nodal support than mitochondrial topologies alone (Figs. 4 vs. 6). In contrast, the merging of nuclear and mitochondrial

data either increased nodal support for clades without evidence of cytonuclear discordance, or alliances congruent with both datasets remained unchanged with nearly equal bootstrap support. For example, *Delphinus delphis* + *Delphinus capensis*, *Globicephala macrorhynchus* + *Globicephala melas*, *Sagmatias obliquidens* + *Sagmatias obscurus*, and *Sotalia* + Delphininae (to the exclusion of *Steno*) were recovered with high bootstrap support in all supermatrix analyses. Similarly *Orcaella* was allied with Globicephalinae with strong support in all topologies except for that of the maximum parsimony mitogenome topology. The alliance of *Orcaella* with Globicephalinae is well corroborated (Caballero et al., 2008; McGowen, 2011; McGowen et al., 2009; Nishida et al., 2007; Steeman et al., 2009; Vilstrup et al., 2011).

Disruption of nu based hypotheses was not, however, the only result of simultaneous molecular analyses of nu + mt data. Hidden support emerged at the base of the delphinid radiation. The placement and branching order of *Orcinus*, *Lagenorhynchus albirostris*, and *Leucopleurus. acutus*, while remaining identical to nuclear supermatrix hypotheses, was recovered with stronger nodal support, even though some relationships conflict with the mitochondrial tree (Fig. 4 vs. Fig. 6). Likewise, the branching order of the three delphinid subfamilies remained identical to nu supermatrix hypotheses, and bootstrap support increased for ML topologies. Although *Stenella longirostris* exhibited moderately supported cytonuclear discordance (Fig. 4), *Stenella longirostris* remained robustly allied with *Delphinus* in the combined topology (Fig. 6). Greater resolution was

also achieved within Globicephalinae; *Feresa attenuata* + *Peponocephala electra*, a relationship marginally supported in mt topologies and non-existent in nu supermatrix hypotheses, was recovered with > 70% BS support in all combined molecular evidence supermatrix topologies.

For ASTRAL and BUCKY, gene tree based nu hypotheses changed with the inclusion of mitochondrial data (Figs. 7 and 8). The most pronounced topological rearrangements occurred for the 31 gene nu ASTRAL analyses (Fig. 7). Although the mt topology was input as a single gene tree, addition of mt data allied *Steno* with Delphininae + *Sotalia*, *Orcinus* with Lissodelphininae, and rendered *Tursiops* paraphyletic (Fig. 7B). However, all three hypotheses were weakly supported. At the same time, incorporation of the mitogenome reduced support for the alliance of *Lagenodelphis hosei* with *Stenella longirostris* + *Delphinus*, and reversed the paraphyly of common dolphins, *Delphinus*, a result found only in the 31 gene nu ASTRAL hypothesis (Fig. 7A vs. 7B).

In general, the combined nu + mt 32 gene ASTRAL topology was largely congruent with supermatrix topologies. Notably, relationships within Globicephalinae and Lissodelphininae were identical to all supermatrix combined molecular analyses. *Leucopleurus acutus* was strongly supported as the basalmost delphinid, and Lissodelphininae was sister to Delphininae + Globicephalinae (Fig. 7B vs. Fig. 4).

Combining the single mitogenome tree with nuclear input trees had less of a pronounced effect upon the 13 gene nu ASTRAL topologies (Fig. 8A-F). Similar to the full 31 nu gene dataset, incorporation of the mt tree allied *Orcinus* with Lissodelphininae for the ASTRAL ML based analysis. For both ASTRAL and BUCKY, *Steno* was recovered as a basal globicephaline, rather than allied with *Sotalia* + Delphininae (Fig. 8D-F). Supernetwork reconstructions, however, presented a large split between alternative hypotheses for *Steno* (Fig. 8H). Similar to observed incongruence between hypotheses for *Tursiops*, gene tree incongruence visualized in split networks could be the result of ILS or hybridization (Huson and Bryant, 2006; Whitfield et al., 2008).

Cytonuclear conflict: hybridization or ILS?

As noted above, conflicting nu and mt hypotheses were evident for numerous delphinids throughout my analyses (Figs. 4, 7, and 8). The strongest instance of cytonuclear incongruence was apparent for *Steno*. But other moderately supported (BS > 70%) instances of cytonuclear incongruence were evident for *Stenella longirostris* and *Lagenodelphis hosei* in supermatrix analyses. More tenuous examples of cytonuclear incongruence were found for *Orcinus*, *Tursiops*, and throughout sub-family Delphininae.

It might be proposed that because of the rapid diversification of Delphinidae (~10-13 Ma; McGowen et al., 2009; Murakami et al., 2014; Steeman et al., 2009), mitochondrial-based trees, rather than trees based on the nuclear genome, more

accurately portray delphinid evolutionary history. The reduced effective population size of the mitochondrial genome, as well as a higher substitution rate relative to the nuclear genome (Brown et al., 1982; Harrison, 1989; Moore, 1995), should make mitochondrial based phylogenetic inference less prone to the effects of ILS over short internodes (Moore, 1995). For this very reason, I compared topologies arising from different genetic loci as well as reconstruction methodologies, and I explicitly accounted for ILS in both nu and nu + mt phylogenetic reconstructions via ASTRAL. Nuclear hypotheses arising from concatenated supermatrices, BUCKy, and ASTRAL were largely congruent (Figs. 4, 7, and 8), which suggests that ILS might not be the source of cytonuclear incongruence for some taxa.

For all methods I employed, the incorporation of mt data into nu datasets either reduced nodal support, increased nodal support, or disrupted certain clades and alliances unique to nu hypotheses (Figs. 4 vs. 6, and Figs. 7 and 8). The outcome of combining nuclear and mitochondrial data into simultaneous analyses (concatenation) has been investigated by Fisher-Reid and Wiens (2011) for 14 vertebrate clades. For the majority of these 14 clades, the prediction that shorter branches would be resolved in favor of mitochondrial hypotheses and longer branches would be resolved in favor of nuclear hypothesis was not always met. In fact, trees recovered from the analysis of combined datasets typically contained a majority of nodes found in nu topologies despite some of these datasets containing 2-3 times more mt data relative to nu data. For plethodontid

salamanders, mt hypotheses dominated simultaneous analyses, and Fisher-Reid and Wiens (2011) reasoned that strongly supported instances of cytonuclear incongruence were suggestive of mitochondrial introgression.

For my simultaneous analyses, resolution of long terminal branches at the base of Delphinidae favored nu hypotheses whereas resolution of short branches, with the exception of placement of *Stenella longirostris*, favored mitochondrial hypotheses (Fig. 4 vs. Fig. 6). While relationships within Delphininae, exclusive of *Delphinus* + *Stenella longirostris* + *Lagenodelphis hosei*, were weakly supported, similar topologies were recovered across nuclear analyses. Specifically, a clade consisting of *Tursiops* + *Stenella frontalis* + *Stenella attenuata* was sister to *Delphinus* + *Stenella longirostris* + *Lagenodelphis hosei*. Placement of *Stenella coeruleoalba* differed between supermatrix and gene tree based topologies (Fig. 4 vs. 7 and 8). Supernetwork reconstructions, while not an explicit graph of evolutionary relationships, recovered similar alliances (Fig. 8); however, as previously mentioned, well-defined splits indicative of phylogenetic incongruence that might arise from ILS or introgressive hybridization were apparent in each delphinine cluster. The number of splits increased with the incorporation of the mt gene tree.

My review of the literature indicated that hybridization within free-ranging delphinines is ongoing (Table 2). For example, interspecific copulations have been observed between *Tursiops truncatus* and *Stenella frontalis* in the vicinity of the

Bahamas (Herzing and Elliser, 2013), and a putative *Tursiops. truncatus* x *Stenella frontalis* calf was documented with photographic evidence (Herzing et al., 2003). *Stenella frontalis* hybrids have also been detected with molecular techniques by Vollmer et al. (2011), but the exact details of the interspecific cross and determination of hybrid status was not made clear. Interspecific copulations between other delphinines have been observed for *Stenella longirostris* and *Stenella attenuata* in the vicinity of Hawaii (Psarakos et al., 2003), and a presumed *Stenella longirostris* x *Stenella. attenuata* calf was identified in the West Atlantic (Silva-Jr. et al., 2005). Kingston et al. (2009) identified at least four (possibly five) *Stenella frontalis* x *Stenella attenuata* hybrids and evidence of bidirectional hybridization as well as probable multi-generational introgression into paternal species. Furthermore, AFLP analyses suggested that low levels of allelic introgression were widespread.

While there were no known examples of hybridization between *Lagenodelphis hosei* and other delphinines, inclusion of mitochondrial data into simultaneous concatenated analyses separated *Lagenodelphis hosei* from *Delphinus* + *Stenella longirostris*, and combined topologies instead recovered *Lagenodelphis. hosei* as a basal delphinine (Figs. 4 and 6). Likewise, incorporation of the mt gene tree reduced nodal support for *Lagenodelphis hosei* + *Stenella longirostris* + *Delphinus* in ASTRAL topologies to < 50%, but the alliance of *Lagenodelphis hosei* with the *Delphinus* group was not disrupted (Figs. 7 and 8). The alliance of *Lagenodelphis hosei* with *Stenella*

longirostris + *Delphinus* is corroborated by the analyses of Caballero et al. (2008), and by the nu topology of McGowen (2011). In contrast, three examples of active hybridization between *Stenella longirostris* and other delphinines have been reported in the literature (Table 2), but well supported cytonuclear discordance observable for *Stenella longirostris* did not disrupt nu hypotheses when mt data were incorporated into supermatrix analyses (Figs. 4, 6, 7, and 8). For gene tree based reconstruction methods, nodal support also increased for placement of *Stenella longirostris* with the incorporation of the mitochondrial tree (Figs. 7 and 8). Despite both *Lagenodelphis hosei* and *Stenella longirostris* exhibiting divergent nu and mt histories, the contrasting effects of incorporating mt data into ASTRAL analyses for these two delphinines are not clear. For *Lagenodelphis hosei*, cytonuclear incongruence is suggestive of mitochondrial introgression, but there are no known examples of wild hybrids to corroborate this possibility, and ILS as the source of incongruence remains plausible. Nevertheless, including an informative locus such as the mitogenome into a coalescent analysis should improve accuracy (Corl and Ellegren, 2013; Lanier et al., 2014), unless mitochondrial introgression is the source of phylogenetic incongruence (Corl and Ellegren, 2013).

The sum total of reported free-ranging hybridization events within delphinines indicates that interspecific pairings occur between taxa that have diverged from one another anywhere from 1.59-4.36 Ma (McGowen et al., 2009; Steeman et al., 2009). Yet an account of free-ranging hybridization, and possible introgression between *Sousa*

chinensis and *Orcaella* was reported (Brown et al., 2014). Two different accounts suggest that hybridization between *Tursiops truncatus* and *Grampus griseus* in waters off of the United Kingdom has been occurring since at least the 1940s (Table 2; est. divergence 8.36-9.44 Ma, McGowen et al., 2009; Steeman et al., 2009). The capacity for *Tursiops truncatus* to hybridize with the globicephalines has been demonstrated in captivity, and fertility of hybrid offspring has been confirmed (Table 3). Additionally, the holotype of the extinct globicephaline, *Protoglobicephala mexicana* (2.2-3.6 ± 0.5 Ma; Aguirre-Fernández et al., 2009), was determined to exhibit intermediate cranial morphology between extant globicephalines and *Tursiops*, which prompted Aguirre-Fernández et al. (2009) to consider, but not to conclude, the possibility that *P. mexicana* was a hybrid.

In light of evidence for ongoing hybridization between Delphininae and Globicephalinae, and because of strongly supported cytonuclear incongruence that affected all phylogenetic reconstruction methods that I employed, it is plausible, but not definitive, that discrepancies between mt and nu hypotheses for *Steno* are the result of past mitochondrial introgression and subsequent fixation. Topologies obtained from the mitogenome and the combined mt dataset strongly group *Steno* with *Sotalia* + Delphininae (Figs. 4 and 5). Moreover, all molecular investigations to date that have analyzed mt datasets either in the absence of nu data or separate from nu data have consistently recovered mt topologies that group *Steno* with *Sotalia* (Agnarsson and May-Collado, 2008; Caballero et al., 2008; Cunha et al., 2011; LeDuc et al., 1999; May-

Collado and Agnarsson, 2006; McGowen et al., 2011; Vilstrup et al., 2011), which suggests that cytonuclear incongruence in *Steno* is ubiquitous. Four nu ML gene topologies (*LALBA*, *MC1R*, *RAG1*, *OR10J1*) allied *Steno* with Globicephalinae and/or Globicephalinae + *Orcaella*, but one ML nu gene topology *(CHRNA1)* allied *Steno* with Delphininae. Regardless, nodal support for the *CHRNA1 Steno* + Delphininae ML topology was <50%, and parsimony branch support for the same alliance was negative (Table 1). Therefore, not one nu locus sampled here supported an alliance of *Steno* + *Sotalia* + *Delphininae*, and both gene tree based reconstruction methods and supermatrix analyses yielded virtually identical nu hypotheses that were strongly supported (Figs. 4 and 7). Nevertheless, it is possible that because of a low number of informative loci, and/or nonrandom missing data for some of the taxa in the 31 gene nu dataset, that the ASTRAL nuclear analysis recovered an erroneous topology (Lanier et al., 2014; Xi et al., 2015). If this was the case, then coalescent and concordance analyses of the reduced gene dataset with complete sampling of loci for each included taxon might have presented alternative hypotheses that allied *Steno* with Delphininae. Instead, the alliance of *Steno* + *Orcaella* + Globicephalinae was robust to the incorporation of mt data into the reduced gene dataset (Fig. 7). Furthermore, aside from the marginally supported mitochondrial alliance of *Orcinus* with Lissodelphininae, no other delphinid besides *Steno* switched sub-family alliances with the incorporation of the mitogenome into analyses of the 31 gene nu dataset (Figs. 4, 6, and 7).

Morphology, fossils, and molecules

Prior to the investigation of Murakami et al. (2014a), no comprehensive morphological cladistic analysis of Delphinidae had been executed. Because of this, morphological synapomorphies that might support recent molecular phylogenies remained unclear (McGowen, 2011). My re-analysis of the morphology matrix of Murakami et al. (2014a) was inclusive of Delphinida and I excluded more distantly related outgroup taxa. The resulting strict consensus tree obtained from analysis of my chosen taxa set (62 extant + extinct members of Delphinida) was less resolved within Delphinidae than the strict consensus incorporating 84 taxa recovered by the morphological cladistics analysis of Murakami et al. (Fig. 9 vs. Fig. 7, Murakami et al., 2014a). It is possible that removal of more distant delphinid outgroup taxa might have affected character polarity within Delphinidae. Whereas Murakami et al. (2014a) recovered a clade consisting of *Orcinus* + *Hemisyntrachelus cortesii* + *Eodelphinus*, that was allied with Globicephalinae, disagreement between equally parsimonious trees obscured similar resolution at the base of Delphinidae for the morphology partition. Likewise, *Etruridelphis giulii*, *Stenella rayi*, *Tursiops osennae*, *Tursiops aduncus*, *Sousa chinensis,* and *Sotalia fluviatilis* were not allied with Delphininae (Fig. 9). Nevertheless, as in Murakami et al. (2014a), *Steno* grouped with members of Delphininae; albeit with marginal support (Bremer Support=1).

Three synapomorphies supported the alliance of *Steno* with Delphininae for the Morph+Foss consensus hypothesis: the number of teeth in the mandible, the aperture for the cochlear aqueduct, and the posterior edge of the inner posterior prominence of the involucrum. Both *Steno* and *Tursiops truncatus* possess similar mandibular tooth counts: 17-27. This quantity of mandibular teeth differs from most delphinines; however, parsimonious reconstruction of mandibular tooth counts onto the Morph+Foss consensus topology unambiguously transitions from delphinids possessing 28-39 mandibular teeth, to *Steno* and *Tursiops* at the base of Delphininae, and subsequently transitions back to ≥ 28 mandibular teeth for more crownward delphinines. Furthermore, the character states for the periotic and tympanic bulla characters listed above are unambiguous synapomorphies for *Steno* + Delphinidae to the exclusion of Globicephalinae.

With the integration of nuDNA, morphology, and fossils, simultaneous analysis of the Nu+Foss dataset resulted in six minimum length trees. The strict consensus of these six trees was largely congruent with hypotheses generated from nuclear data alone (Fig. 10 vs. Figs. 4, 7A, 8A-C). A few notable exceptions in comparison to molecular supermatrix topologies were monophyly of the spotted dolphins, *Stenella frontalis* and *Stenella attenuata*, a clade consisting of *Sousa chinensis* + *Sotalia fluviatillis* allied with Delphininae, and a sister relationship for *Lagenorhynchus albirostris* and *Leucopleurus acutus*. The former two alliances were recovered in different molecular reconstructions, but the sister relationship of *Lagenorhynchus albirostris* and *Leucopleurus acutus* was

unique to the Nu+Foss consensus hypothesis. Likewise, the integration of nuDNA and fossils recovered the basal delphinid clade consisting of *Orcinus* + *Hemisyntrachelus cortesii* + *Eodelphinus*, which was identical to the morphology and backbone constraint analyses of Murakami et al. (2014a).

Congruent with all nuclear analyses, both *Orcaella* and *Steno* were allied with Globicephalinae in the Nu+Foss consensus topology. A single character transition for the deltoid crest on the anterior edge of the humerus supported the alliance of *Steno* with Globicephalinae to the exclusion of Delphininae. However, the same character state was present in *Sotalia fluviatilis* as an autapomorphy, and both *Globicephala macrorhynchus* and *Pseudorca crassidens* were not scored for this character by Murakami et al. (2014a). In and of itself, this single character is not a convincing synapomorphy for the alliance of *Steno* with Globicephalinae to the exclusion of *Sotalia fluviatilis* + Delphininae. Nuclear DNA likely dominated phylogenetic resolution of *Steno* in the Nu + Foss analysis.

Arguably, the most novel portion of my investigation was the combination of fossils and molecules into simultaneous analyses of crown Delphinidae. The total evidence and Nu + Foss consensus hypotheses recovered here are unique to this synthesis. While Murakami et al. (2014a) did combine morphology, fossils, and molecules, they utilized an altered molecular scaffold derived from McGowen et al. (2009) (Gatesy, pers. comm.; Murakami, pers. comm.). Essentially, the molecular constraint tree of Murakami et al. (2014a) was not recovered by McGowen et al. (2009),

and was obtained by accidentally altering the topology of McGowen et al. (2009) in MacClade (Murakami, pers. comm.). Consequently, direct comparison of my total evidence consensus topology and that of Murakami et al. (2014a) would likely result in incongruences that are not strictly the result of incorporating a greater amount of molecular data into simultaneous analysis with fossils.

As has been consistent throughout my analyses, incorporation of all available mitochondrial data into simultaneous analysis altered the Nu + Foss consensus hypothesis (Fig. 10 vs. Fig. 11). Furthermore, placement of extinct delphinids was altered despite the absence of molecular characters in these taxa. The potential for molecular data to alter the placement of extinct taxa has been previously shown (e.g., Gatesy et al., 2003; O'Leary and Gatesy, 2008; Wiens et al., 2010). Likewise, the ability of morphological characters to influence and in some instances overturn molecular hypotheses is known to occur (Gatesy et al., 2013; Wiens et al., 2010). In this instance, it would appear that incorporation of the mitogenome into simultaneous analyses obscured delphinid relationships and the Nu + Foss consensus is likely a more accurate hypothesis of delphinid evolutionary history, primarily because the nuclear dataset is comprised of multiple loci. Nevertheless, addition of the entire mitochondrial partition into the Nu + Foss dataset increased nodal support for relationships within Globicephalinae, Lissodelphininae, and Phocoenidae (Figs. 10 vs. Figs. 11), and enabled character optimization for *Steno* + *Sotalia fluviatilis*. Two characters supported the hypothesis of

Steno + *Sotalia fluviatilis*: mandibular tooth count and rostrum length. Although *Steno* and *Tursiops truncatus* have identical tooth counts, *Steno* and *Sotalia fluviatilis* have overlapping tooth counts (*Steno*: 17-27 vs. *Sotalia fluviatilis*: 24-39). Both possess a long rostrum, expressed as the percentage of skull length. The same rostral length is found in crownward delphinines. However, *Peponocephala electra* not only possesses a relatively long rostrum, but also a tooth count similar to that of *Sotalia fluviatilis*: 24-39. Therefore, synapomorphies for *Steno* + *Sotalia fluviatilis* were present as autapomorphies in one globicephaline for the total evidence consensus hypothesis.

Conclusions

The largest datasets assembled to date were analyzed with a combination of methodologies to arrive at improved phylogenetic hypotheses for Delphinidae (e.g., Figs. 6 and 11). Concomitantly, discordant signals arising from individual datasets for different taxa were highlighted in individual analyses. The single greatest source of discordance for some delphinids was found to be cytonuclear incongruence. Nevertheless, because of the low information content of the nuclear data partitions (Fig. 4, Fig. 7A, Fig. 8A-C, Appendix B) statistical measures of phylogenetic certainty, bootstrap nodal support, remained low for many taxa in multilocus nuclear topologies (e.g., resolution of Delphininae). For this reason, it remains equivocal to what extent actual cytonuclear incongruence, and possible mitochondrial introgression, is a pervasive phenomena within

much of Delphinidae. Because of the nascence of the delphinid radiation, low information content combined with the effects of ILS might be responsible for much of the phylogenetic uncertainty in this group.

I accounted for ILS based upon the sampling efforts here, but could not simultaneously account for contemporary or past nuclear gene flow among divergent lineages. Methods are sorely needed that can accommodate introgression, if ILS is to be explicitly modeled (Nakhleh, 2013; Ronquist and Deans, 2010). Simulation studies have shown that coalescent species tree methods are susceptible to genetic exchanges between taxa (Chung and Ané, 2011; Leaché et al., 2014). Furthermore, gene tree reconciliation methods can suffer when faced with inaccurate reconstruction of gene trees (Gatesy and Springer, 2014; Springer and Gatesy, 2016). For this reason, I executed the most rigorous gene tree searches currently available with three different phylogenetic programs and utilized the most likely trees for gene tree reconciliation methods.

The sum total of available evidence provided in this investigation suggests that cytonuclear discordance in *Steno* is likely caused by past introgressive hybridization. However, there was not strong evidence of nuclear introgression. Parsimony analysis of osteological characters revealed several synapomorphies for *Steno* + Delphininae. Nevertheless, ILS could also be the cause of cytonuclear discordance and morphological similarities might represent convergences.

A strong result highlighted here exposed that competing hypotheses for the phylogenetic affinity of *Steno* that have pervaded the literature (e.g., Agnarsson and May-Collado, 2008; Cunha et al., 2011; LeDuc et al., 1999; Steeman et al., 2009; Vilstrup et al., 2011 vs. Caballero et al., 2008; McGowen, 2011; McGowen et al., 2009, 2008) are strictly an artifact of mitochondrial phylogenetics. Not one of my nuclear analyses allied Steno with *Sotalia* + *Delphininae*. The Achilles heel of mitochondrial based phylogenetic inference, mitochondrial introgression, has long been known (Ballard and Whitlock, 2004; Funk and Omland, 2003; Harrison, 1989b; Moore, 1995).

Essentially, genome scale data are needed to firmly resolve some delphinid relationships; notably, the monophyly of *Tursiops*, relationships within the delphinine radiation, select nodes within Lissodelphininae, and the affinity of *Orcinus* based upon nuclear data alone. Placement of *Orcinus* was strongly supported in the combined molecular hypothesis (Fig. 6); however, combining nuDNA with fossils recovered *Orcinus* as the basalmost extant delphinid. For these reasons, until genome scale nuclear data are available, *Orcinus* should remain *incertae sedis*. Notwithstanding, if introgressive hybridization has been rampant throughout the evolutionary history of Delphinidae, increasing the amount of informative data might confound bifurcating trees. The reported amount of contemporary hybridization within this group of marine mammals is likely an underestimate (Crossman et al., 2016; Kingston et al., 2009).

REFERENCES

Abbott, R., Albach, D., Ansell, S., Arntzen, J.W., Baird, S.J.E., Bierne, N., Boughman, J., Brelsford, a., Buerkle, C. a., Buggs, R., Butlin, R.K., Dieckmann, U., Eroukhmanoff, F., Grill, a., Cahan, S.H., Hermansen, J.S., Hewitt, G., Hudson, a. G., Jiggins, C., Jones, J., Keller, B., Marczewski, T., Mallet, J., Martinez-Rodriguez, P., Möst, M., Mullen, S., Nichols, R., Nolte, a. W., Parisod, C., Pfennig, K., Rice, a. M., Ritchie, M.G., Seifert, B., Smadja, C.M., Stelkens, R., Szymura, J.M., Väinölä, R., Wolf, J.B.W., Zinner, D., 2013. Hybridization and speciation. J. Evol. Biol. 26, 229–246.

Acevedo-Gutiérrez, a., DiBerardinis, A., Larkin, S., Larkin, K., Forestell, P., 2005. Social interactions between tucuxis and bottlenose dolphins in Gandoca-Manzanillo, Costa Rica. Lat. Am. J. Aquat. Mamm. 4, 49–54.

Agnarsson, I., May-Collado, L.J., 2008. The phylogeny of Cetartiodactyla: The importance of dense taxon sampling, missing data, and the remarkable promise of cytochrome b to provide reliable species-level phylogenies. Mol. Phylogenet. Evol. 48, 964–985.

Aguirre-Fernández, G., Barnes, L.G., Aranda-Manteca, F.J., Fernández-Rivera, J.R., 2009. *Protoglobicephala mexicana*, a new genus and species of Pliocene fossil dolphin (Cetacea; Odontoceti; Delphinidae) from the Gulf of California, Mexico. Boletín la Soc. Geológica Mex. 61, 245–65.

Alexander, A., Steel, D., Slikas, B., Hoekzema, K., Carraher, C., Parks, M., Cronn, R., Baker, C.S., 2013. Low diversity in the mitogenome of sperm whales revealed by next-generation sequencing. Genome Biol. Evol. 5, 113–129.

Allendorf, F.W., Leary, R.F., Spruell, P., Wenburg, J.K., 2001. The problems with hybrids: Setting conservation guidelines. Trends Ecol. Evol. 16, 613–622.

Amaral, A.R., Gretchen, L., Maria M, C., George, A., Howard C, R., 2014. Hybrid speciation in a marine mammal: The clymene dolphin (*Stenella clymene*). PLoS One 9, 1–8. doi:10.1371/journal.pone.0083645

Amaral, A.R., Jackson, J. a., Möller, L.M., Beheregaray, L.B., Manuela Coelho, M., 2012. Species tree of a recent radiation: The subfamily Delphininae (Cetacea, Mammalia). Mol. Phylogenet. Evol. 64, 243–253.

Anderson, E., 1949. Introgressive hybridization. John Wiley and Sons, Inc., New York, Chapman and Hall, Ltd., London.

Anderson, E., Hubricht, L., 1938. Hybridization in *Tradescantia* . III . The evidence for introgressive hybridization. Am. J. Bot. 25, 396–402.

Anderson, E., Stebbins, Jr., G.L., 1954. Hybridization as an evolutionary stimulus. Evolution. 8, 378–388.

Ané, C., Larget, B., Baum, D. a., Smith, S.D., Rokas, A., 2007. Bayesian estimation of concordance among gene trees. Mol. Biol. Evol. 24, 412–426.

Arnason, U., 1980. C- and G-banded karyotypes of three delphinids : *Stenella clymene* , *Lagenorhynchus albirostris* and *Phocoena phocoena.* Hereditas 92, 179–187.

Arnason, U., Benirschke, K., 1973. Karyotypes and idiograms of sperm and pygmy sperm whales. Hereditas 75, 67–74.

Arnason, U., Spilliaert, R., Pálsdóttir, a, Arnason, a, 1991. Molecular identification of hybrids between the two largest whale species, the blue whale (*Balaenoptera musculus*) and the fin whale (*B. physalus*). Hereditas 115, 183–189.

Arnason, U., Xullberg, A., and Janke, A. 2004. Mitogenomic analyses provide new insights into cetacean origin and evolution. Gene 333: 27-34.

Arnold, M.L., 1992. Natural hybridization as an evolutionary process. Annu. Rev. Ecol. Syst. 23, 237–261.

Arnold, M.L., Meyer, A., 2006. Natural hybridization in primates: One evolutionary mechanism. Zoology 109, 261–276.

Baird, R.W., Willis, P.M., Guenther, T.J., Wilson, P.J., White, B.N., 1998. An intergeneric hybrid in the family Phocoenidae. Can. J. Zool. 76, 198–204.

Ballard, J.W.O., Whitlock, M.C., 2004. The incomplete natural history of mitochondria. Mol. Ecol. 13, 729–744.

Banguera-Hinestroza, E., Hayano, A., Crespo, E., Hoelzel, a. R., 2014. Delphinid systematics and biogeography with a focus on the current genus *Lagenorhynchus*: Multiple pathways for antitropical and trans-oceanic radiation. Mol. Phylogenet. Evol. 80, 217–230.

Bazinet, A.L., Zwickl, D.J., Cummings, M.P., 2014. A gateway for phylogenetic analysis powered by grid computing featuring GARLI 2.0. Syst. Biol. 63, 812–818.

Bérubé, M., 2002. Hybridism, in: Perrin, W., Würsig, B., Thewissen, J.G.M. (Eds.), Encyclopedia of Marine Mammals. Academic Press, San Diego, pp. 596–600.

Bérubé, M., Aguilar, A., 1998. A new hybrid between a blue whale, *Balaenoptera musculus*, and a fin whale, *B. physalus*: frequency and implications of hybridization. Mar. Mammal Sci. 14, 82–98.

Bininda-Emonds, O.R.P., 2007. Fast genes and slow clades: Comparative rates of molecular evolution in mammals. Evol. Bioinform. Online 3, 59–85.

Bonifácio, H.L., da Silva, V.M.F., Martin, A.R., Feldberg, E., 2012. Molecular cytogenetic characterization of the Amazon River dolphin *Inia geoffrensis*. Genetica 140, 307–315.

Brelsford, A., Milá, B., Irwin, D.E., 2011. Hybrid origin of Audubon's warbler. Mol. Ecol. 20, 2380–2389.

Bremer, K., 1994. Branch support and tree stability. Cladistics 10, 295–304.

Brown, A.M., Kopps, A.M., Allen, S.J., Bejder, L., Littleford-Colquhoun, B., Parra, G.J., Cagnazzi, D., Thiele, D., Palmer, C., Frère, C.H., 2014. Population differentiation and hybridisation of Australian snubfin (*Orcaella heinsohni*) and Indo-Pacific humpback (*Sousa chinensis*) dolphins in North-Western Australia. PLoS One 9, 1–14. doi:10.1371/journal.pone.0101427

Brown, W.M., Prager, E.M., Wang, A., Wilson, A.C., 1982. Mitochondrial DNA sequence of primates: Tempo and mode of evolution. J. Mol. Evol. 18, 225–239.

Buerkle, C.A., Morris, R.J., Asmussen, M. a., Rieseberg, L.H., 2000. The likelihood of homoploid hybrid speciation. Heredity 84, 441–451.

Caballero, S., Baker, C.S., 2010. Captive-born intergeneric hybrid of a Guiana and bottlenose dolphin: *Sotalia guianensis*×*Tursiops truncatus*. Zoo Biol. 29, 647–657.

Caballero, S., Jackson, J., Mignucci-Giannoni, A. a., Barrios-Garrido, H., Beltrán-Pedreros, S., Montiel-Villalobos, M.G., Robertson, K.M., Baker, C.S., 2008. Molecular systematics of South American dolphins *Sotalia*: Sister taxa determination and phylogenetic relationships, with insights into a multi-locus phylogeny of the Delphinidae. Mol. Phylogenet. Evol. 46, 252–268.

Cahill, J. a., Stirling, I., Kistler, L., Salamzade, R., Ersmark, E., Fulton, T.L., Stiller, M., Green, R.E., Shapiro, B., 2015. Genomic evidence of geographically widespread effect of gene flow from polar bears into brown bears. Mol. Ecol. 24, 1205–1217.

Cassens, I., Vicario, S., Waddell, V.G., Balchowsky, H., Van Belle, D., Ding, W., Fan, C., Mohan, R.S., Simões-Lopes, P.C., Bastida, R., Meyer, A., Stanhope, M.J., Milinkovitch, M.C., 2000. Independent adaptation to riverine habitats allowed survival of ancient cetacean lineages. Proc. Natl. Acad. Sci. 97, 11343–7.

Chung, Y., Ané, C., 2011. Comparing two Bayesian methods for gene tree/species tree reconstruction: Simulations with incomplete lineage sorting and horizontal gene transfer. Syst. Biol. 60, 261–275.

Cocks, A.H., 1887. The fin whale fishery of 1886 on the Lapland coast. Zoologist 11, 207–222.

Consortium, T.H.G., 2012. Butterfly genome reveals promiscuous exchange of mimicry adaptations among species. Nature 487, 94–98.

Corl, A., Ellegren, H., 2013. Sampling strategies for species trees: The effects on phylogenetic inference of the number of genes, number of individuals, and whether loci are mitochondrial, sex-linked, or autosomal. Mol. Phylogenet. Evol. 67, 358–366.

Crossman, C.A., Barrett-lennard, L.G., Taylor, E.B., 2014. Population structure and intergeneric hybridization in harbour porpoises *Phocoena phocoena* in British Columbia , Canada. Endanger. Species Res. 26, 1–12.

Crossman, C.A., Taylor, E.B., Barrett-Lennard, L.G., 2016. Hybridization in the Cetacea: Widespread occurrence and associated morphological, behavioral, and ecological factors. Ecol. Evol. 1293-1303. doi:10.1002/ece3.1913

Cummings, M.P., Otto, S.P., Wakeley, J., 1995. Sampling properties of DNA sequence data in phylogenetic analysis. Mol. Biol. Evol. 12, 814–822.

Cunha, H. a., Moraes, L.C., Medeiros, B. V., Lailson-Brito, J., da Silva, V.M.F., Solé-Cava, A.M., Schrago, C.G., 2011. Phylogenetic status and timescale for the diversification of *Steno* and *Sotalia* dolphins. PLoS One 6, 1–7. doi:10.1371/journal.pone.0028297

Darriba, D., Taboada, G.L., Doallo, R., Posada, D., 2012. jModelTest 2: More models, new heuristics and parallel computing. Nat. Methods 9, 772.

Dobzhansky, T., 1940. Speciation as a stage in evolutionary divergence. Am. Nat. 74, 312–321.

Dohl, T.P., Norris, K.S., Kang, I., 1974. A porpoise hybrid: *Tursiops* x *Steno*. J. Mammal. 55, 217–221.

Donoghue, M.J., Doyle, J. a, Gauthier, J., Kluge, a G., Rowe, T., 1989. The importance of fossils in phylogeny reconstruction. Annu. Rev. Ecol. Syst. 20, 431–460.

Doroshenko, N. V, 1970. A whale with features of fin whale and blue whale. Tinro 70, 255–257.

Duffield, D.A., 1998. Examples of captive hybridisation and a genetic point of view. Page 421 in Evans, P.G.H. and Parsons, E.C.M. (Eds), in: World Marine Mammal Science Conference. Vol. 12, Monaco. p. 421.

Felsenstein, J., 1985. Confidence limits on phylogenies: An approach using the bootstrap. Evolution 39, 783–791.

Fish, F.E., Nicastro, A.J., Weihs, D., 2006. Dynamics of the aerial maneuvers of spinner dolphins. J. Exp. Biol. 209, 590–598.

Fisher-Reid, M.C., Wiens, J., 2011. What are the consequences of combining nuclear and mitochondrial data for phylogenetic analysis? Lessons from Plethodon salamanders and 13 other vertebrate clades. Bmc Evol. Biol. 11, 300.

Fitzpatrick, B.M., 2004. Rates of evolution of hybrid inviability in birds and mammals. Evolution 58, 1865–1870.

Frantzis, A., Herzing, D.L., 2002. Mixed-species associations of striped dolphins (*Stenella coeruleoalba*), short-beaked common dolphins (*Delphinus delphis*), and Risso's dolphins (*Grampus griseus*) in the Gulf of Corinth (Greece , Mediterranean Sea). Aquat. Conserv. Mar. Freshw. Ecosyst. 28, 188–197.

Fraser, F.C., 1940. Three anomalous dolphins from Blacksod Bay, Ireland. Proceeding R. Irish Acad. B Biol. Geol. Chem. Sci. 45, 413–455.

Funk, D.J., Omland, K.E., 2003. Species-level paraphyly and polyphyly: Frequency, causes, and consequences, with insights from animal mitochondrial DNA. Annu. Rev. Ecol. Evol. Syst. 34, 397–423.

Gatesy, J., Amato, G., Norell, M., DeSalle, R., Hayashi, C., 2003. Combined support for wholesale taxic atavism in gavialine crocodylians. Syst. Biol. 52, 403–422.

Gatesy, J., Geisler, J.H., Chang, J., Buell, C., Berta, A., Meredith, R.W., Springer, M.S., McGowen, M.R., 2013. A phylogenetic blueprint for a modern whale. Mol. Phylogenet. Evol. 66, 479–506.

Gatesy, J. and Springer, M.S., 2014. Phylogenetic analysis at deep timescales: Unreliable gene trees, bypassed hidden support, and the coalescence/concatalescence conundrum. Mol. Phylogenet. Evol. 80, 231-266.

Gauthier, J., Kluge, A.G., Rowe, T., 1988. Amniote phylogeny and the importance of fossils. Cladistics 4, 105–209.

Geisler, J.H., McGowen, M.R., Yang, G., Gatesy, J., 2011. A supermatrix analysis of genomic, morphological, and paleontological data from crown Cetacea. BMC Evol. Biol. 11, 112. doi:10.1186/1471-2148-11-112

Gibson, M.L., Geisler, J.H., 2009. A new Pliocene dolphin (Cetacea: Pontoporiidae), from the Lee Creek Mine, North Carolina. J. Vertebr. Paleontol. 29, 966–971.

Glover, K. a, Kanda, N., Haug, T., Pastene, L. a, Øien, N., Seliussen, B.B., Sørvik, A.G.E., Skaug, H.J., 2013. Hybrids between common and Antarctic minke whales are fertile and can back-cross. BMC Genet. 14, 25. doi:10.1186/1471-2156-14-25

Glover, K.A., Kanda, N., Haug, T., Pastene, L.A., Oien, N., Goto, M., Seliussen, B.B., Skaug, H.J., 2010. Migration of Antarctic minke whales to the Arctic. PLoS One 5, e15197. doi:10.1371/journal.pone.0015197

Goujon, M., McWilliam, H., Li, W., Valentin, F., Squizzato, S., Paern, J., Lopez, R., 2010. A new bioinformatics analysis tools framework at EMBL-EBI. Nucleic Acids Res. 38, W695–9. doi:10.1093/nar/gkq313

Hailer, F., Kutschera, V.E., Hallstrom, B.M., Klassert, D., Fain, S.R., Leonard, J. a., Arnason, U., Janke, a., 2012. Nuclear genomic sequences reveal that polar bears are an old and distinct bear lineage. Science. 336, 344–347.

Harlin-Cognato, A.D., Honeycutt, R.L., 2006. Multi-locus phylogeny of dolphins in the subfamily Lissodelphininae: character synergy improves phylogenetic resolution. BMC Evol. Biol. 6, 87. doi:10.1186/1471-2148-6-87

Harrison, R.G., 1989a. Animal mitochondrial DNA as a genetic marker in population and evolutionary biology. Trends Ecol. Evol. 4, 6–11.

Hassanin, A., Delsuc, F., Ropiquet, A., Hammer, C., van Vuuren, B.J., Matthee, C., Ruiz-Garcia, M., Catzeflis, F., Areskoug, V., Nguyen, T.T. and Couloux, A., 2012. Pattern and timing of diversification of Cetartiodactyla (Mammalia, Laurasiatheria), as revealed by a comprehensive analysis of mitochondrial genomes. Comptes rendus biologies, 335, 32-50.

Heide-Jorgensen, M.P., Reeves, R.R., 1993. Description of an anomalous monodontid skull from West Greenland: A possible hybrid? Mar. Mammal Sci. 9, 258–268.

Heinzelmann, L., Chagastelles, P.C., Danilewicz, D., Chies, J. a B., Andrades-Miranda, J., 2009. The karyotype of franciscana dolphin (*Pontoporia blainvillei*). J. Hered. 100, 119–122.

Hermansen, J.S., Sæther, S. a., Elgvin, T.O., Borge, T., Hjelle, E., Sætre, G.P., 2011. Hybrid speciation in sparrows I: Phenotypic intermediacy, genetic admixture and barriers to gene flow. Mol. Ecol. 20, 3812–3822.

Herzing, D., Johnson, C., 1997. Interspecific interactions between Atlantic spotted dolphins (*Stenella frontalis)* and bottlenose dolphins (*Tursiops truncatus)* in the Bahamas, 1985–1995. Aquat. Mamm. 23.2, 85-99.

Herzing, D.L., Elliser, C.R., 2013. Directionality of sexual activities during mixed-species encounters between Atlantic spotted dolphins (*Stenella frontalis*) and bottlenose dolphins (*Tursiops truncatus*). Int. J. Comp. Psychol. 26, 124–134.

Herzing, D.L., Moewe, K., Brunnick, B.J., 2003. Interspecies interactions between Atlantic spotted dolphins, *Stenella frontalis* and bottlenose dolphins, *Tursiops truncatus*, on Great Bahama Bank, Bahamas. Aquat. Mamm. 29.3, 335-341.

Hodgins, N.K., Dolman, S.J., Weir, C.R., 2014. Potential hybridism between free-ranging Risso's dolphins (*Grampus griseus)* and bottlenose dolphins (*Tursiops truncatus*) off north-east Lewis (Hebrides, UK). Mar. Biodivers. Rec. 7, 1–7.

Hudson, R.R., 1990. Gene genealogies and the coalescent process. Ox. Surv. Evol. Biol. 7, 1–44.

Huson, D.H., Bryant, D., 2006. Application of phylogenetic networks in evolutionary studies. Mol. Biol. Evol. 23, 254–267.

Jackson, J. a., Baker, C.S., Vant, M., Steel, D.J., Medrano-González, L., Palumbi, S.R., 2009. Big and slow: Phylogenetic estimates of molecular evolution in baleen whales (Suborder Mysticeti). Mol. Biol. Evol. 26, 2427–2440.

Jefferson, T.A., 2002. Rough-toothed dolphin *Steno bredanensis*. In: Perrin, W.,Würsig, B., Thewissen, J.G.M. (Eds.), Encyclopedia of Marine Mammals. Academic Press, New York, pp. 310–314.

Kingston, S.E., Adams, L.D., Rosel, P.E., 2009. Testing mitochondrial sequences and anonymous nuclear markers for phylogeny reconstruction in a rapidly radiating group: molecular systematics of the Delphininae (Cetacea: Odontoceti: Delphinidae). BMC Evol. Biol. 9, 245. doi:10.1186/1471-2148-9-245

Kluge, A.G., 1989. A Concern for evidence and a phylogenetic hypothesis of relationships among Epicrates (Boidae, Serpentes). Syst. Zool. 38, 7–25.

Koito, T., Kubokawa, K., Tanabe, S., Miyazaki, N., 2010. Phylogenetic analyses in cetacean species of the family Delphinidae using a short wavelength sensitive opsin gene sequence. Fish. Sci. 76, 571–576.

Kulemzina, A.I., Trifonov, V. a., Perelman, P.L., Rubtsova, N. V., Volobuev, V., Ferguson-Smith, M. a., Stanyon, R., Yang, F., Graphodatsky, A.S., 2009. Cross-species chromosome painting in Cetartiodactyla: Reconstructing the karyotype evolution in key phylogenetic lineages. Chromosom. Res. 17, 419–436.

Kutschera, V.E., Bidon, T., Hailer, F., Rodi, J.L., Fain, S.R., Janke, A., 2014. Bears in a forest of gene trees: Phylogenetic inference is complicated by incomplete lineage sorting and gene flow. Mol. Biol. Evol. 31, 2004–2017.

Lanfear, R., Calcott, B., Ho, S.Y.W., Guindon, S., 2012. PartitionFinder: Combined selection of partitioning schemes and substitution models for phylogenetic analyses. Mol. Biol. Evol. 29, 1695–1701.

Lanier, H.C., Huang, H., Knowles, L.L., 2014. How low can you go? The effects of mutation rate on the accuracy of species-tree estimation. Mol. Phylogenet. Evol. 70, 112–119.

Larget, B.R., Kotha, S.K., Dewey, C.N., Ané, C., 2010. BUCKy: gene tree/species tree reconciliation with Bayesian concordance analysis. Bioinformatics 26, 2910–1.

Larkin, M.A., Blackshields, G., Brown, N.P., Chenna, R., McGettigan, P.A., McWilliam, H., Valentin, F., Wallace, I.M., Wilm, A., Lopez, R., Thompson, J.D., Gibson, T.J., Higgins, D.G., 2007. Clustal W and Clustal X version 2.0. Bioinformatics 23, 2947–8.

Larsen, P. a, Marchán-Rivadeneira, M.R., Baker, R.J., 2010. Natural hybridization generates mammalian lineage with species characteristics. Proc. Natl. Acad. Sci. U. S. A. 107, 11447–11452.

Leaché, A.D., Harris, R.B., Rannala, B., Yang, Z., 2014. The influence of gene flow on species tree estimation: A simulation study. Syst. Biol. 63, 17–30.

LeDuc, R.G., Perrin, W.F., Dizon, a E., 1999. Phylogenetic relationships among the delphinid cetaceans based on full cytochrome B sequences. Mar. Mammal Sci. 15, 619–648.

Maddison, W.P., 1997. Gene trees in species trees. Syst. Biol. 46, 523–536.

Mallet, J., 2007. Hybrid speciation. Nature 446, 279–283.

Mallet, J., 2005. Hybridization as an invasion of the genome. Trends Ecol. Evol. 20, 229–237.

Marshall, D., Simon, C., Buckley, T., 2006. Accurate branch length estimation in partitioned Bayesian analyses requires accommodation of among-partition rate variation and attention to branch length priors. Syst. Biol. 55, 993–1003.

Martien, K.K., Baird, R.W., Hedrick, N.M., Gorgone, A.M., Thieleking, J.L., Mcsweeney, D.J., Robertson, K.M., Webster, D.L., 2012. Population structure of island-associated dolphins: Evidence from mitochondrial and microsatellite markers for common bottlenose dolphins (*Tursiops truncatus*) around the main Hawaiian Islands. Mar. Mammal Sci. 28, 208–232.

Mavárez, J., Linares, M., 2008. Homoploid hybrid speciation in animals. Mol. Ecol. 17, 4181–4185.

May-Collado, L., Agnarsson, I., 2006. Cytochrome b and Bayesian inference of whale phylogeny. Mol. Phylogenet. Evol. 38, 344–354.

Mayr, E., 1942. Systematics and the origin of species, from the viewpoint of a zoologist. Harvard University Press.

McGowen, M.R., 2011. Toward the resolution of an explosive radiation-A multilocus phylogeny of oceanic dolphins (Delphinidae). Mol. Phylogenet. Evol. 60, 345–357.

McGowen, M.R., Clark, C., Gatesy, J., 2008. The vestigial olfactory receptor subgenome of odontocete whales: Phylogenetic congruence between gene-tree reconciliation and supermatrix methods. Syst. Biol. 57, 574–590.

McGowen, M.R., Montgomery, S.H., Clark, C., Gatesy, J., 2011. Phylogeny and adaptive evolution of the brain-development gene microcephalin (MCPH1) in cetaceans. BMC Evol. Biol. 11, 98. doi:10.1186/1471-2148-11-98

McGowen, M.R., Spaulding, M., Gatesy, J., 2009. Divergence date estimation and a comprehensive molecular tree of extant cetaceans. Mol. Phylogenet. Evol. 53, 891–906.

McGuire, J. a., Linkem, C.W., Koo, M.S., Hutchison, D.W., Lappin, a. K., Orange, D.I., Lemos-Espinal, J., Riddle, B.R., Jaeger, J.R., 2007. Mitochondrial introgression and incomplete lineage sorting through space and time: Phylogenetics of crotaphytid lizards. Evolution. 61, 2879–2897.

Messenger, S.L., McGuire, J.A., 1998. Morphology, molecules, and the phylogenetics of cetaceans. Syst. Biol. 47, 90–124.

Miller, M.A., Pfeiffer, W., Schwartz, T., 2010. Creating the CIPRES science gateway for inference of large phylogenetic trees, in: Gateway Computing Environments Workshop (GCE). New Orleans, pp. 1–8.

Miralles, L., Lens, S., Rodríguez-Folgar, A., Carrillo, M., Martín, V., Mikkelsen, B., Garcia-Vazquez, E., 2013. Interspecific introgression in cetaceans: DNA markers reveal post-F1 status of a pilot whale. PLoS One 8, e69511. doi:10.1371/journal.pone.0069511

Mirarab, S., Reaz, R., Bayzid, M.S., Zimmermann, T., Swenson, M.S., Warnow, T., 2014. ASTRAL: genome-scale coalescent-based species tree estimation. Bioinformatics 30, i541–i548.

Mirarab, S., Warnow, T., 2015. ASTRAL-II: coalescent-based species tree estimation with many hundreds of taxa and thousands of genes. Bioinformatics 31, i44–i52.

Moore, W.S., 1995. Inferring phylogenies from mtDNA variation: Mitochondrial gene trees versus nuclear gene trees. Evolution. 49, 718–726.

Muizon, C., 1984. Les vertebres fossiles de la Formation Pisco (Perou) II: Les Odontocetes (Cetacea, Mammalia) du Pliocene inferieur de Sud-Sacaco. Inst. Fr. d'Etudes Andin. Ed. Rech. sur les Civilizations Mem. 50, 1–188.

Murakami, M., Shimada, C., Hikida, Y., Soeda, Y., 2014a. *Eodelphinus kabatensis* , a replacement name for *Eodelphis kabatensis* (Cetacea: Delphinoidea: Delphinidae). J. Vertebr. Paleontol. 34, 1261–1261.

Murakami, M., Shimada, C., Hikida, Y., Soeda, Y., Hirano, H., 2014b. *Eodelphis kabatensis*, a new name for the oldest true dolphin *Stenella kabatensis* Horikawa, 1977 (Cetacea, Odontoceti, Delphinidae), from the upper Miocene of Japan, and the phylogeny and paleobiogeography of Delphinoidea. J. Vertebr. Paleontol. 34, 491–511.

Nabholz, B., Glémin, S., Galtier, N., 2008. Strong variations of mitochondrial mutation rate across mammals - The longevity hypothesis. Mol. Biol. Evol. 25, 120–130.

Nadeau, N., Whibley, A., Jones, R., Davey, J., Dasmahapatra, K., Baxter, S., Quail, M., Joron, M., Ffrench-Constant, R., Blaxter, M., Mallet, J., Jiggins, C., 2012. Genomic islands of divergence in hybridizing Heliconius butterflies identified by large-scale targeted sequencing. Philos. Trans. R. Soc. Lond. B. Biol. Sci. 367, 343–353.

Nakhleh, L., 2013. Computational approaches to species phylogeny inference and gene tree reconciliation. Trends Ecol. Evol. 28, 719–728.

Nice, C.C., Gompert, Z., Fordyce, J. a., Forister, M.L., Lucas, L.K., Buerkle, C.A., 2013. Hybrid speciation and independent evolution in lineages of alpine butterflies. Evolution. 67, 1055–1068.

Nishida, S., Goto, M., Pastene, L. a, Kanda, N., Koike, H., 2007. Phylogenetic relationships among cetaceans revealed by Y-chromosome sequences. Zoolog. Sci. 24, 723–732.

Nishiwaki, M., Tobayama, T., 1982. Morphological study on the hybrid between *Tursiops* and *Psuedorca*. Sci. Reports Whale Res. Inst. Tokyo 34, 109–121.

Nixon, K., and Carpenter, J.M., 1996. On simultaneous analysis. Cladistics 12, 221–241.

Nylander, J. a a, Wilgenbusch, J.C., Warren, D.L., Swofford, D.L., 2008. AWTY (are we there yet?): A system for graphical exploration of MCMC convergence in Bayesian phylogenetics. Bioinformatics 24, 581–583.

O'Leary, M.A., Gatesy, J., 2008. Impact of increased character sampling on the phylogeny of Cetartiodactyla (Mammalia): Combined analysis including fossils. Cladistics 24, 397–442.

Onbe, K., Nishida, S., Sone, E., Kanda, N., Goto, M., Pastene, L. a, Tanabe, S., Koike, H., 2007. Sequence variation in the Tbx4 gene in marine mammals. Zoolog. Sci. 24, 449–464.

Pause, K.C., Bonde, R.K., McGuire, P.M., Zori, R.T., Gray, B. a, 2006. G-banded karyotype and ideogram for the North Atlantic right whale (*Eubalaena glacialis*). J. Hered. 97, 303–306.

Perrin, W.F., Mitchell, E.D., Mead, J.G., Caldwell, D.K., van Bree, P.J.H., 1981. *Stenella clymene*, a rediscovered tropical dolphin of the Atlantic. J. Mammal. 62, 583–598.

Perrin, W.F., Rosel, P.E., Cipriano, F., 2013. How to contend with paraphyly in the taxonomy of the delphinine cetaceans? Mar. Mammal Sci. 29, 567–588.

Psarakos, S., Herzing, D.L., Marten, K., 2003. Mixed-species associations between pantropical spotted dolphins (*Stenella attenuata*) and hawaiian spinner dolphins (*Stenella longirostris*) off Oahu, Hawaii. Aquat. Mamm. 29, 390–395.

Rannala, B. and Yang, Z., 2003. Bayes estimation of species divergence times and ancestral population sizes using DNA sequences from multiple loci. Genetics, 164, 1645-1656.

Regier, J.C., Zwick, A., Cummings, M.P., Kawahara, A.Y., Cho, S., Weller, S., Roe, A., Baixeras, J., Brown, J.W., Parr, C., Davis, D.R., Epstein, M., Hallwachs, W., Hausmann, A., Janzen, D.H., Kitching, I.J., Solis, M.A., Yen, S.-H., Bazinet, A.L., Mitter, C., 2009. Toward reconstructing the evolution of advanced moths and butterflies (Lepidoptera: Ditrysia): an initial molecular study. BMC Evol. Biol. 9, 280. doi:10.1186/1471-2148-9-280

Reyes, J.C., 1996. A possible case of hybridism in wild dolphins. Mar. Mammal Sci. 12, 301–307.

Rhymer, J.M., Simberloff, D., 1996. Extinction by hybridization and introgression. Annu. Rev. Ecol. Syst. 27, 83–109.

Robinson, D.F., Foulds, L.R., 1981. Comparison of phylogenetic trees. Math. Biosci. 53, 131–147.

Ronquist, F., Deans, A.R., 2010. Bayesian phylogenetics and its influence on insect systematics. Annu. Rev. Entomol. 55, 189–206.

Ronquist, F., Teslenko, M., van der Mark, P., Ayres, D.L., Darling, A., Höhna, S., Larget, B., Liu, L., Suchard, M.A., Huelsenbeck, J.P., 2012. MrBayes 3.2: efficient Bayesian phylogenetic inference and model choice across a large model space. Syst. Biol. 61, 539–42.

Rubinoff, D., Holland, B.S., 2005. Between two extremes: mitochondrial DNA is neither the panacea nor the nemesis of phylogenetic and taxonomic inference. Syst. Biol. 54, 952–961.

Schumer, M., Rosenthal, G.G., Andolfatto, P., 2014. How common is homoploid hybrid speciation? Evolution 68, 1553–1560.

Shimura, E., Numachi, K., Sezaki, K., Hirosaki, Y., Watabe, S., Hashimoto, K., 1986. Biochemical evidence of hybrid formation between the two species of dolphin *Tursiops truncatus* and *Grampus griseus*. Bull. Japanese Soc. Sci. Fish. 52, 725–730.

Shurtliff, Q.R., 2013. Mammalian hybrid zones: A review. Mamm. Rev. 43, 1–21.

Silva-Jr., J.M., Silva, F.J.L., Sazima, I., 2005. Two presumed interspecific hybrids in the genus *Stenella* (Delphinidae) in the tropical west Atlantic. Aquat. Mamm. 31, 467–471.

Song, Y., Endepols, S., Klemann, N., Richter, D., Matuschka, F.R., Shih, C.H., Nachman, M.W., Kohn, M.H., 2011. Adaptive introgression of anticoagulant rodent poison resistance by hybridization between old world mice. Curr. Biol. 21, 1296–1301.

Sorenson, M.D., Franzosa, E.A., 2007. TreeRot, version 3. Boston University, Boston, MA.

Spilliaert, R., Vikingsson, G., Arnason, U., Palsdottir, A., Sigurjonsson, J., Arnason, A., 1991. Species hybridization between a female blue whale (*Balaenoptera musculus*) and a male fin whale (*B. physalus*): molecular and morphological documentation. J. Hered. 82, 269–274.

Springer, M.S., Gatesy, J., 2016. The gene tree delusion. Mol. Phylogenet. Evol. 94, 1–33.

Stamatakis, A., 2014. RAxML version 8: A tool for phylogenetic analysis and post-analysis of large phylogenies. Bioinformatics 30, 1312–1313.

Stanhope, M.J., Smith, M.R., Waddell, V.G., Porter, C.A., Shivji, M.S., Goodman, M., 1996. Mammalian evolution and the interphotoreceptor retinoid binding protein (IRBP) gene: Convincing evidence for several superordinal clades. J. Mol. Evol. 43, 83–92.

Steeman, M.E., Hebsgaard, M.B., Fordyce, R.E., Ho, S.Y.W., Rabosky, D.L., Nielsen, R., Rahbek, C., Glenner, H., Sørensen, M. V., Willerslev, E., 2009. Radiation of extant cetaceans driven by restructuring of the oceans. Syst. Biol. 58, 573–585.

Stensland, E., Angerbjorn, A., Berggren, P., 2003. Mixed species groups in mammals. Mamm. Rev. 33, 205–223.

Sugiura, N., 1978. Further analysts of the data by akaike' s information criterion and the finite corrections. Commun. Stat. - Theory Methods 7, 13–26.

Sukumaran, J., Holder, M.T., 2010. DendroPy: a Python library for phylogenetic computing. Bioinformatics 26, 1569–71.

Sullivan, J., Demboski, J.R., Bell, K.C., Hird, S., Sarver, B., Reid, N., Good, J.M., 2014. Divergence with gene flow within the recent chipmunk radiation (*Tamias*). Heredity. 113, 185–194.

Swofford, D.L., 2002. PAUP*. Phylogenetic Analysis Using Parsimony (* and Other Methods). Sinauer Associates, Sunderland, MA.

Sylvestre, J.-P., Tasaka, S., 1985. On the intergeneric hybrids in cetaceans. Aquat. Mamm.11.3,101-108.

Toews, D.P.L., Brelsford, A., 2012. The biogeography of mitochondrial and nuclear discordance in animals. Mol. Ecol. 21, 3907–3930.

Vilstrup, J.T., Ho, S.Y., Foote, A.D., Morin, P. a, Kreb, D., Krützen, M., Parra, G.J., Robertson, K.M., de Stephanis, R., Verborgh, P., Willerslev, E., Orlando, L., Gilbert, M.T.P., 2011. Mitogenomic phylogenetic analyses of the Delphinidae with an emphasis on the Globicephalinae. BMC Evol. Biol. 11, 65. doi:10.1186/1471-2148-11-65

Vollmer, N.L., Viricel, A., Wilcox, L., Katherine Moore, M., Rosel, P.E., 2011. The occurrence of mtDNA heteroplasmy in multiple cetacean species. Curr. Genet. 57, 115–131.

Vrana, P.B., 2007. Genomic imprinting as a mechanism of reproductive isolation in mammals. J. Mammal. 88, 5–23.

Whitfield, J.B., Cameron, S. a, Huson, D.H., Steel, M. a, 2008. Filtered Z-closure supernetworks for extracting and visualizing recurrent signal from incongruent gene trees. Syst. Biol. 57, 939–947.

Wiens, J.J., Kuczynski, C. a., Townsend, T., Reeder, T.W., Mulcahy, D.G., Sites, J.W., 2010. Combining phylogenomics and fossils in higher-level squamate reptile phylogeny: Molecular data change the placement of fossil taxa. Syst. Biol. 59, 674–688.

Wilgenbusch, J.C., Warren, D.L., Swofford, D.L., 2004. AWTY: A system for graphical exploration of MCMC convergence in Bayesian phylogenetic inference. doi:http://ceb.csit.fsu.edu/awty

Willis, P.M., Crespi, B.J., Dill, L.M., Baird, R.W., Hanson, M.B., 2004. Natural hybridization between Dall's porpoises (*Phocoenoides dalli*) and harbour porpoises (*Phocoena phocoena*). Can. J. Zool. Can. Zool. 82, 828–834.

Xi, Z., Liu, L., Davis, C.C., 2015. The impact of missing data on species tree estimation. Mol. Biol. Evol. 33, 838-860.

Xiong, Y., Brandley, M.C., Xu, S., Zhou, K., Yang, G., 2009. Seven new dolphin mitochondrial genomes and a time-calibrated phylogeny of whales. BMC Evol. Biol. 9, 20. doi:10.1186/1471-2148-9-20

Yan, J., Zhou, K., Yang, G., 2005. Molecular phylogenetics of "river dolphins" and the baiji mitochondrial genome. Mol. Phylogenet. Evol. 37, 743–750.

Yazdi, P., 2002. A possible hybrid between the dusky dolphin (*Lagenorhynchus obscurus*) and the southern right whale dolphin (*Lissodelphis peronii*). Aquat. Mamm. 28, 211–217.

Zeh, D.W., Zeh, J.A., 2000. Reproductive mode and speciation: the viviparity-drive conflict hypothesis. Bioessays 22, 938–946.

Zeh, J.A., Zeh, D.W., 2008. Viviparity-driven conflict: More to speciation than meets the fly. Ann. N. Y. Acad. Sci. 1133, 126–148.

Zhang, P., Han, J., Zhichuang, L., Chen, R., 2014. Molecular evidence of a captive-born intergeneric hybridization between bottlenose and Risso's dolphins: *Tursiops truncatus* x *Grampus griseus*. Aquat. Mamm. 40, 5–8.

Zornetzer, H.R., Duffield, D. a, 2003. Captive-born bottlenose dolphin x common dolphin (*Tursiops truncatus* x *Delphinus capensis)* intergeneric hybrids. Can. J. Zool. 81, 1755–1762. doi:10.1139/z03-150

Zwickl, D.J., 2006. Genetic algorithm approaches for the phylogenetic analysis of large biological sequence datasets under the maximum likelihood criterion. Ph.D. dissertation, The University of Texas at Austin.

Table 1. Parsimony constraint results for individual genes. Genes are denoted by gene symbol. Sequence type is listed as: I=intron, E=exon, P=pseudogene, UTR=untranslated region, mt=mitochondrial sequence. Number of characters (No. Characters), and the number of parsimony informative characters (Pars. Inform. Characters) are given for each gene. Branch support, defined as the difference in the number of steps for a topology lacking a clade of interest minus the number of steps for a topology containing a clade of interest, for four different constraints is abbreviated Con. 1, Con. 2, Con. 3, and Con. 4. Constraints are as follows: 1. *Steno* + *Sotalia*, 2. *Steno* + *Sotalia* + Delphininae, 3. *Steno* + Globicephalinae, 4. *Steno* + *Orcaella* + Globicephalinae.

Gene	Type	No. Characters	Pars. inform. Characters	Con.1	Con. 2	Con. 3	Con. 4
ACTA2	I	1207	59	-5	-5	0	0
AMBN	E	467	19	0	0	0	0
ATP7A	E	677	15	-1	-1	-1	-1
BTN1A1	I	670	17	0	0	0	-5
CAT	E, I	626	12	0	0	-2	-2
CHRNA1	E, I	368	15	-4	-2	-3	-3
CSN2	E	424	17	0	0	0	N/A
GBA	E, I	308	9	-1	-1	0	0
IFNA1	I	337	4	-1	0	0	0
RBP3	E	1101	45	-1	-3	-2	N/A

LALBA	E, I	1115	64	-5	-5	0	2
MAS1	E	772	17	-2	0	0	N/A
MC1R	E	1053	29	-3	-2	0	1
MCPH1	E, I	1224	60	-10	-1	-1	N/A
OPN1SW	P	1116	39	0	0	0	N/A
OR1I1	P	517	36	-6	-3	0	0
OR2AT1P	P	518	9	N/A	-2	0	N/A
OR6M1	P	514	10	N/A	0	-1	N/A
OR10AB1P	P	521	15	N/A	-5	0	N/A
OR10J1	P	515	7	N/A	-2	2	N/A
OR10J2P	P	518	5	N/A	0	0	N/A
OR13F1	P	520	3	N/A	0	0	N/A
OR13J1	P	510	2	N/A	0	0	N/A
PKDREJ	E	558	23	0	0	-1	N/A
PRM1	E, I, U	422	26	-1	-1	0	0

RAG1	E	811	36	-6	-7	1	N/A
SPTBN1	E, I	875	30	0	0	0	0
STAT5A	E, I	773	31	-8	-7	0	-5
TBX4	E	1339	24	-2	-2	0	0
TSHB	E, I	730	17	0	0	0	N/A
Yintrons	I	1248	38	-6	0	0	-1
MT-12s	mt	985	152	2	0	-7	-4
MT-16s	mt	1604	212	2	-3	-2	-6
MT-ND1	mt	958	280	2	0	-9	-10
MT-ND2	mt	1042	319	3	-3	-8	-11
MT-CO1	mt	1551	430	9	3	-20	-18
MT-CO2	mt	684	211	0	-2	-2	-5
MT-ATP8	mt	192	68	0	-1	-1	-3
MT-ATP6	mt	684	238	1	2	-10	-11
MT-CO3	mt	785	228	1	-5	-4	-5
MT-ND3	mt	346	118	-1	0	-6	-7

MT-ND4L	mt	297	94	1	-1	-7	-6
MT-ND4	mt	1379	419	8	-1	-19	-21
MT-ND5	mt	1825	593	1	-2	-14	-16
MT-ND6	mt	528	168	-7	-4	-2	-3
MT-CYB	mt	1140	362	2	0	-7	-10
MT-tRNAs	mt	1589	257	2	2	-9	-13

Table 2. Reported Occurrences of Hybridization in the Wild

Family	Species Involved	Method of Detection	Estimated Divergence* (million years)	Reported number of hybrids	Reference
Delphinidae	*T. truncatus* x *G. griseus*	Morphological	8.36 / 9.44	7	Fraser, (1940), Hodgins et al. (2014)
Delphinidae	*T. truncatus x T. aduncus*	Molecular	1.59 / 2.19	2	Martien et al. (2012)
Delphinidae	*D. capensis x L. obscurus*	Morphological	8.85 / 8.14	1	Reyes (1996)
Delphinidae	*S. frontalis* x *S. attenuata*	Molecular	1.94 / 3.63	4	Kingston et al. (2009)
Delphinidae	*S. frontalis x T. truncatus*	Morphological	1.94 / 3.63	1	Herzing et al. (2003)
Delphinidae	*S. longirostris* x *S. attenuata*	Morphological	3.51 / 4.36	1	Silva-Jr. et al. (2005)
Delphinidae	*S. longirostris x S. clymene*	Morphological	3.51 / 4.36	1	Silva-Jr. et al. (2005)

Delphinidae	*S. longirostris* x *S. coeruleoalba*	Molecular	3.51 / 4.36	*S. clymene*	Amaral et al. (2014)
Delphinidae	*O. heinsohni x S. chinensis*	Molecular	8.36 / 9.44	1+	Brown et al. (2014)
Delphinidae	*L. obscurus x L. peronii*	Morphological	4.32 / 5.26	1	Yazdi (2002)
Delphinidae	*G. macrorhynchus* x *G. melas*	Molecular	0.66 / 1.47	1	Miralles et al. (2013)
Phocoenidae	*P. phocoena x P. dalli*	Molecular	3.75 / 3.71	38+	Baird et al (1998), Willis et al (2004), Crossman et al (2014)
Monodontidae	*D. leucas x M. monoceros*	Morphological	6.28 / 5.47	1	Heide-Jørgensen and Reeves (1993)
Balaenopteridae	*B. physalus* x *B. musculus*	Morphological and Molecular	10 / 10-18	11+	Arnason et al. (1991, Bérubé and Aguilar (1998), Cocks (1887), Doroshenko (1970) Spilliaert et al. (1991)
Balaenopteridae	*B. acutorostrata* x *B. bonaerensis*	Molecular	4.92 / 5.28	2	Glover et al. (2013, 2010)

* Estimated divergence from McGowen et al. (2009)/ Steeman et al. (2009)

Table 3. Reported Occurrences of Hybridization in Captivity

Family	Species Involved	Method of Detection	Estimated Divergence* (million years)	Reported number of hybrids	Reference
Delphinidae	*T. truncatus* x *G. griseus*	Morphological and Molecular	8.36 / 9.44	14	Shimura et al. (1986), Sylvestre and Tasaka (1985), Zhang et al. (2014)
Delphinidae	*T. truncatus x D. delphis*	Morphological	2.18/3.63	2	Duffield (1998)
Delphinidae	*T. truncatus* x *D. capensis*	Morphological and Molecular	2.18/3.63	4	Zornetzer and Duffield, (2003)
Delphinidae	*T. truncatus x P. crassidens*	Morphological	8.36/7.51	6+	Duffield (1998); Nishiwaki and Tobayama (1982)
Delphinidae	*T. truncatus x Steno*	Morphological	8.36/7.51	1	Dohl et al. (1974)
Delphinidae	*T. truncatus x S. guianensis*	Morphological and Molecular	6.98/7.51	1	Caballero and Baker (2010)
Delphinidae	*T. truncatus x G. macrorhynchus*	Morphological	8.36/9.44	2	Duffield (1998)

* Estimated divergence from McGowen et al. (2009)/ Steeman et al. (2009)

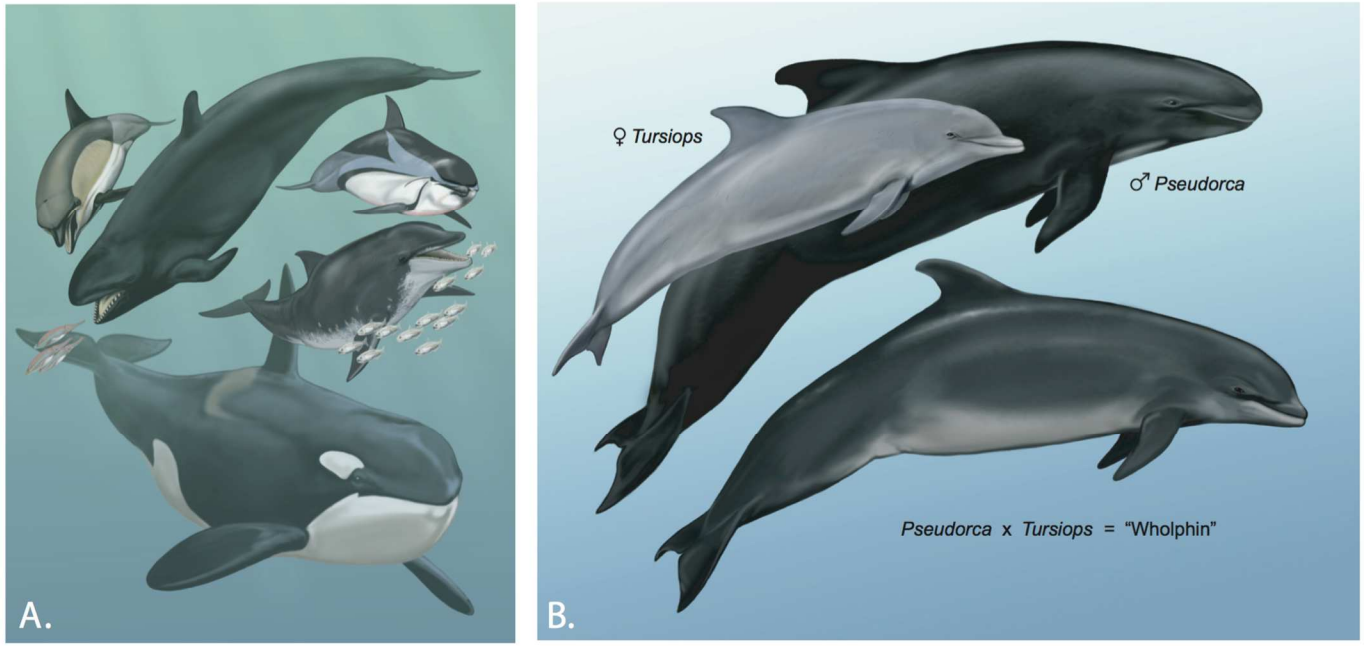

Figure 1. A.) Illustration of diversity in delphinid body forms and size for five different species: (clockwise starting from bottom) *Orcinus orca*, *Delphinus delphis*, *Pseudorca crassidens*, *Stenella coeruleoalba*, and *Steno bredanensis*. B.) Illustration of body forms and size differences for captive hybridization between the false killer whale, *Pseudorca crassidens*, and the bottlenose dolphin, *Tursiops truncatus*. The resultant viable and fertile hybrid is intermediate in form to both parental species. Artwork is by Carl Buell.

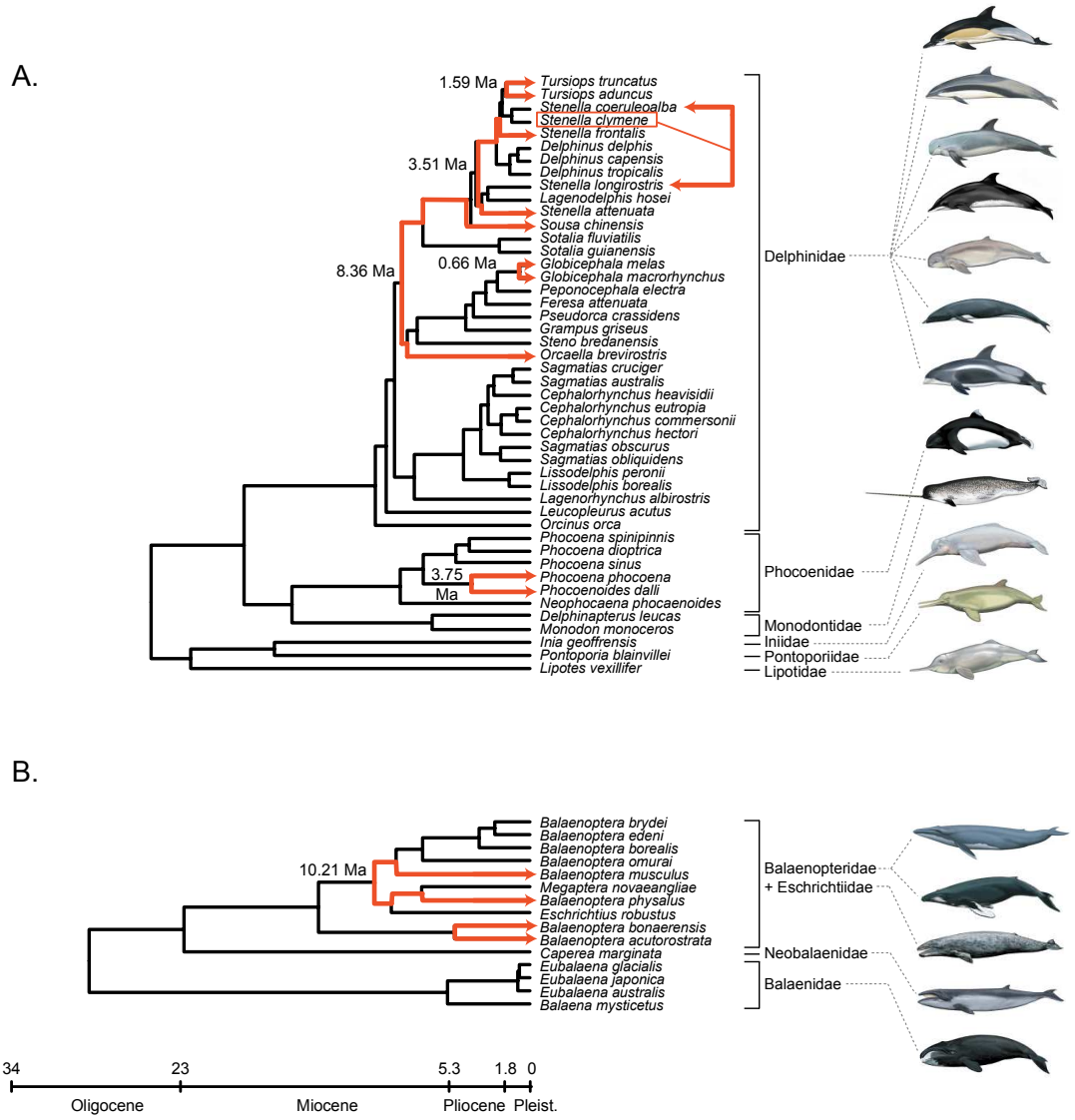

Figure 2. Bayesian phylogenetic hypotheses for A.) Delphinida, and B.) Mysticeti obtained from McGowen et al. (2009). All other cetacean clades have been removed for simplicity. Branch lengths are scaled to time. Hybridization events that have been documented with molecular evidence are denoted with orange lineages to the left of taxa names, and end with terminal arrows for hybridizing species. Divergence dates for hybridizing taxa are Ma (million years). Orange arrows to the right of *Stenella longirostris* and *Stenella coeruleoalba*, denote putative reticulation in which *Stenella clymene* originated from parental taxa *Stenella longirostris* and *Stenella coeruleoalba*

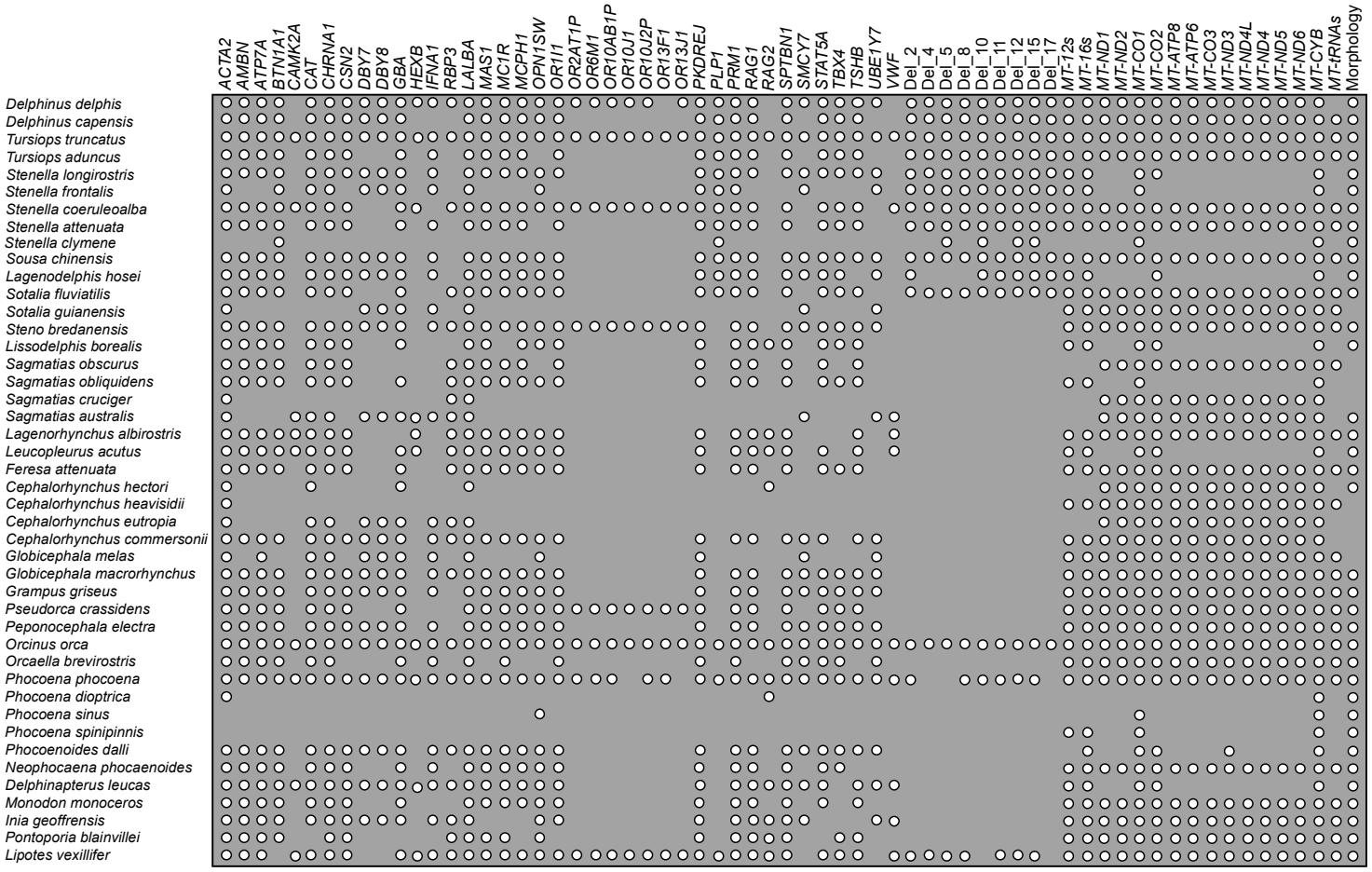

Figure 3. Taxonomic coverage for all datasets.

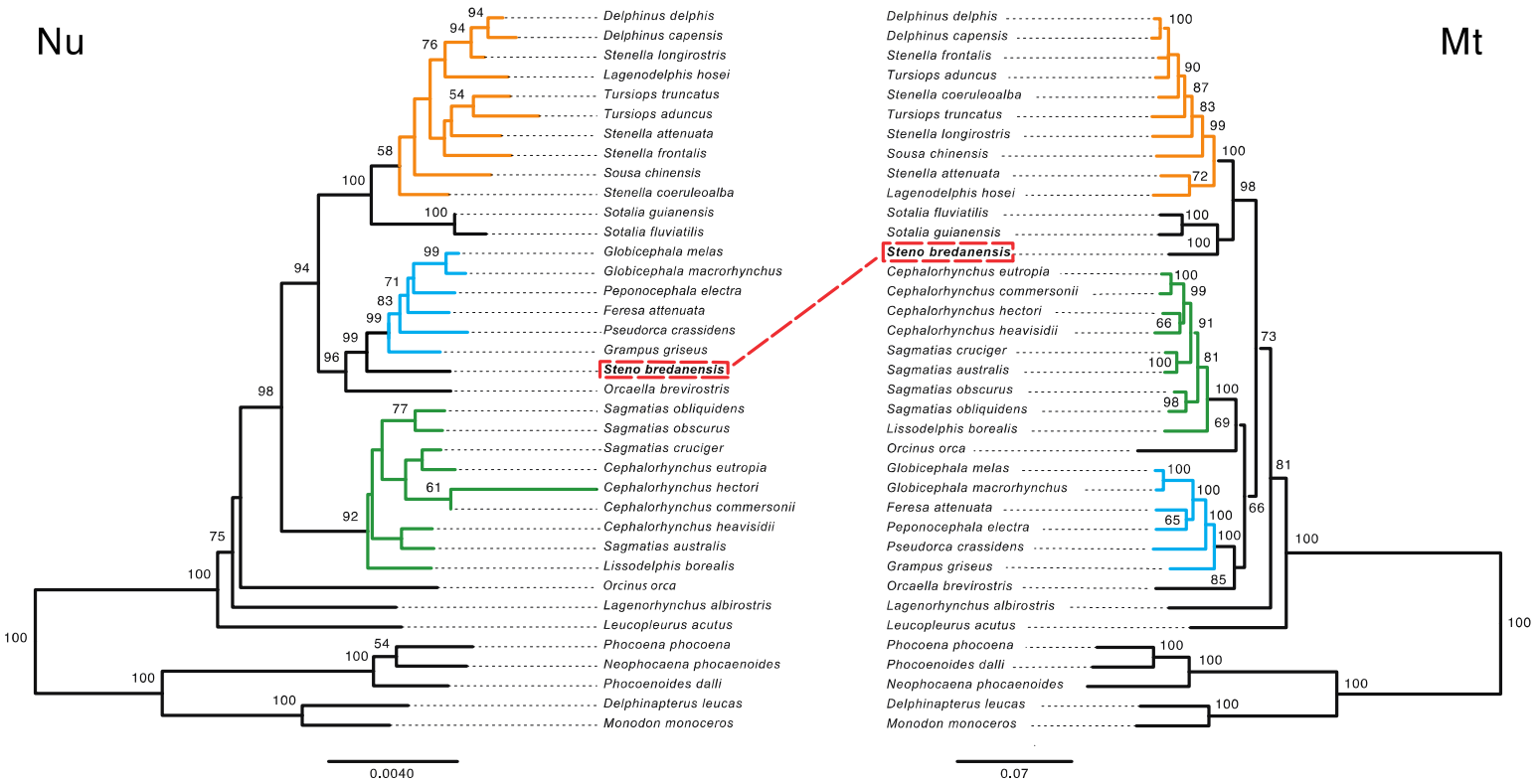

Figure 4. Nuclear (Nu; left) and mitochondrial (Mt; right) partitioned GARLI 2.1 maximum likelihood hypotheses. Delphinid subfamilies are colored as Delphininae: orange, Globicephalinae: blue, Lissodelphininae: green. Note that alternative placements of *S. bredanensis* are highly supported (≥ 99% BS: bootstrap support). Also note weakly supported phylogenetic incongruence for numerous other taxa, including *Orcinus*. Nodal support < 50% BS is not shown.

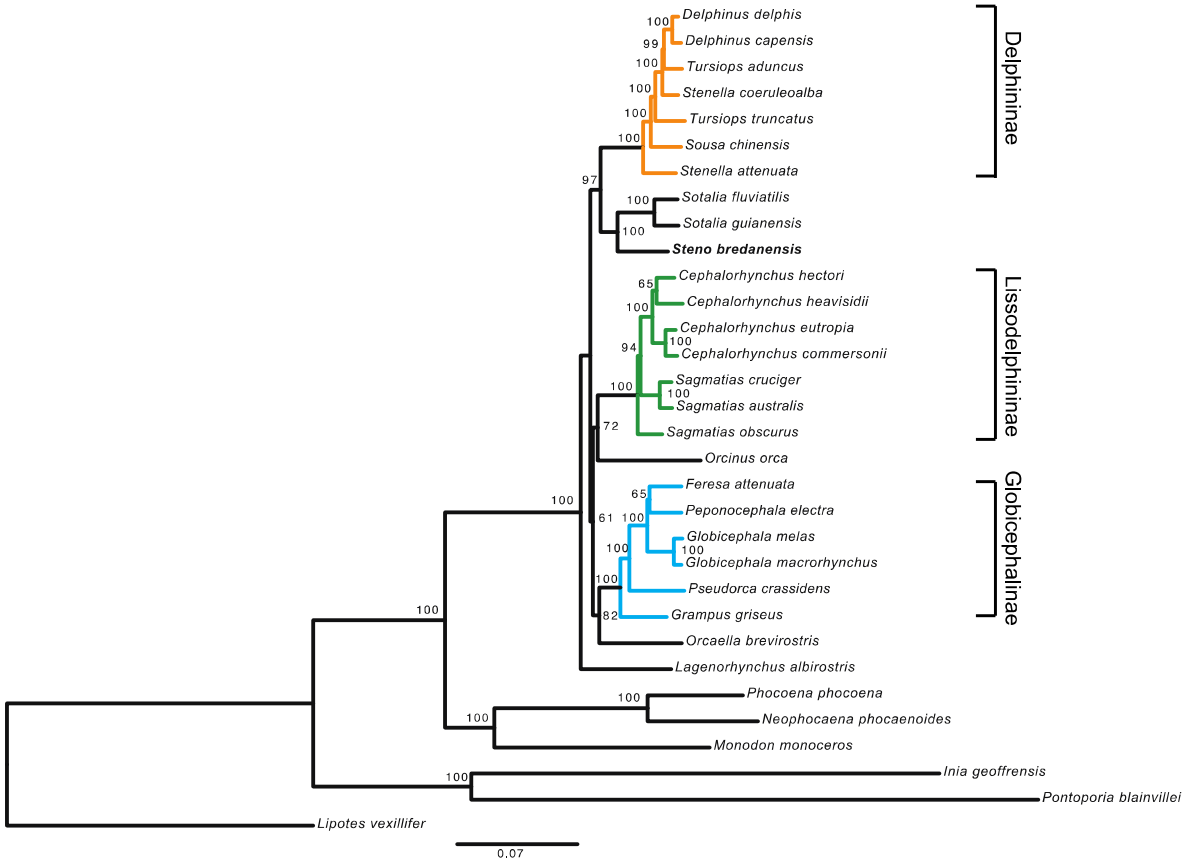

Figure 5. Partitioned mitogenome GARLI 2.1 maximum likelihood hypothesis. Sub-families are color coded as in Fig. 4. Nodal support < 50% BS is not shown.

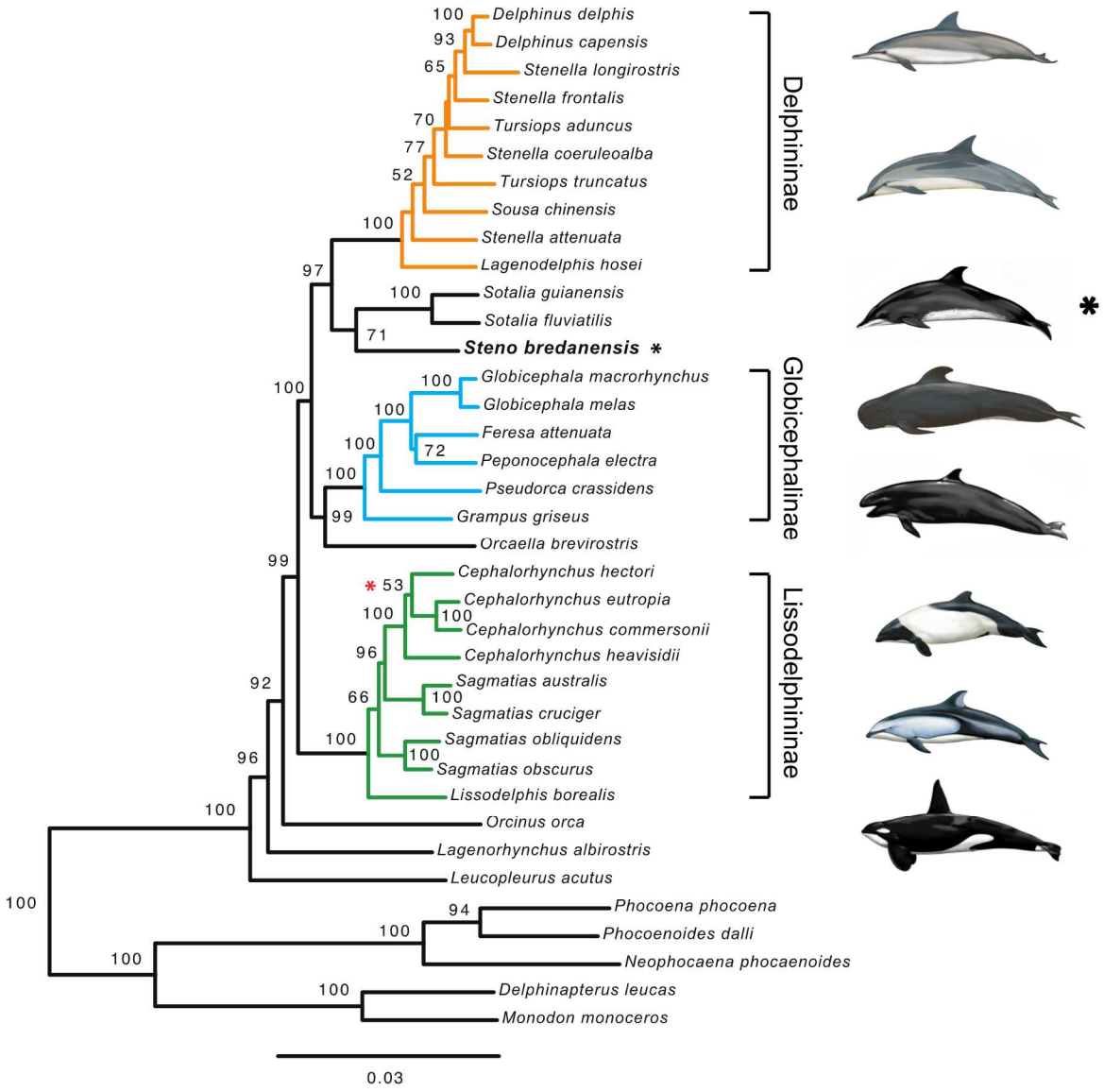

Figure 6. Combined nuclear + mitochondrial partitioned GARLI 2.1 maximum likelihood hypothesis. The red asterisk denotes a conflicting node between GARLI, RAxML, and PAUP* topologies (see text). The black asterisk denotes placement of *Steno*. Nodal support < 50% BS is not shown.

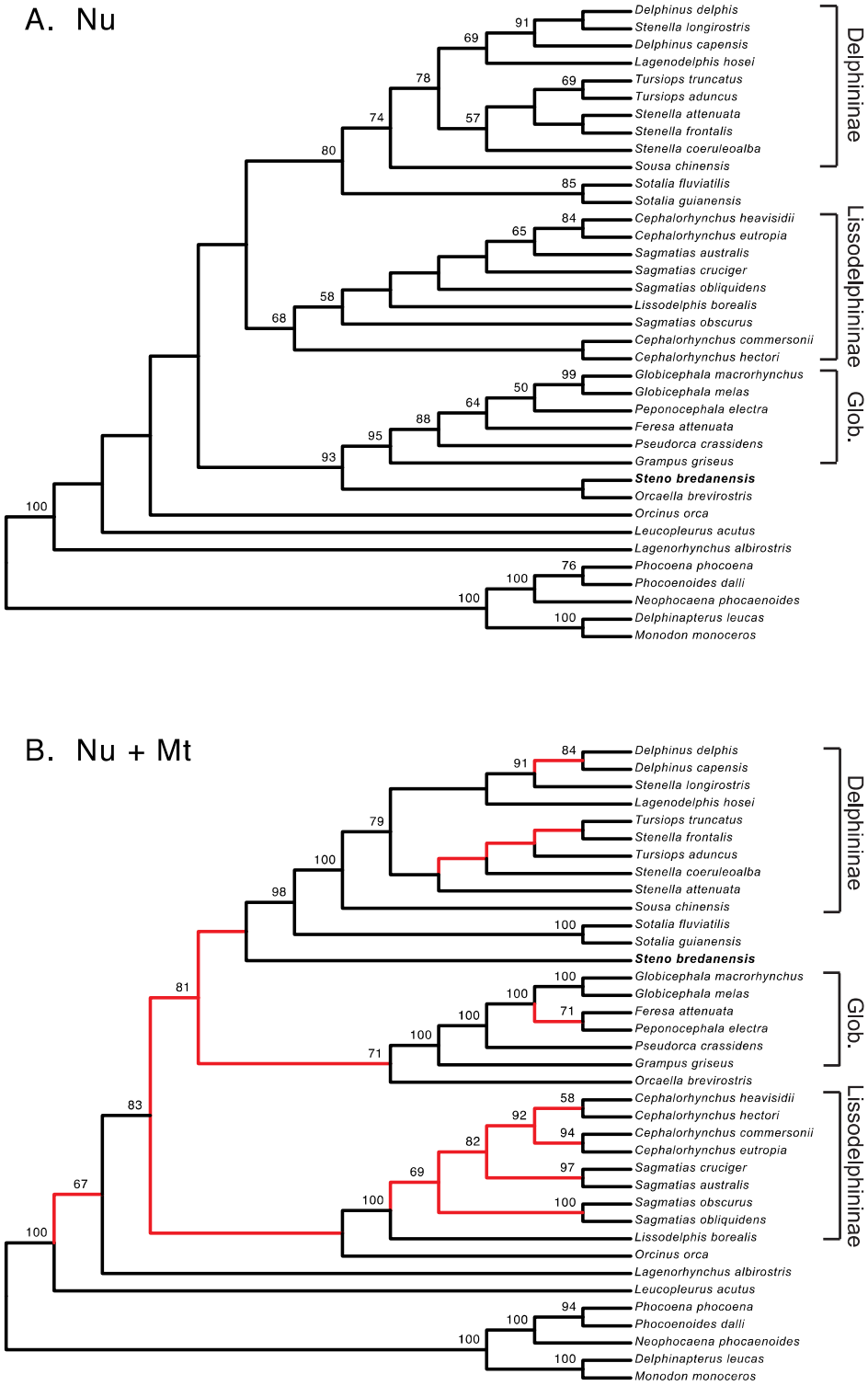
A. Nu
Delphininae
Lissodelphininae
Glob.
Delphinus delphis
Stenella longirostris
Delphinus capensis
Lagenodelphis hosei
Tursiops truncatus
Tursiops aduncus
Stenella attenuata
Stenella frontalis
Stenella coeruleoalba
Sousa chinensis
Sotalia fluviatilis
Sotalia guianensis
Cephalorhynchus heavisidii
Cephalorhynchus eutropia
Sagmatias australis
Sagmatias cruciger
Sagmatias obliquidens
Lissodelphis borealis
Sagmatias obscurus
Cephalorhynchus commersonii
Cephalorhynchus hectori
Globicephala macrorhynchus
Globicephala melas
Peponocephala electra
Feresa attenuata
Pseudorca crassidens
Grampus griseus
Steno bredanensis
Orcaella brevirostris
Orcinus orca
Leucopleurus acutus
Lagenorhynchus albirostris
Phocoena phocoena
Phocoenoides dalli
Neophocaena phocaenoides
Delphinapterus leucas
Monodon monoceros
B. Nu + Mt
Delphininae
Glob.
Lissodelphininae
Delphinus delphis
Delphinus capensis
Stenella longirostris
Lagenodelphis hosei
Tursiops truncatus
Stenella frontalis
Tursiops aduncus
Stenella coeruleoalba
Stenella attenuata
Sousa chinensis
Sotalia fluviatilis
Sotalia guianensis
Steno bredanensis
Globicephala macrorhynchus
Globicephala melas
Feresa attenuata
Peponocephala electra
Pseudorca crassidens
Grampus griseus
Orcaella brevirostris
Cephalorhynchus heavisidii
Cephalorhynchus hectori
Cephalorhynchus commersonii
Cephalorhynchus eutropia
Sagmatias cruciger
Sagmatias australis
Sagmatias obscurus
Sagmatias obliquidens
Lissodelphis borealis
Orcinus orca
Lagenorhynchus albirostris
Leucopleurus acutus
Phocoena phocoena
Phocoenoides dalli
Neophocaena phocaenoides
Delphinapterus leucas
Monodon monoceros

Figure 7. ASTRAL II hypotheses obtained with A.) 31 nuclear gene trees as input data. B.) 31 nuclear gene trees + the mitochondrial tree. Red lineages denote clades not present in hypothesis A. Nodal support <50% BS is not shown.

A. ASTRAL 13 Nu

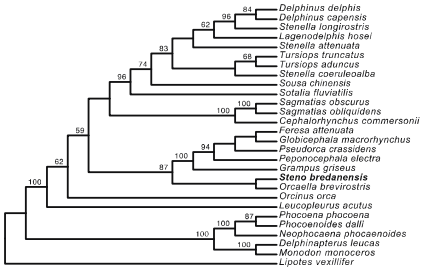

B. BUCKy 13 Nu

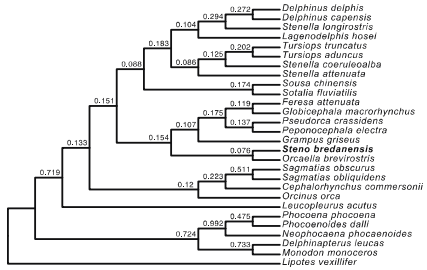

C. ASTRAL 13 Nu Bayes Trees

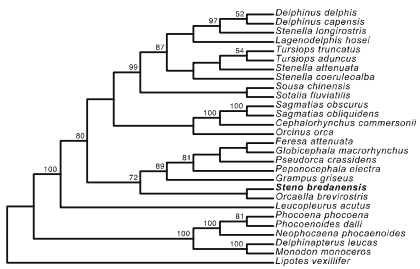

D. ASTRAL 13 Nu + Mt

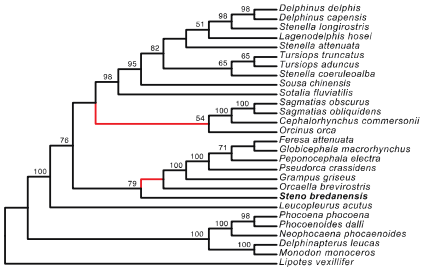

E. BUCKy 13 Nu + Mt

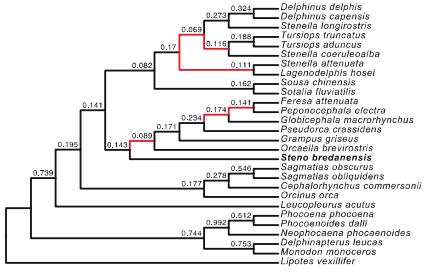

F. ASTRAL 13 Nu + Mt Bayes Trees

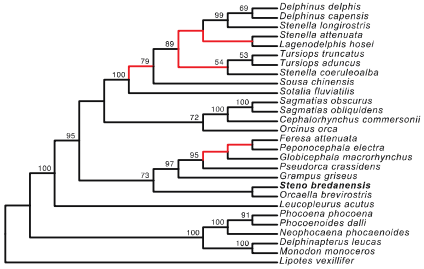

Splits Tree
Filtered Super Networks

(Showing only splits present in 5 or more gene trees)

G. 13 Nu

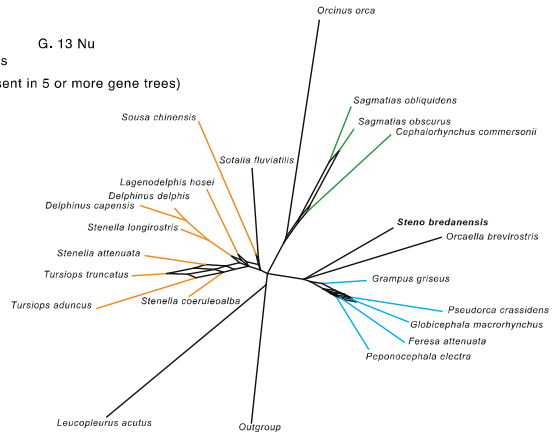

H. 13 Nu + Mt

Figure 8. ASTRAL II hypotheses obtained with optimal GARLI 2.1 maximum likelihood trees (A. & D.), BUCKy primary concordance topologies (B. & E.), and ASTRAL II hypotheses obtained with Bayesian consensus topologies (C. & F.). Red lineages in D., E., and F., represent clades not present in A., B., and C., respectively, that result by addition of the mitochondrial gene tree to 13 nuclear gene trees. Nodal support < 50% BS is not shown. Primary concordance factors are placed above nodes in BUCKy topologies (B. & E.). SplitsTree supernetworks are shown for 13 nuclear loci (G.) and for 13 nuclear loci plus mitochrondrial DNA(H.). Taxa represented in supernetworks are color coded as in Figs. 4-6. Tree filters were set to 5 for both supernetwork reconstructions (G. & H.).

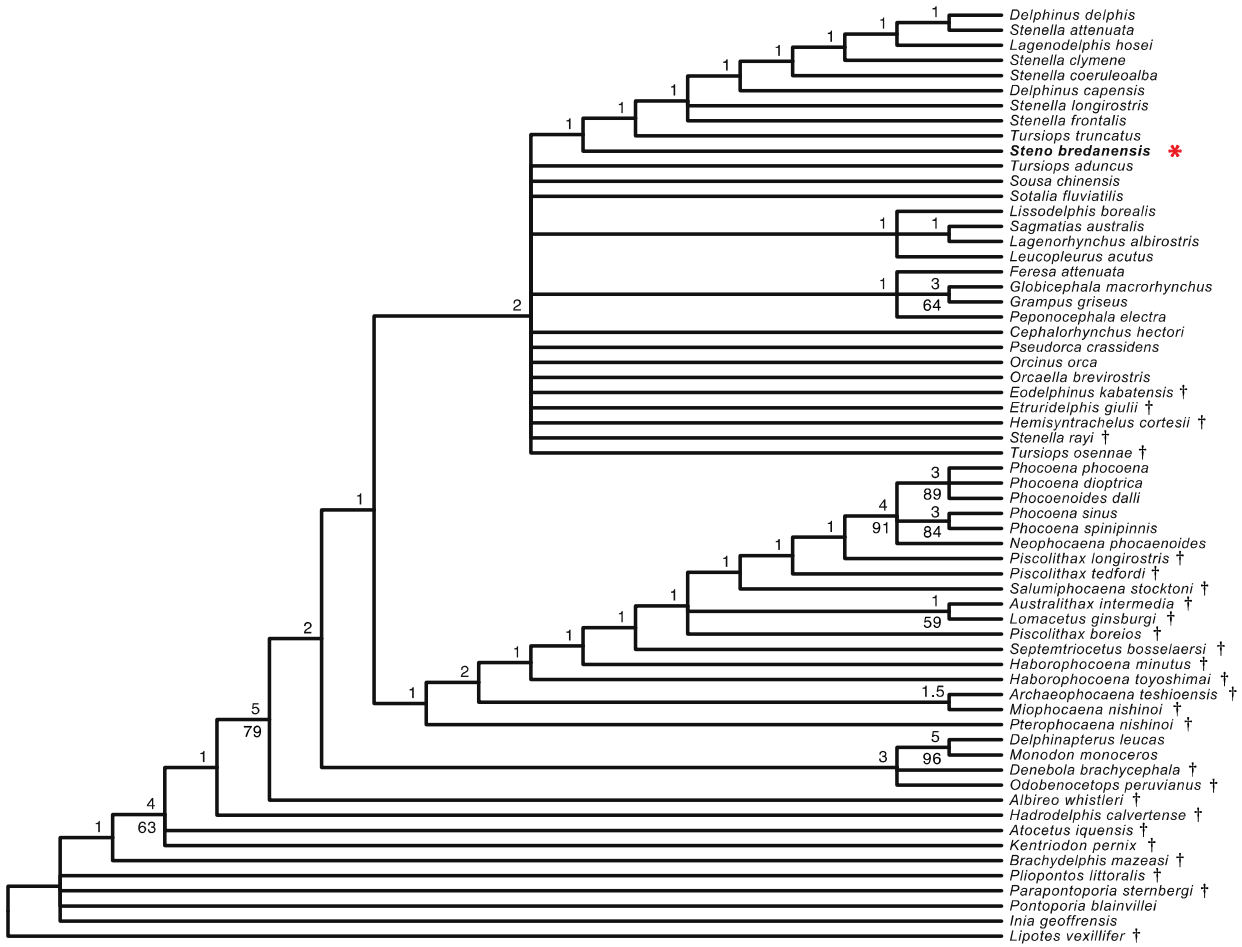

Figure 9. PAUP* strict consensus hypothesis for the morphology + fossils dataset. Numbers above nodes represent branch support values (Bremer support), whereas numbers below nodes represent bootstrap support. The red asterisk denotes placement of *Steno*. † denotes extinct taxa.

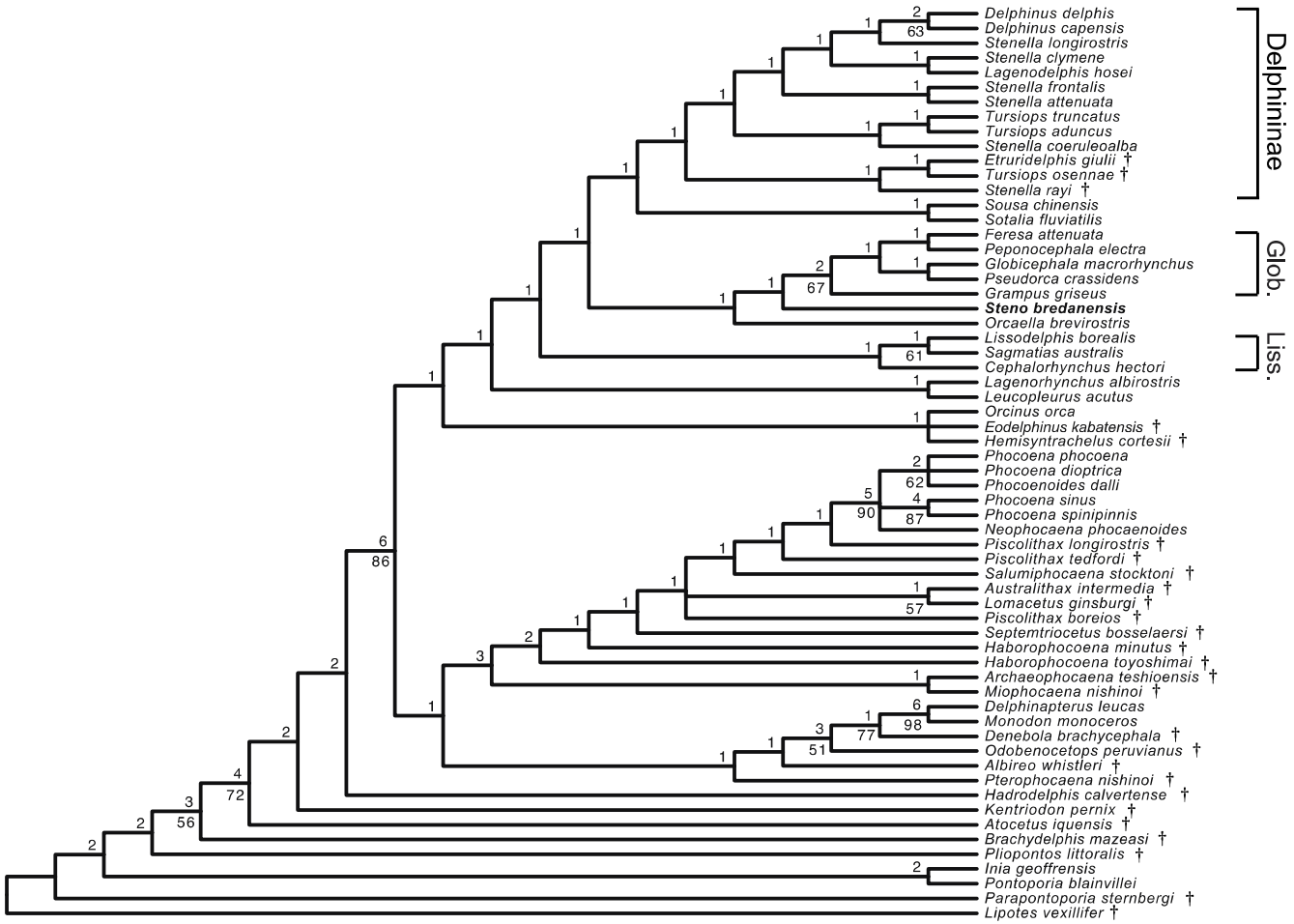

Figure 10. PAUP* consensus hypothesis for the nuclear DNA + fossils dataset. Numbers above nodes represent Bremer Support values, whereas numbers below nodes represent bootstrap support. Subfamilies Globicephalinae and Lissodelphininae are abbreviated as Glob. and Liss. respectively. † denotes extinct taxa.

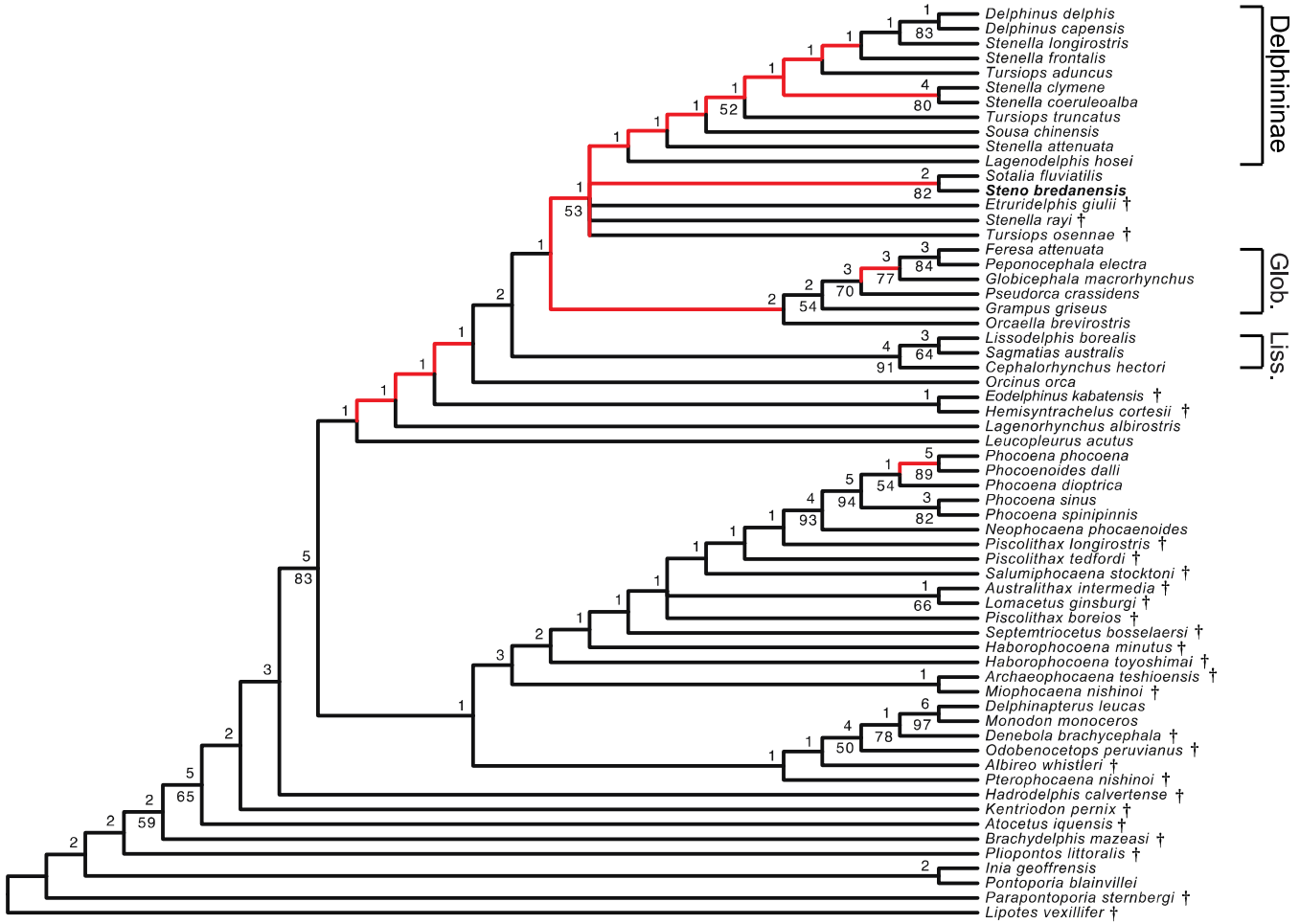

Figure 11. PAUP* total evidence consensus hypothesis (nuclear DNA + mitochondrial DNA + fossils). Numbers above nodes represent Bremer Support values, whereas numbers below nodes represent bootstrap support. Subfamilies Globicephalinae and Lissodelphininae are abbreviated as Glob. and Liss. respectively. † denotes extinct taxa.

APPENDIX A. Best-fit substitution models and partitioning schemes for molecular datasets. "G" refers to the gamma distribution of rate variation among sites and "I" refers to the proportion of invariant sites. The GTR+G model of sequence evolution was used for all RAxML analyses and partitioning schemes. The GTR+G+I model of sequence evolution was the best model found for unpartitioned nuclear and mitochondrial GARLI supermatrix analyses.

Nuclear Partitioning Scheme: GARLI

Subset	Best Model	Subset Partitions
1	TVM+G	DBY7, ACTA2
2	GTR+I+G	MAS1, OR6M1, LALBA
3	HKY+I	AMBN
4	HKY+I	ATP7A
5	K81uf+I+G	BTN1A1
6	TVM+I	CAT, DBY8, TSHB
7	TrNef+G	CHRNA1
8	TVM+G	CSN2
9	TVM+I	SMCY7
10	K80+I+G	PKDREJ, RAG1, UBE1Y7

11	TIM+I	GBA, TBX4
12	TVMef+I	IFNA1
13	TVM+I+G	RBP3, PRM1
14	TrN+G	MC1R, OR13J1
15	HKY+G	MCPH1
16	K81uf+G	OPN1SW, SPTBN1
17	TrN+G	OR1I1, OR2AT1P
18	HKY+I	STAT5A
19	TrN+I	OR10AB1P, OR10J1
20	K81uf	OR10J2P, OR13F1

Mitogenome Partitioning Scheme: GARLI

Subset	Best Model	Subset Partitions
1	GTR+I+G	12s, tRNA_1, tRNA_3
2	GTR+I+G	tRNA_12, tRNA_2, tRNA_5
3	HKY+I+G	tRNA_10, tRNA_4, tRNA_6, tRNA_7, tRNA_9
4	GTR+I+G	16s, tRNA_11, tRNA_8

5	TrN+I+G	ATP6_pos2
6	GTR+I+G	ATP6_pos3, COII_pos3, COI_pos3
7	GTR+I+G	ATP6_pos1, ND5_pos1
8	TrN+G	ATP8_pos1
9	GTR+I+G	ATP8_pos2, ND5_pos2
10	TrN+I+G	ATP8_pos3, ND4_pos1
11	GTR+I+G	COIII_pos1, COII_pos1, COI_pos1
12	HKY+I	COI_pos2
13	HKY+I+G	COIII_pos2, COII_pos2, Cytb_pos2, ND1_pos2, ND4L_pos2
14	TrN+I+G	COIII_pos3, ND4L_pos3
15	GTR+I+G	Cytb_pos1, ND1_pos1, ND3_pos1, ND4L_pos1, ND4_pos2
16	GTR+I+G	Cytb_pos3, ND1_pos3
17	GTR+I+G	ND2_pos1
18	GTR+I+G	ND2_pos2, ND3_pos2
19	TrN+G	ND2_pos3, ND3_pos3
20	GTR+I+G	ND4_pos3

21	TrN+I+G	ND5_pos3
22	GTR+G	ND6_pos1
23	HKY+G	ND6_pos2
24	GTR+G	ND6_pos3

Nuclear Partitioning Scheme: RAxML

Subset	Subset Partitions
1	ACTA2, DBY7
2	LALBA, MAS, OR6M1, OR10AB1P, OR10J1, OR10J2P, OR13F1
3	AMBN, MCPH1, PRM1
4	ATP7
5	BTN1A, CAT
6	CHRNA1, UBE1Y7, PKDREJ, RAG1
7	CSN2
8	DBY8, SMCY7, TSHB
9	GBA, TBX4

10	IFNA1
11	RBP3
12	MC1R, OR13J1
13	OPN1SW, SPTBN1, STAT5A
14	OR1I1, OR2AT1P

Mitogenome Partitioning Scheme: RAxML

Subset	Subset Partitions
1	12s, 16s, tRNA_1, tRNA_11, tRNA_8
2	tRNA_12, tRNA_2, tRNA_5
3	tRNA_10, tRNA_3, tRNA_4, tRNA_6, tRNA_7, tRNA_9
4	ATP6_pos2
5	ATP6_pos3, ATP8_pos3, COIII_pos3, ND1_pos3, ND4L_pos3, ND4_pos1
6	ATP6_pos1, ND5_pos1
7	ATP8_pos1, ATP8_pos2
8	COIII_pos1, COII_pos1, COI_pos1

9	COI_pos2
10	COII_pos3, COI_pos3
11	COIII_pos2, COII_pos2, Cytb_pos2, ND1_pos2, ND4L_pos2
12	Cytb_pos1, ND1_pos1, ND3_pos1, ND4L_pos1, ND4_pos2
13	Cytb_pos3, ND2_pos3, ND3_pos3
14	ND2_pos1
15	ND2_pos2, ND3_pos2
16	ND4_pos3
17	ND5_pos2
18	ND5_pos3
19	ND6_pos1
20	ND6_pos2
21	ND6_pos3

Individual Nuclear Loci: GARLI

Gene	Best Model
ACTA2	TPM2uf+G
AMBN	HKY+I
ATP7A	HKY
BTN1A1	TPM3uf+G
CAT	TPM1uf
CHRNA1	TrNef
CSN2	TPM3uf+G
GBA	TrN
IFNA1	TPM2+I
RBP3	HKY+G
LALBA	TIM2+I+G
MAS1	TIM2+G
MC1R	TrN
MCPH1	TPM2uf+I
OPN1SW	TPM1uf+G

OR1I1	TrN+G
OR2AT1P	TIM2
OR6M1	HKY+I
OR10AB1P	TrN+I
OR10J1	K80+G
OR10J2P	TPM3uf
OR13F1	TPM1uf
OR13J1	HKY
PKDREJ	K80+G
PRM1	TPM3uf+G
RAG1	TPM2+I
SPTBN1	TIM1+I
STAT5A	HKY+I
TBX4	TPM1uf+G
TSHB	TPM3uf+I

Yintrons Partitioning Scheme: GARLI

Subset	Best Model	Subset Partitions
1	HKY	DBY7, DBY8
2	HKY+I	SMCY7
3	SYM+I	UBE1Y7

Yintrons Partitioning Scheme: RAxML

Subset	Subset Partitions
1	DBY7, DBY8, SMCY7
2	UBE1Y7

APPENDIX B. Individual gene trees/consensus bootstrap trees for 30 nuclear loci and concatenated Yintrons. Topologies were recovered with PAUP*, GARLI, and RAxML.

Alpha-2-actin
(ACTA2)

PAUP* Parsimony

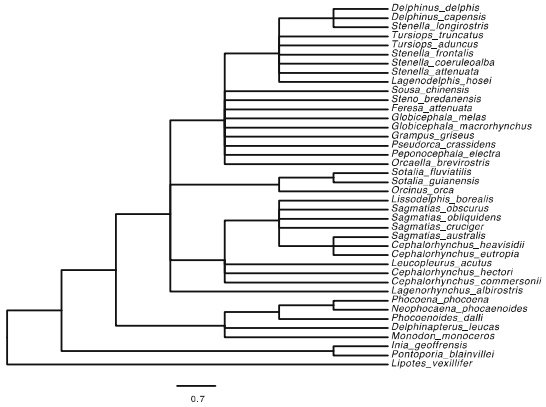

Garli ML

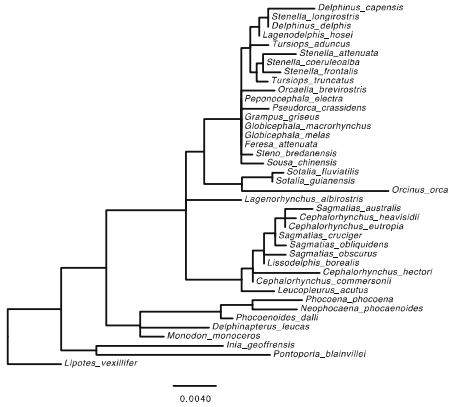

RAxML

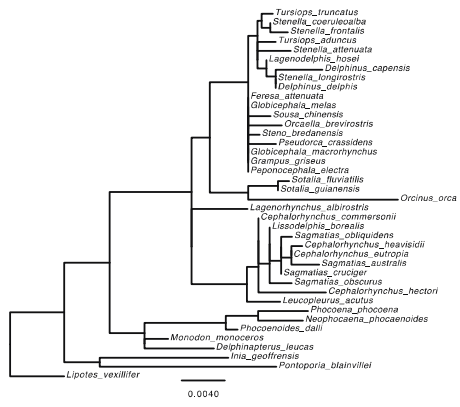

Bootstrap: PAUP* Parsimony

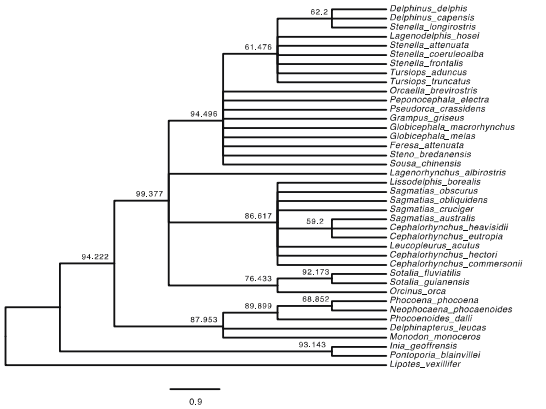

Bootstrap: Garli ML

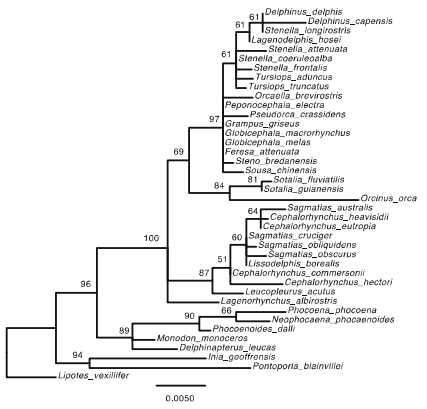

Bootstrap: RAxML

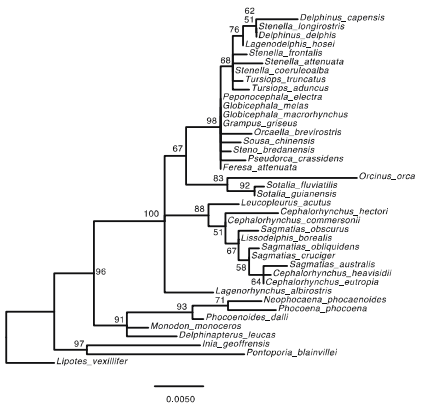

Ameloblastin (AMBN)

PAUP* Parsimony

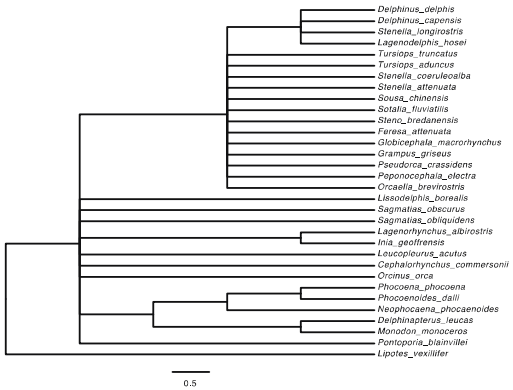

Garli ML

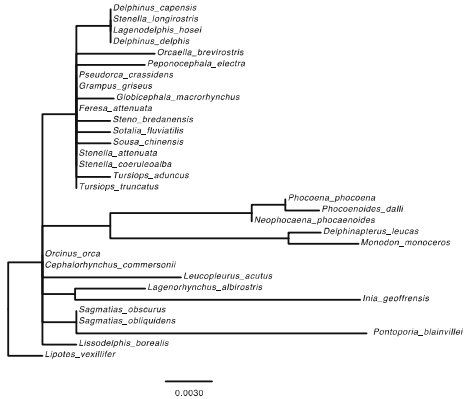

RAxML

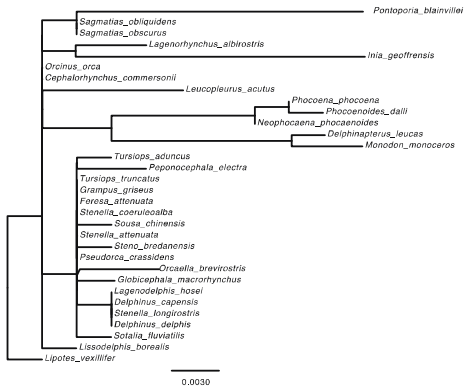

Bootstrap: PAUP* Parsimony

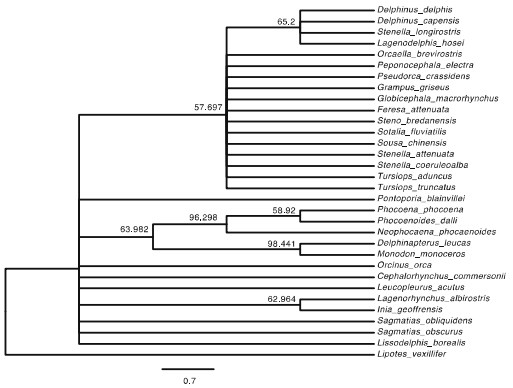

Bootstrap: Garli ML

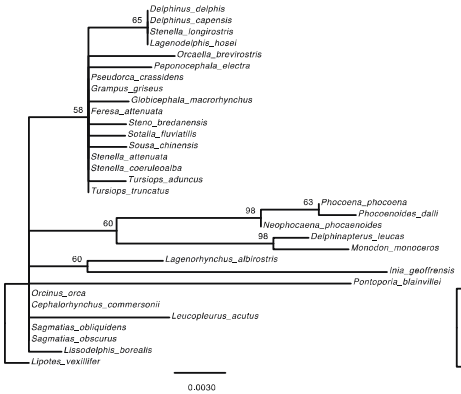

Bootstrap: RAxML

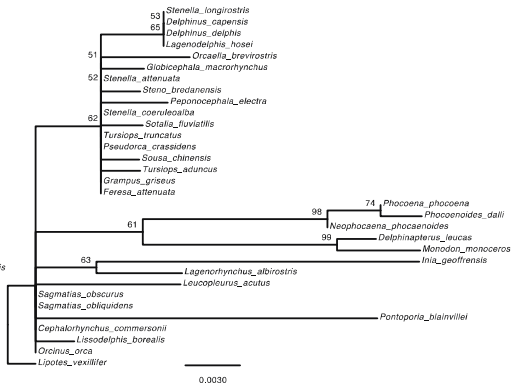

ATPase copper transporting alpha (ATP7A)

PAUP* Parsimony

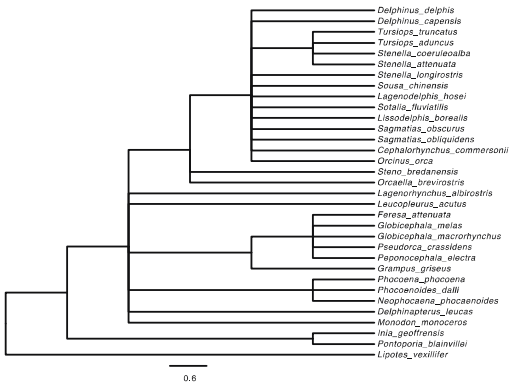

Garli ML

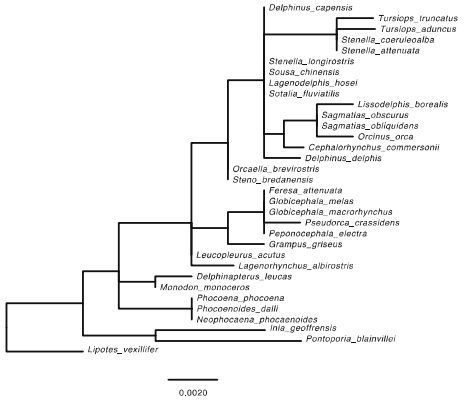

RAxML

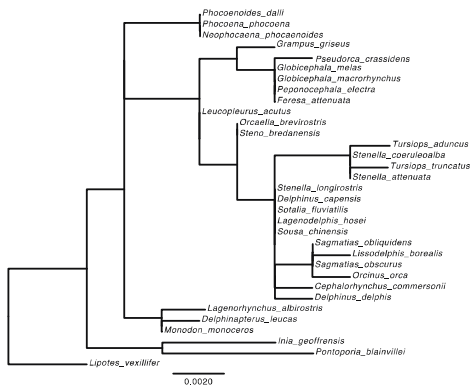

Bootstrap: PAUP* Parsimony

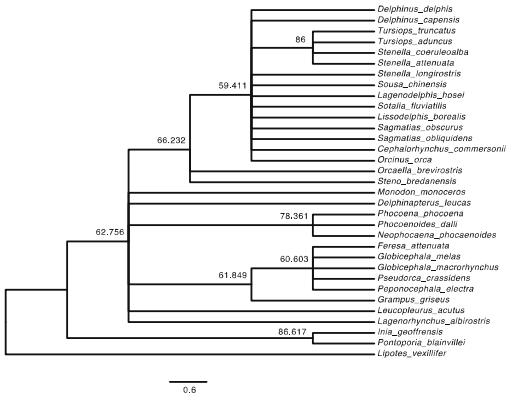

Bootstrap: Garli ML

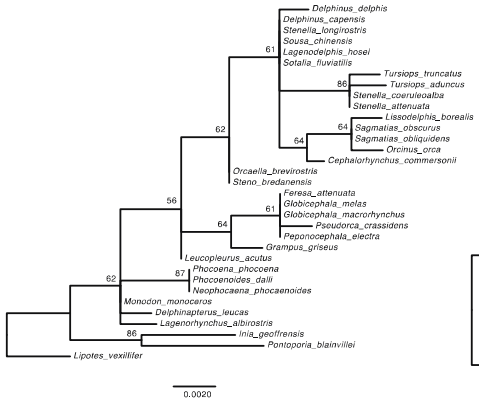

Bootstrap: RAxML

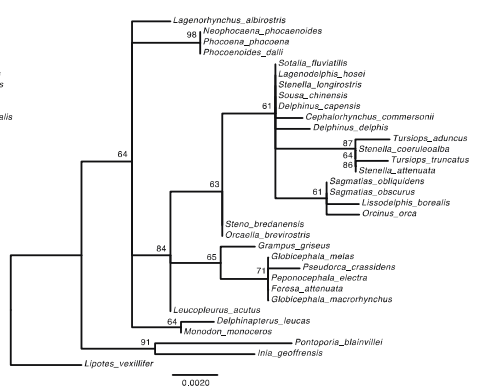

Butyrophilin 1A1
(BTN1A1)

PAUP* Parsimony

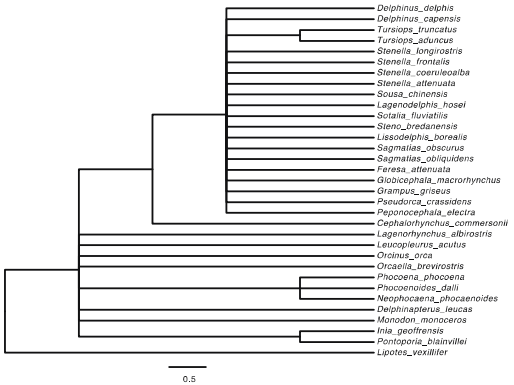

Garli ML

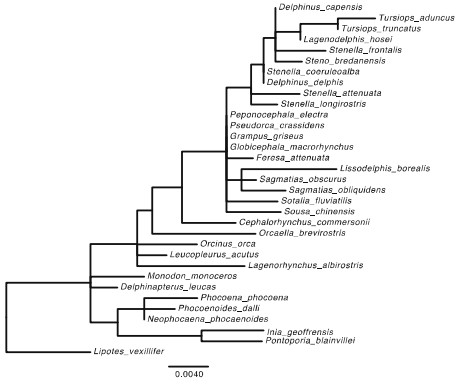

RAxML

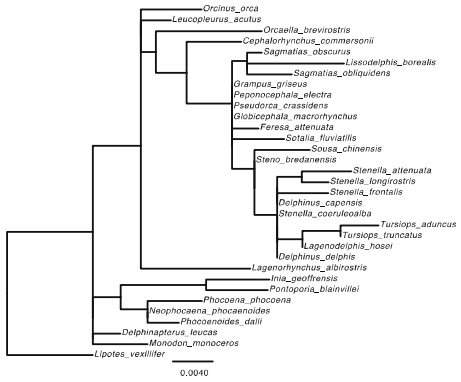

Bootstrap: PAUP* Parsimony

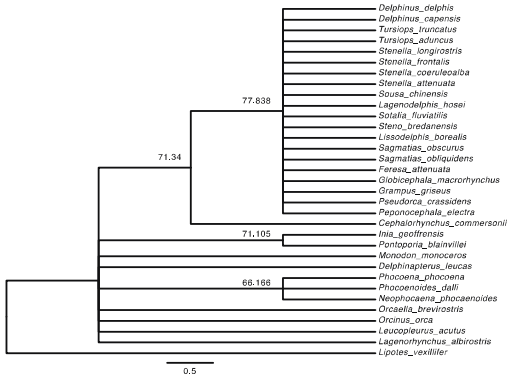

Bootstrap: Garli ML

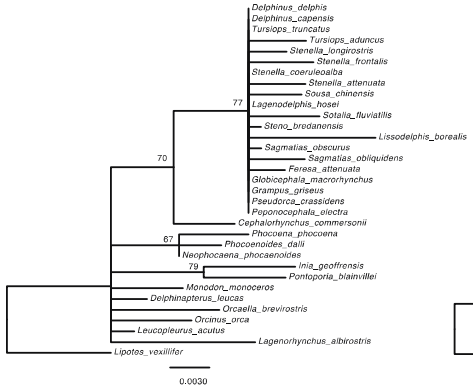

Bootstrap: RAxML

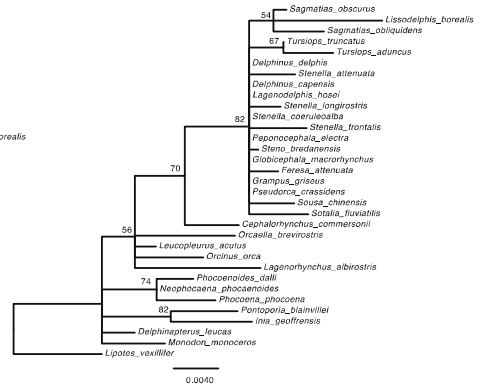

Catalase (CAT)

PAUP* Parsimony

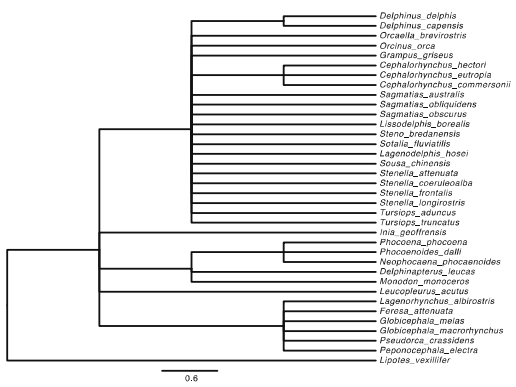

Garli ML

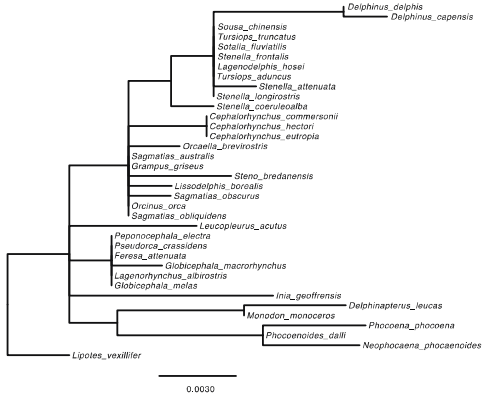

RAxML

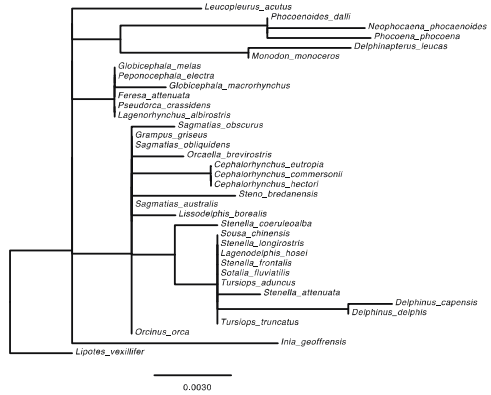

Bootstrap: PAUP* Parsimony

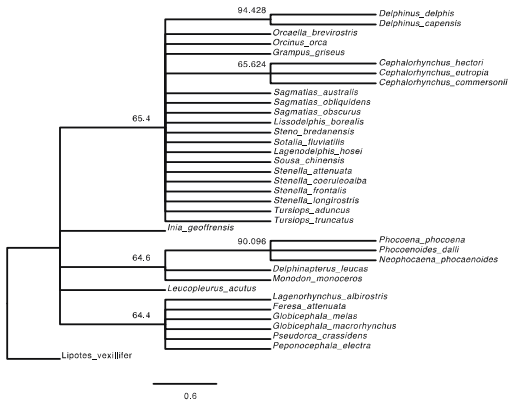

Bootstrap: Garli ML

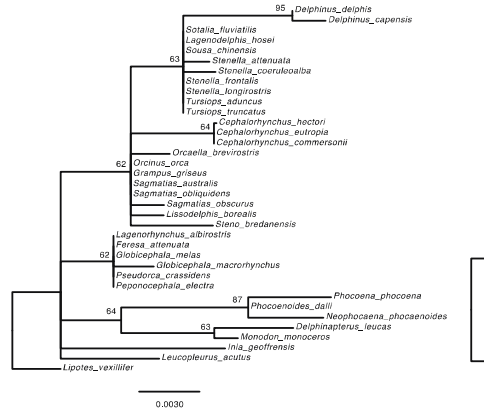

Bootstrap: RAxML

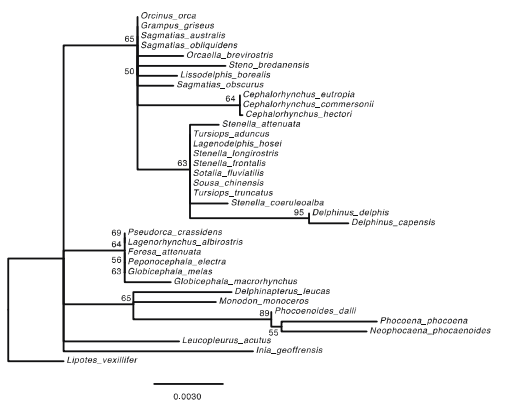

Cholinergic receptor nicotinic alpha 1 subunit (CHRNA1)

PAUP* Parsimony

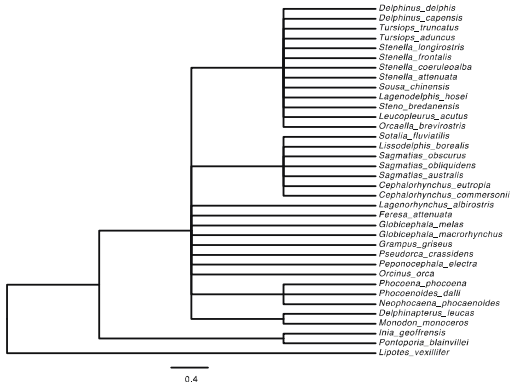

Garli ML

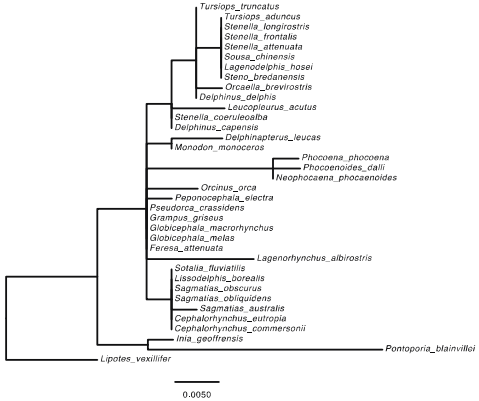

RAxML

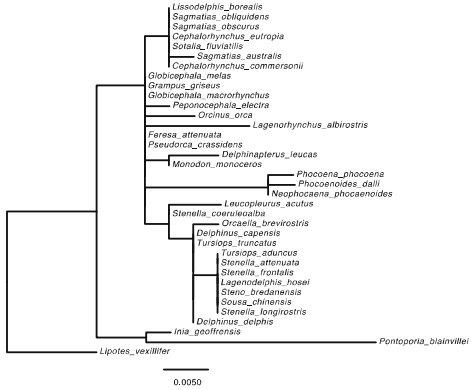

Bootstrap: PAUP* Parsimony

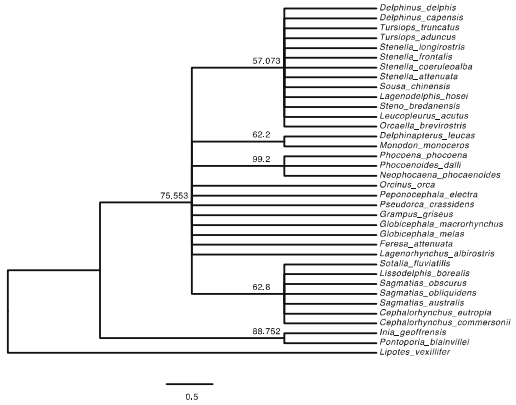

Bootstrap: Garli ML

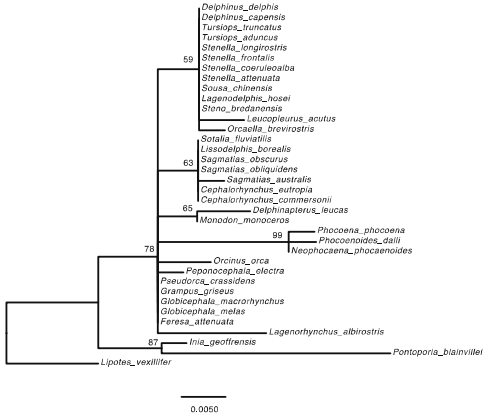

Bootstrap: RAxML

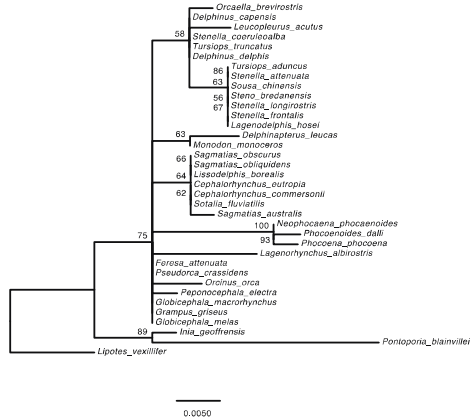

Casein beta
(CSN2)

PAUP* Parsimony

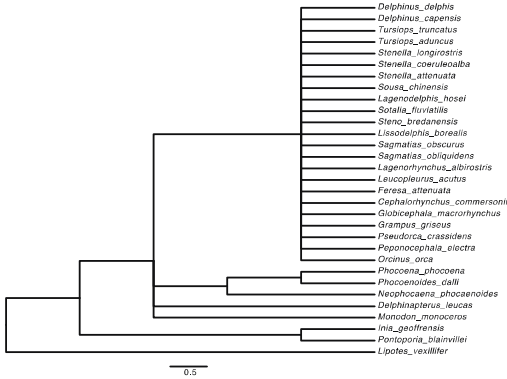

Garli ML

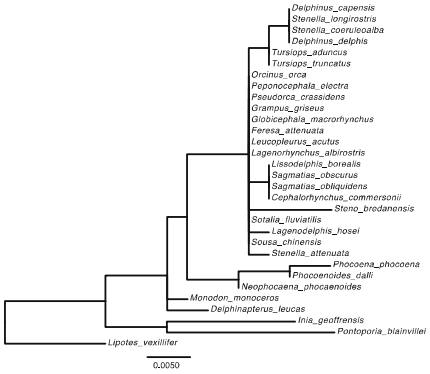

RAxML

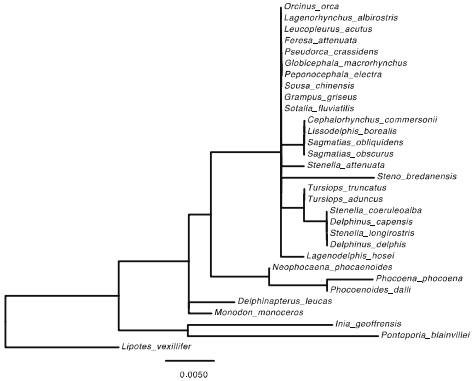

Bootstrap: PAUP* Parsimony

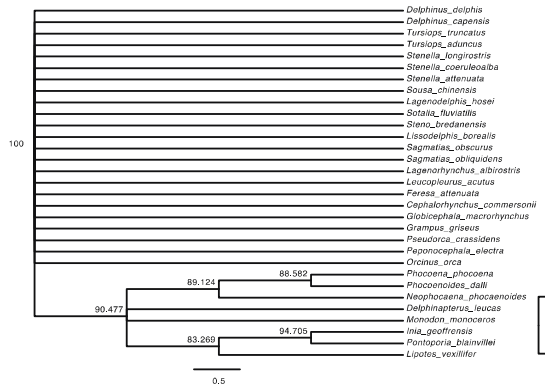

Bootstrap: Garli ML

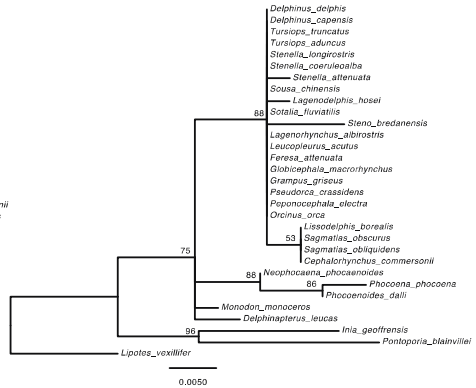

Bootstrap: RAxML

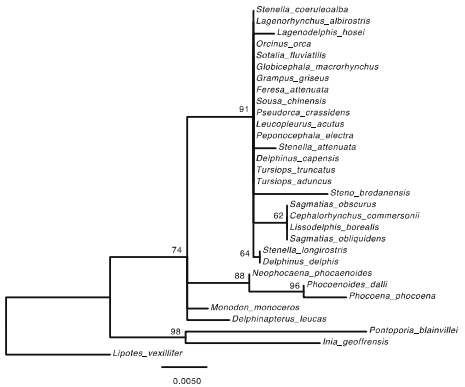

Glucosylceramidase beta (GBA)

PAUP* Parsimony

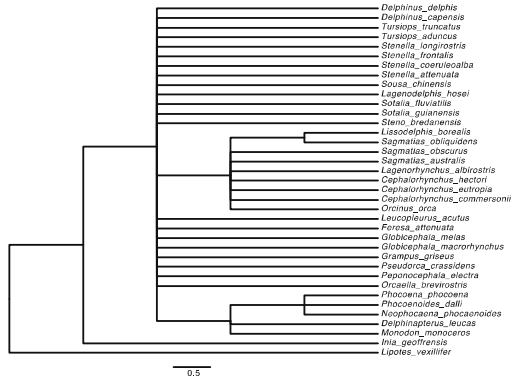

Garli ML

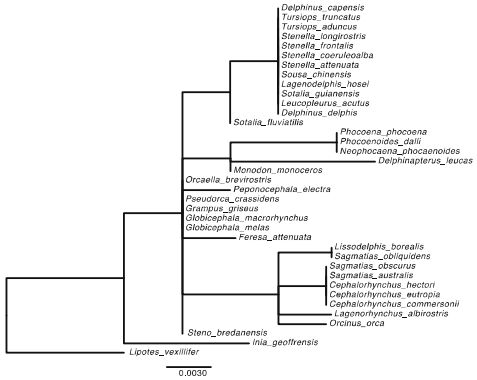

RAxML

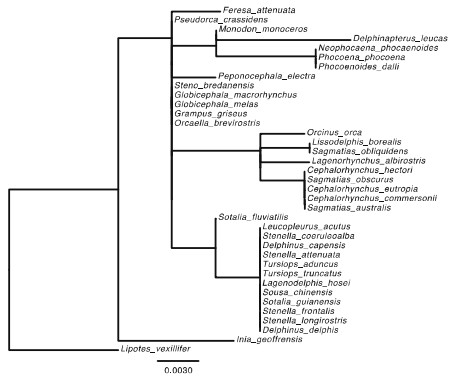

Bootstrap: PAUP* Parsimony

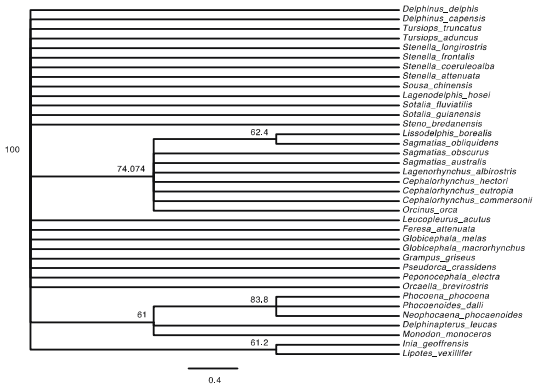

Bootstrap: Garli ML

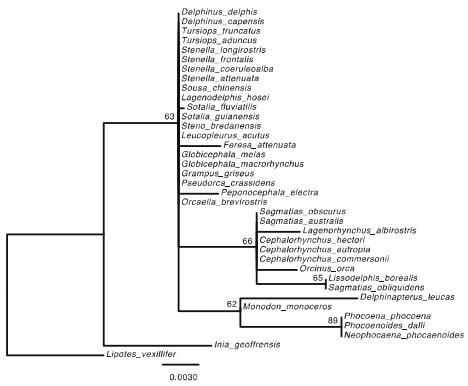

Bootstrap: RAxML

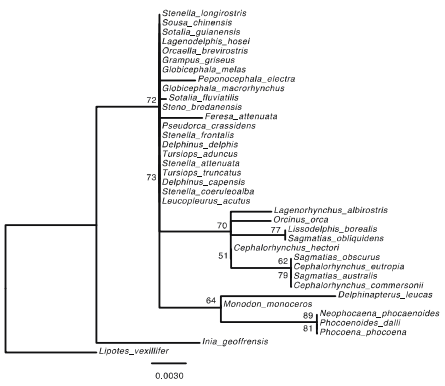

Interferon, alpha 1
(IFNA1)

PAUP* Parsimony

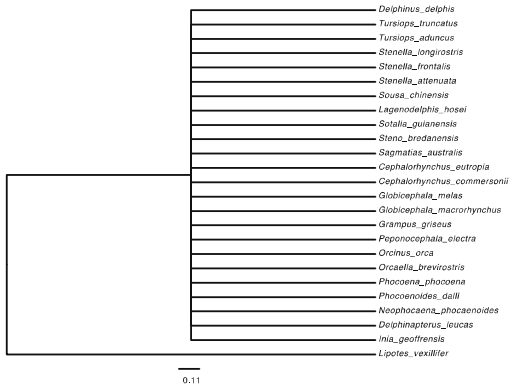

Garli ML

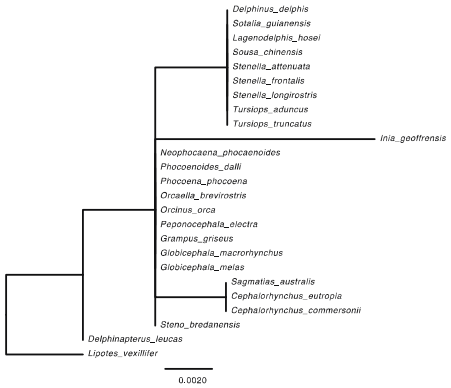

RAxML

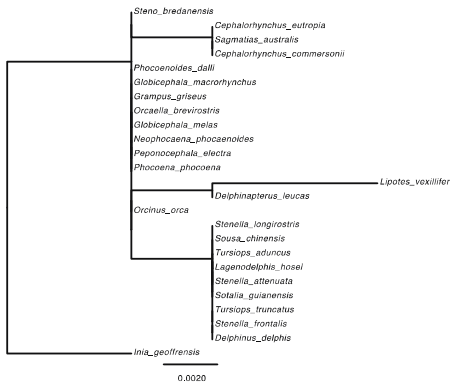

Bootstrap: PAUP* Parsimony

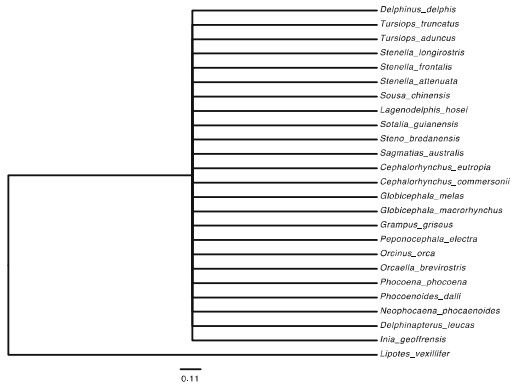

Bootstrap: Garli ML

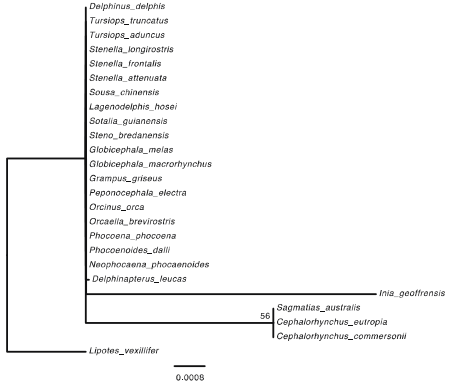

Bootstrap: RAxML

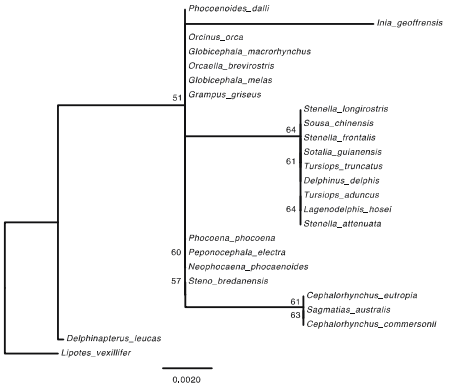

Lactalbumin alpha
(LALBA)

PAUP* Parsimony

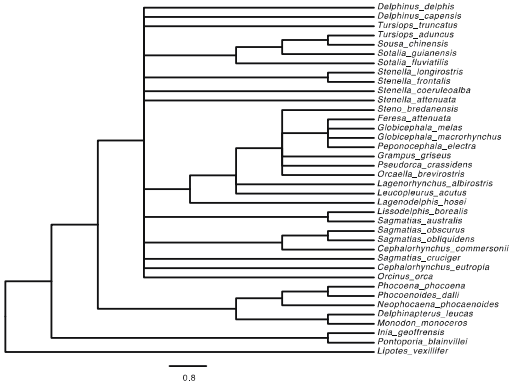

Garli ML

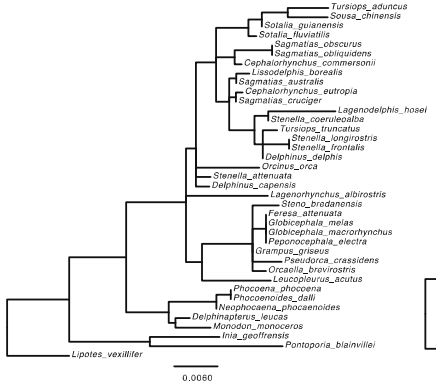

RAxML

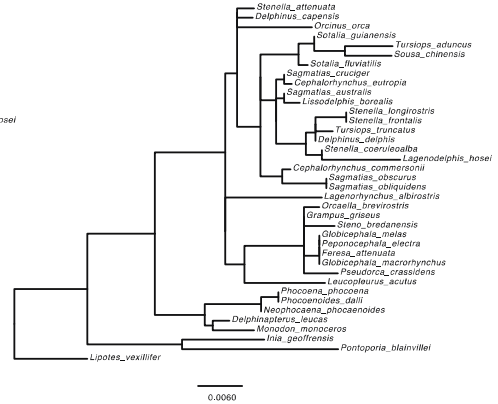

Bootstrap: PAUP* Parsimony

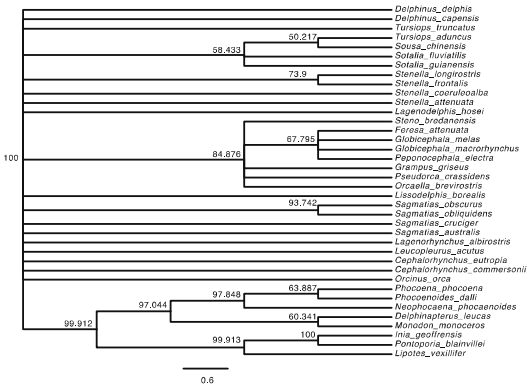

Bootstrap: Garli ML

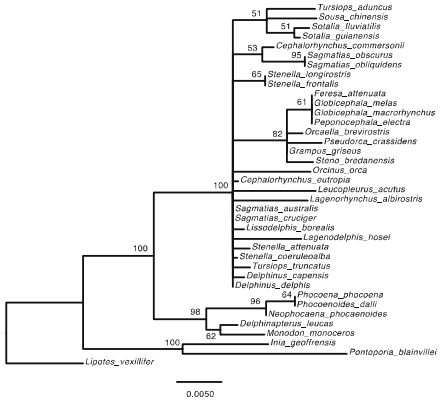

Bootstrap: RAxML

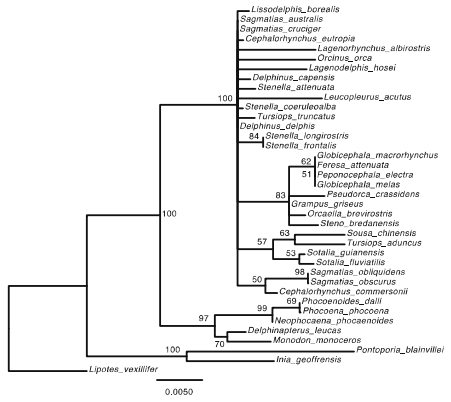

MAS1 proto-oncogene (MAS1)

PAUP* Parsimony

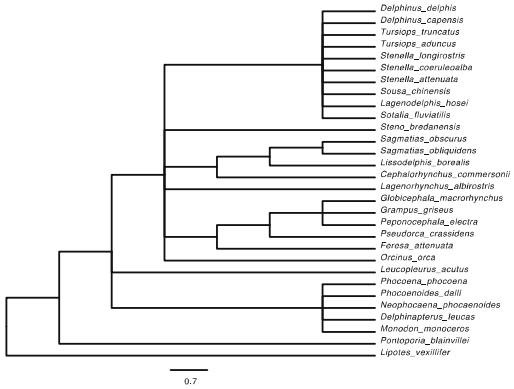

Garli ML

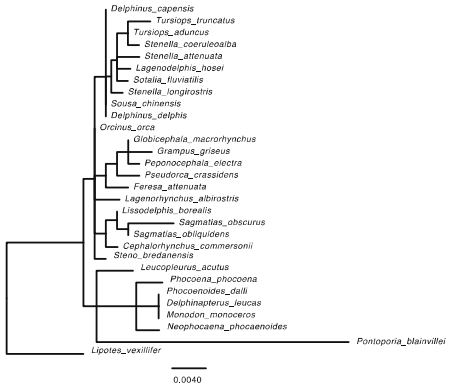

RAxML

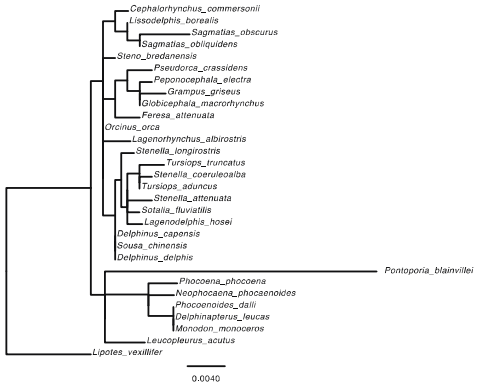

Bootstrap: PAUP* Parsimony

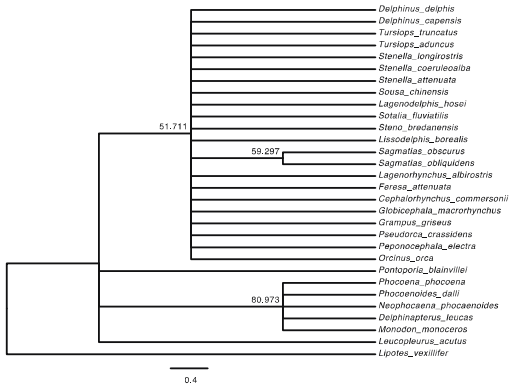

Bootstrap: Garli ML

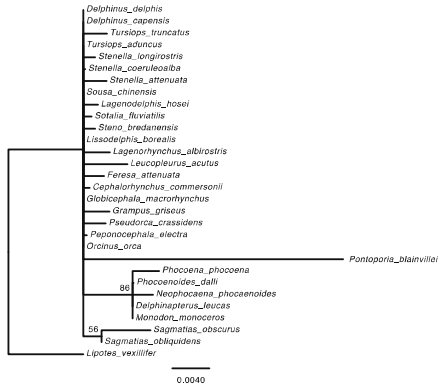

Bootstrap: RAxML

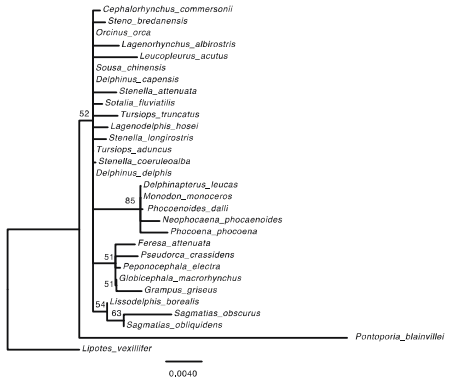

Melanocortin 1 receptor (MC1R)

PAUP* Parsimony

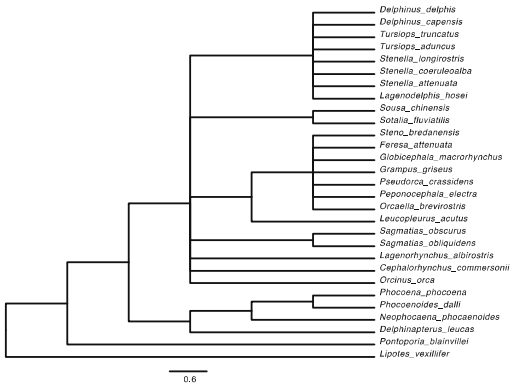

Garli ML

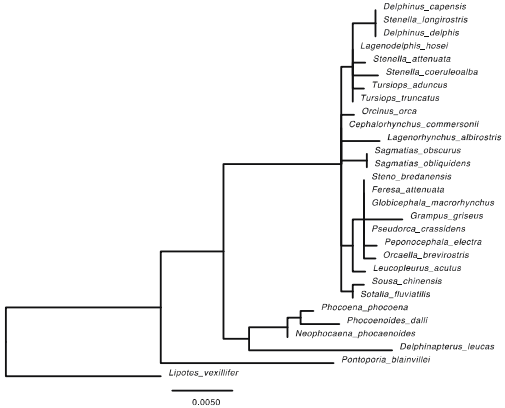

RAxML

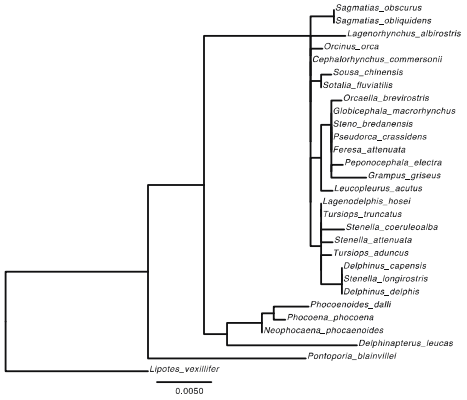

Bootstrap: PAUP* Parsimony

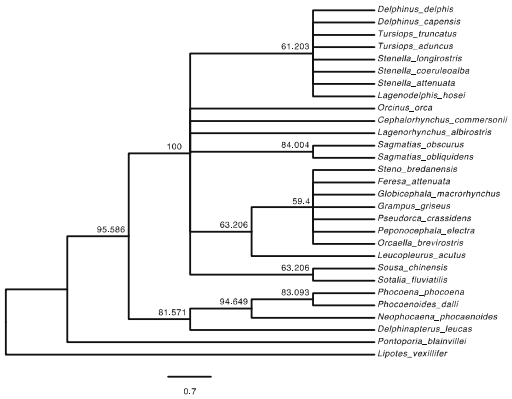

Bootstrap: Garli ML

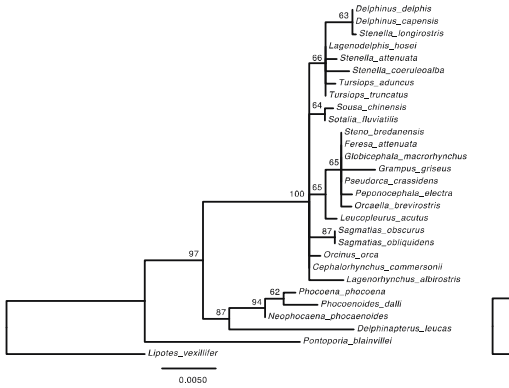

Bootstrap: RAxML

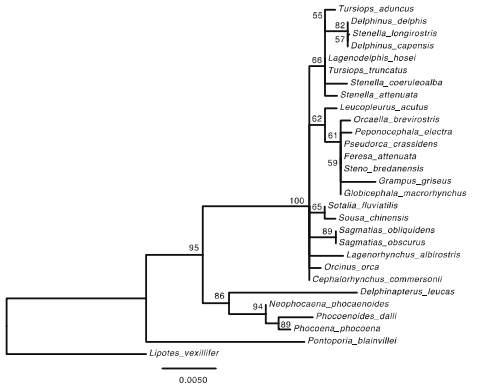

Microcephalin 1
(MCPH1)

PAUP* Parsimony

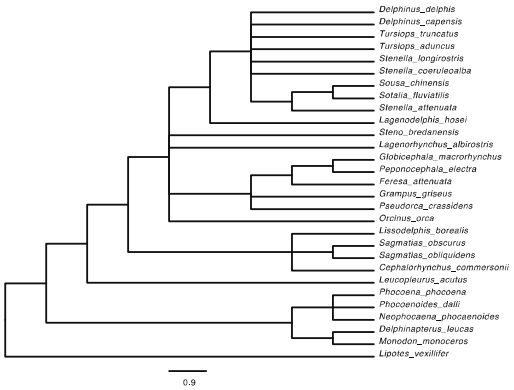

Garli ML

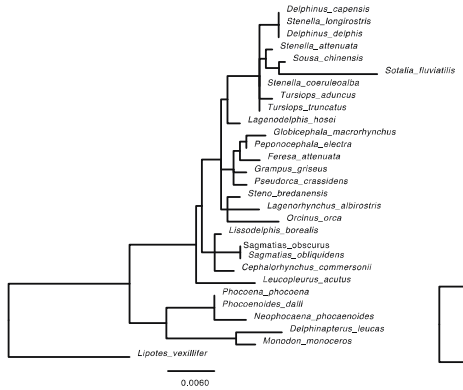

RAxML

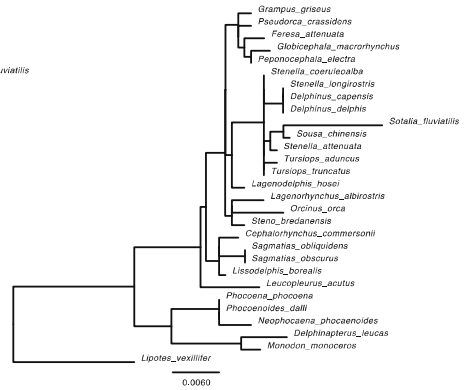

Bootstrap: PAUP* Parsimony

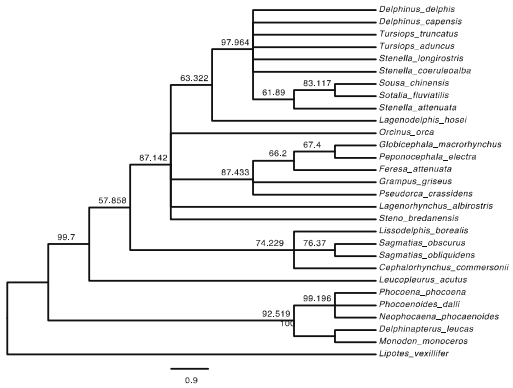

Bootstrap: Garli ML

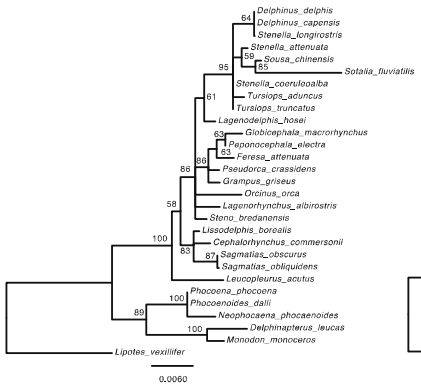

Bootstrap: RAxML

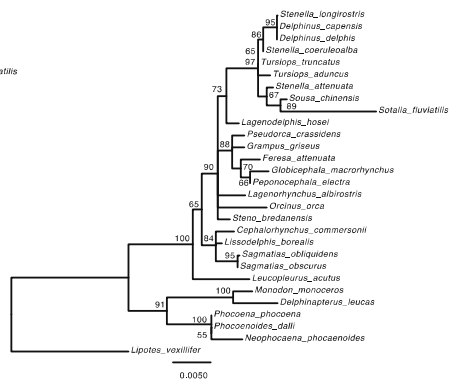

Opsin 1, short-wave-sensitive (OPN1SW)

PAUP* Parsimony

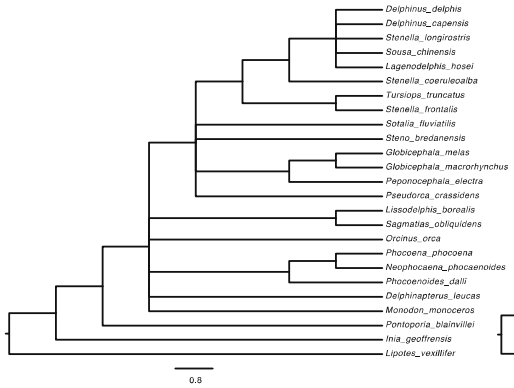

Garli ML

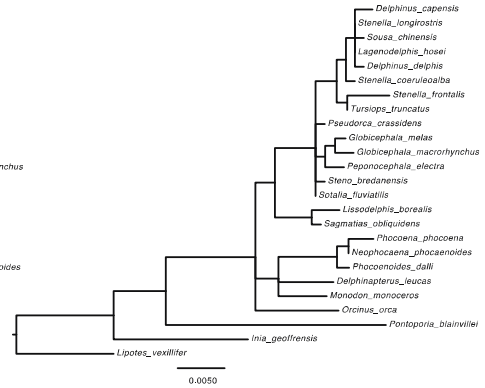

RAxML

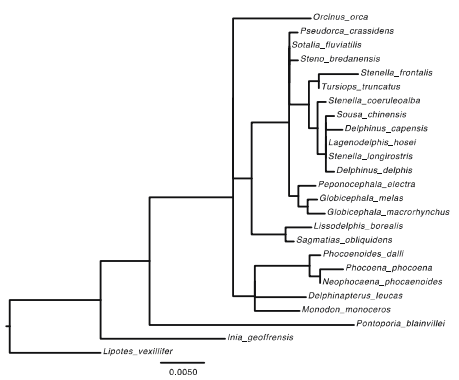

Bootstrap: PAUP* Parsimony

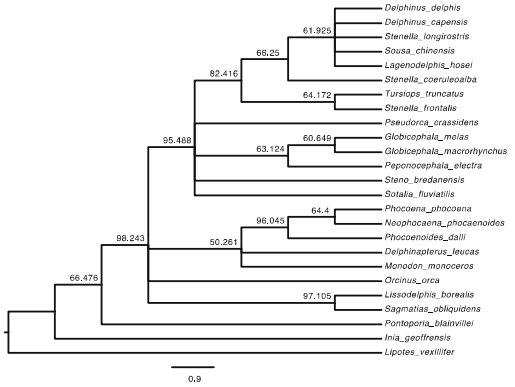

Bootstrap: Garli ML

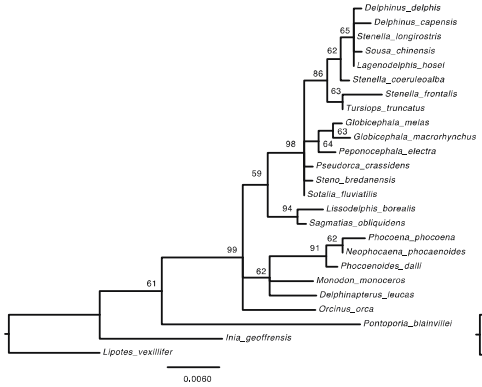

Bootstrap: RAxML

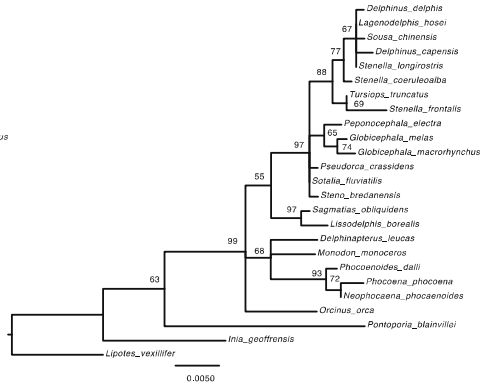

Olfactory receptor 1I1
(OR1I1)

PAUP* Parsimony

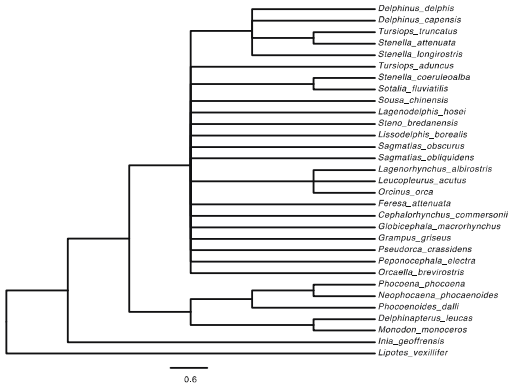

Garli ML

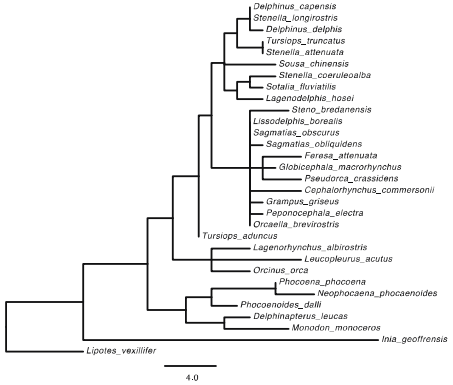

RAxML

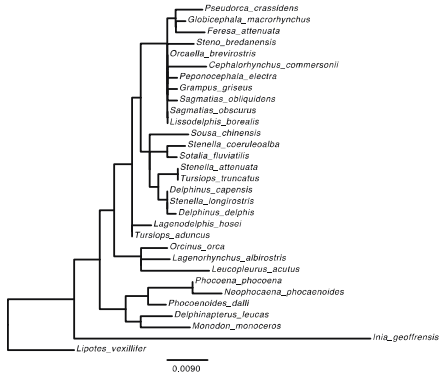

Bootstrap: PAUP* Parsimony

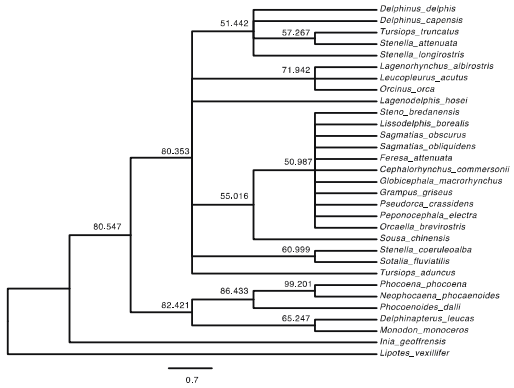

Bootstrap: Garli ML

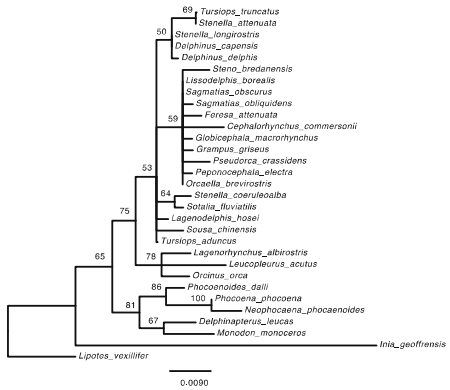

Bootstrap: RAxML

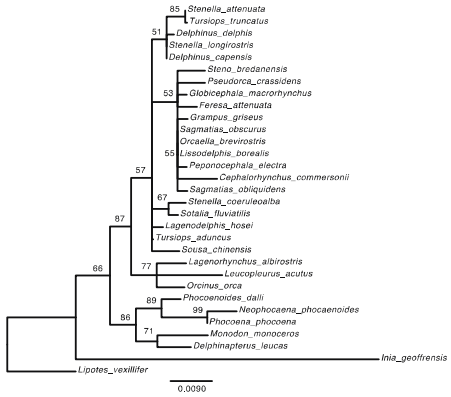

Olfactory receptor 2AT1
(OR2AT1P)

PAUP* Parsimony

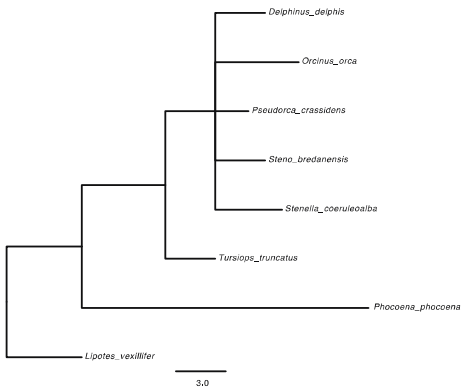

Garli ML

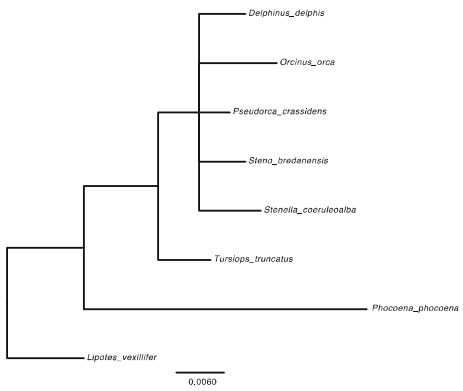

RAxML

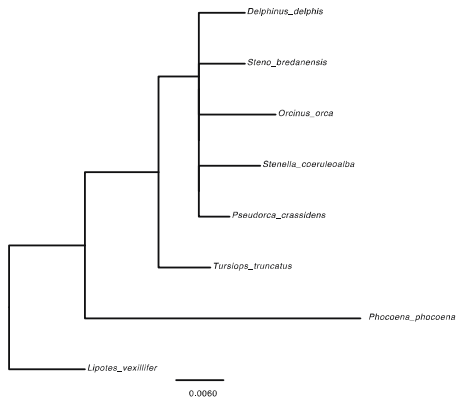

Bootstrap: PAUP* Parsimony

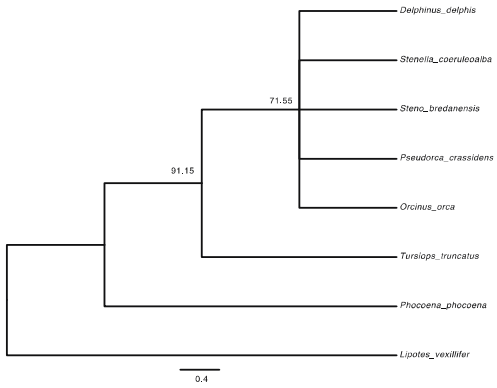

Bootstrap: Garli ML

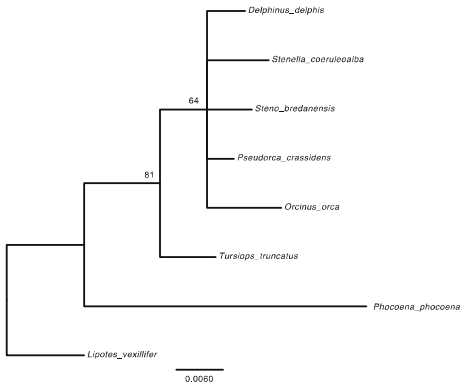

Bootstrap: RAxML

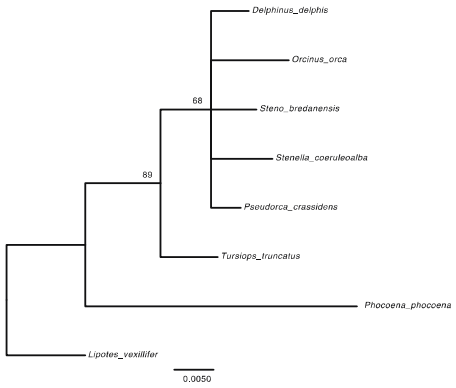

Olfactory receptor 6M1
(OR6M1)

PAUP* Parsimony

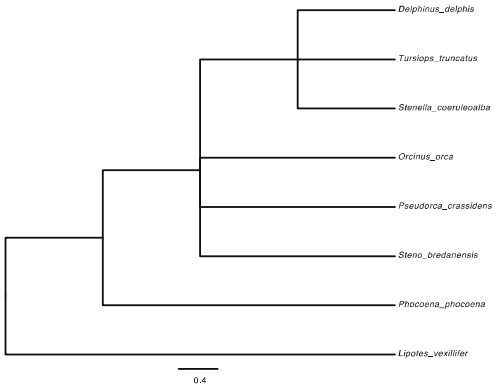

Garli ML

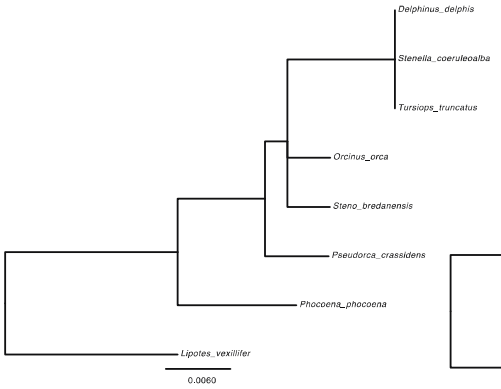

RAxML

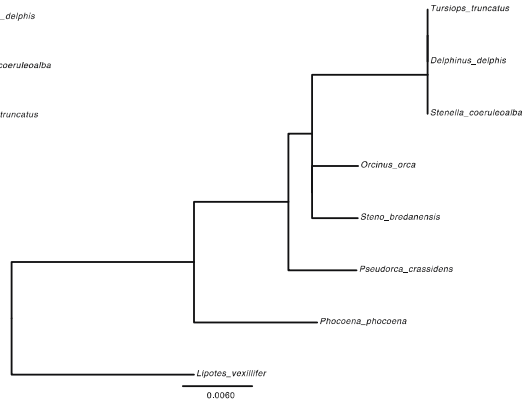

Bootstrap: PAUP* Parsimony

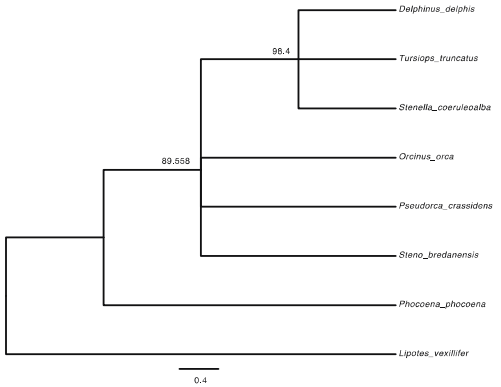

Bootstrap: Garli ML

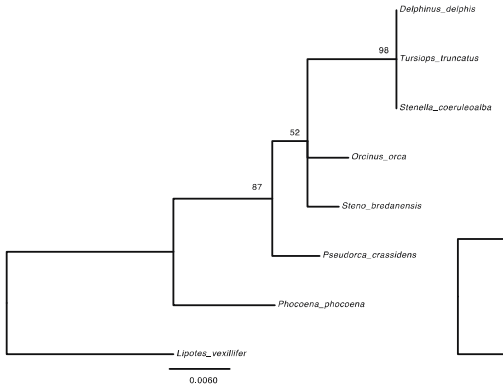

Bootstrap: RAxML

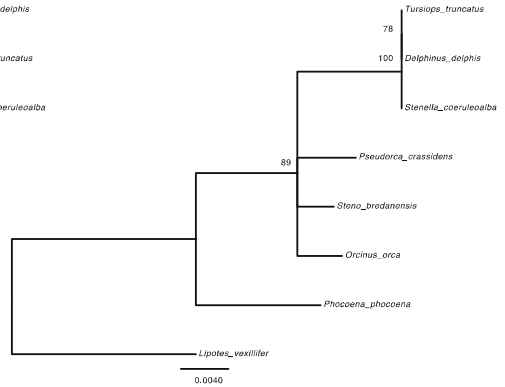

Olfactory receptor 10AB1
(OR10AB1P)

PAUP* Parsimony

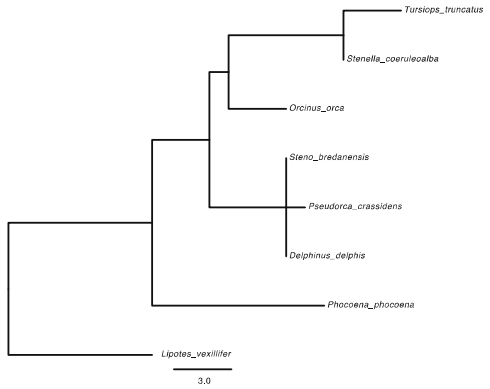

Garli ML

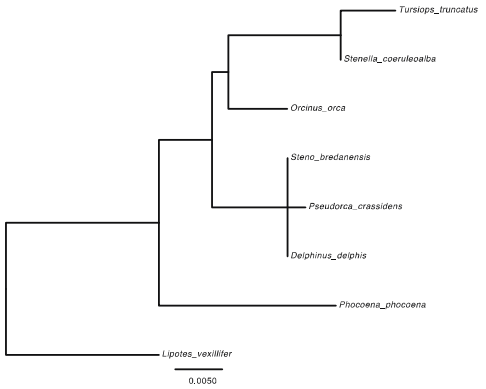

RAxML

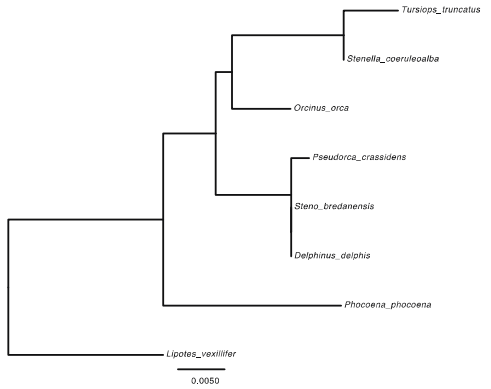

Bootstrap: PAUP* Parsimony

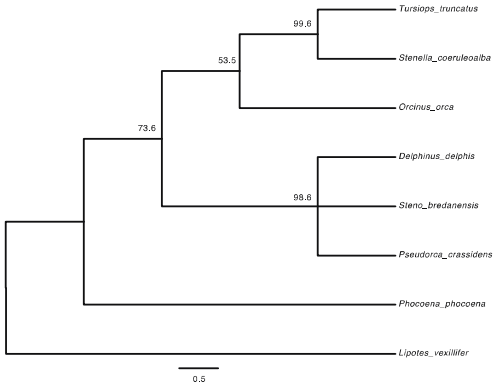

Bootstrap: Garli ML

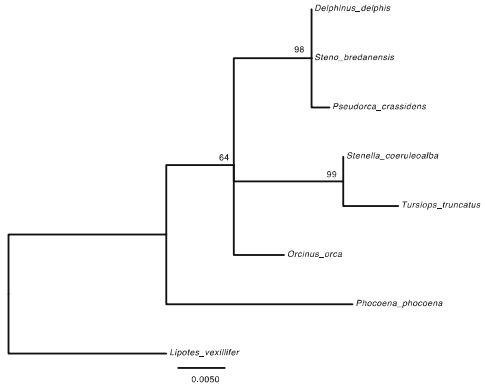

Bootstrap: RAxML

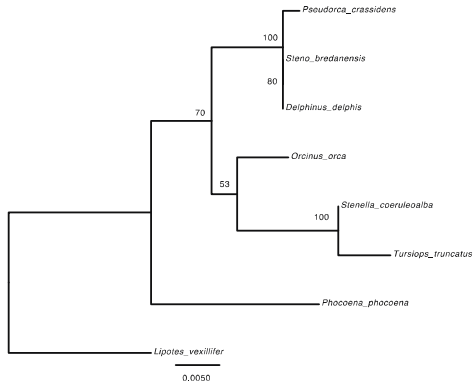

Olfactory receptor 10J1
(OR10J1)

PAUP* Parsimony

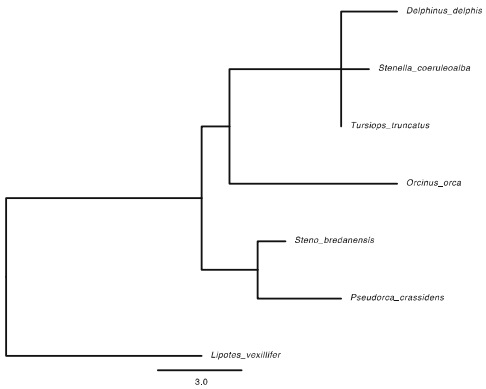

Garli ML

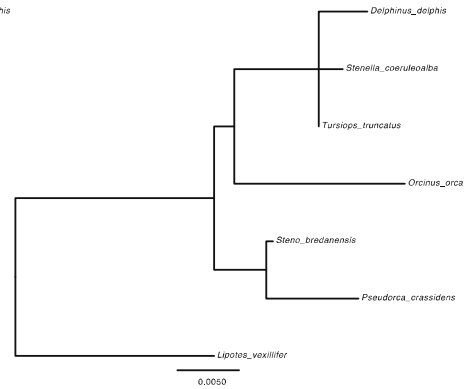

RAxML

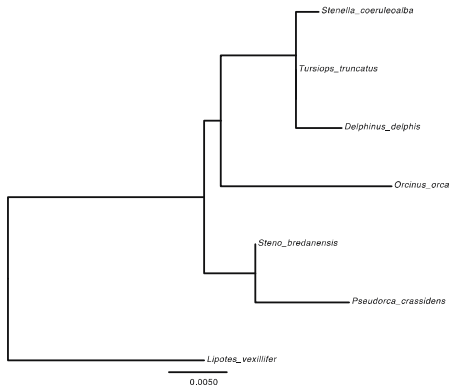

Bootstrap: PAUP* Parsimony

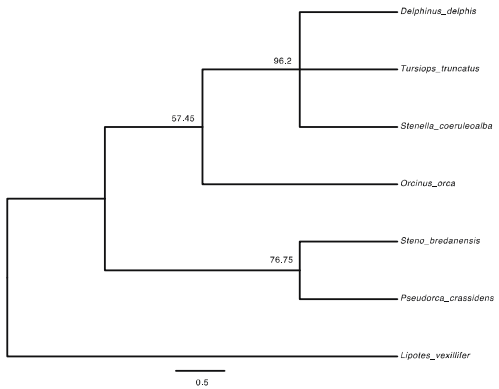

Bootstrap: Garli ML

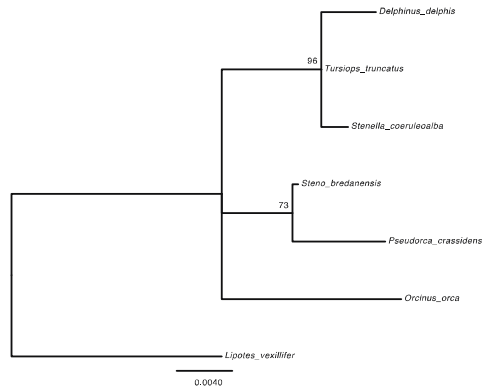

Bootstrap: RAxML

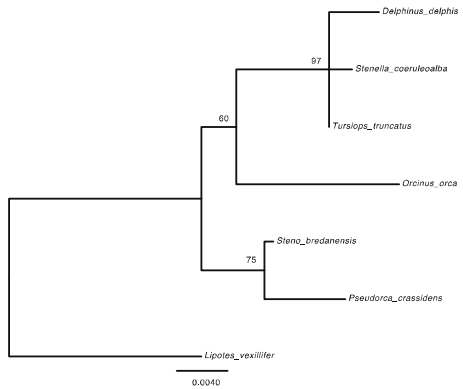

Olfactory receptor 10J2
(OR10J2P)

PAUP* Parsimony

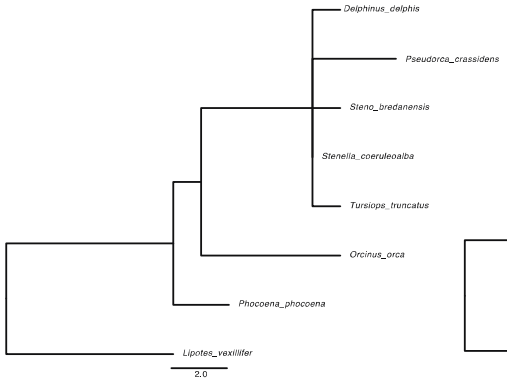

Garli ML

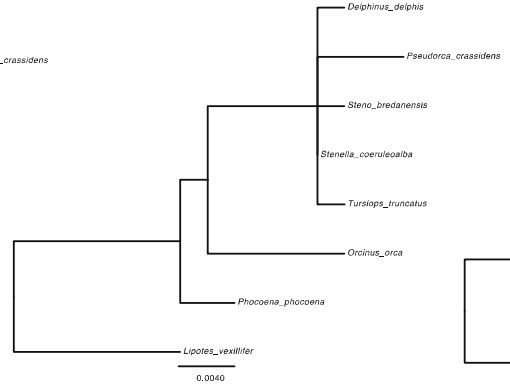

RAxML

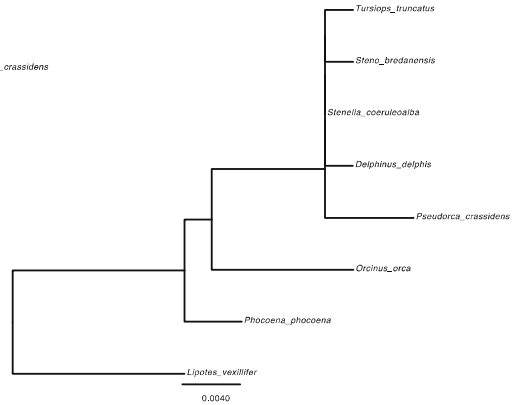

Bootstrap: PAUP* Parsimony

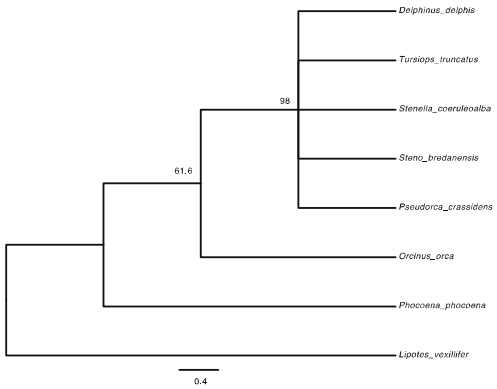

Bootstrap: Garli ML

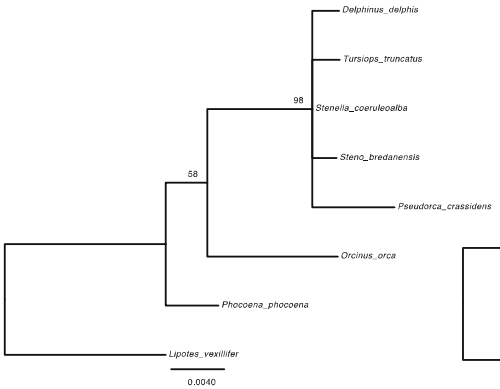

Bootstrap: RAxML

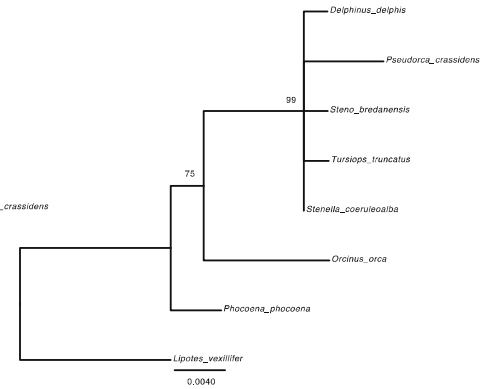

Olfactory receptor 13F1
(OR13F1)

PAUP* Parsimony

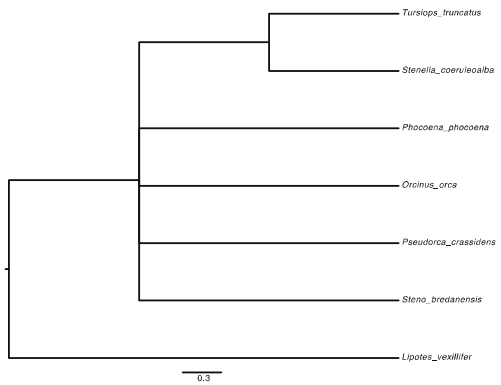

Garli ML

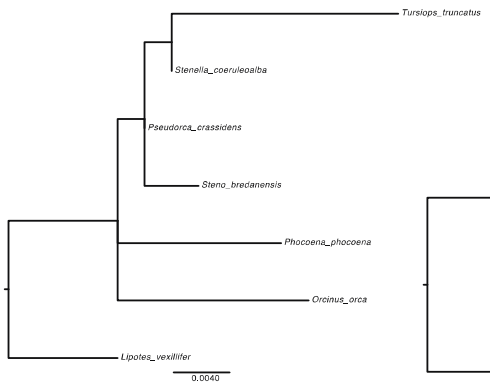

RAxML

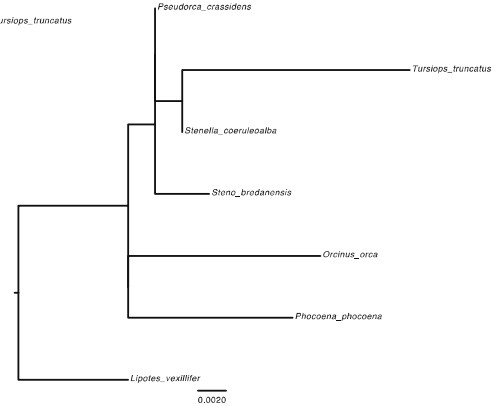

Bootstrap: PAUP* Parsimony

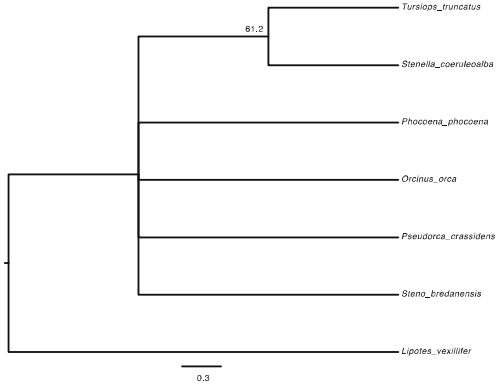

Bootstrap: Garli ML

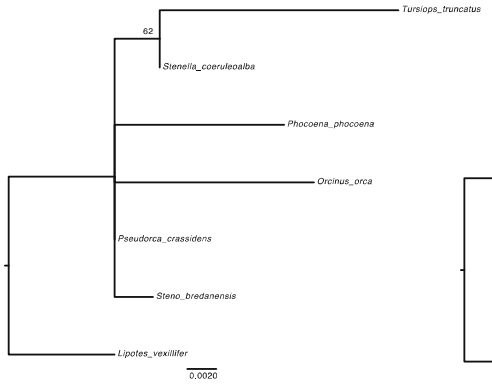

Bootstrap: RAxML

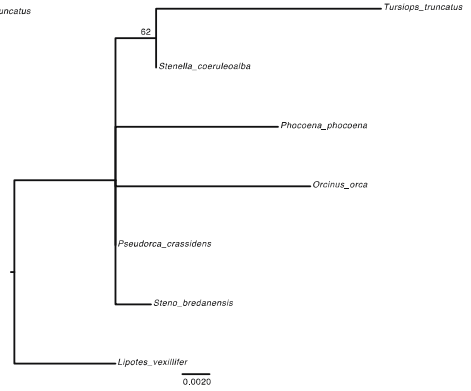

Olfactory receptor 13J1
(OR13J1)

PAUP* Parsimony

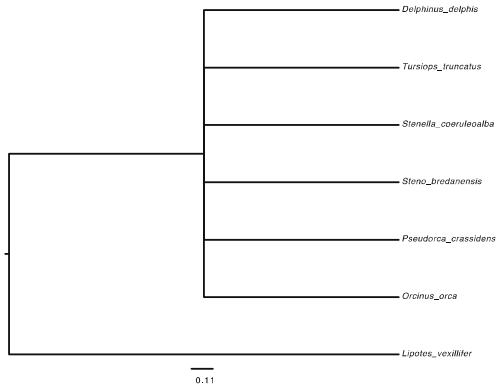

Garli ML

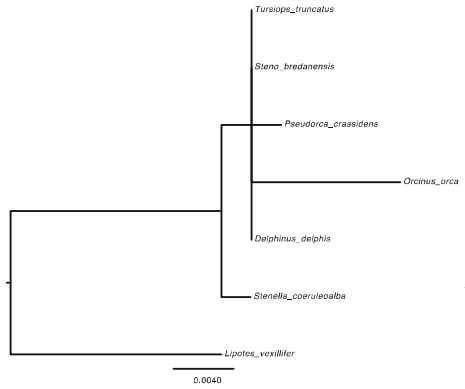

RAxML

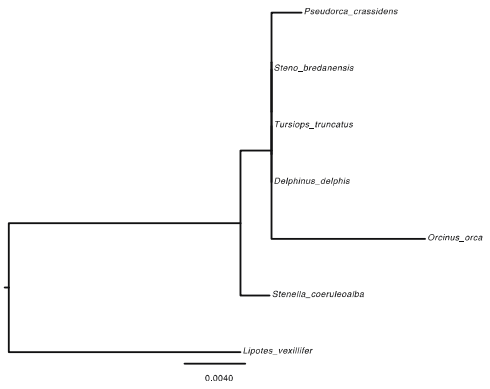

Bootstrap: PAUP* Parsimony

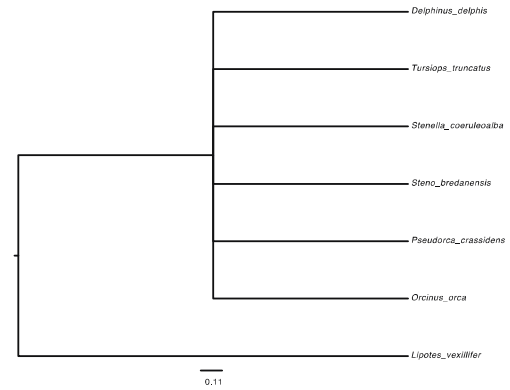

Bootstrap: Garli ML

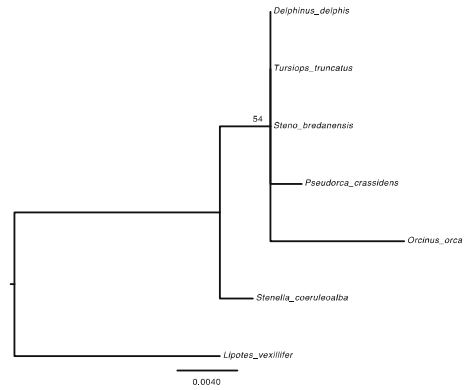

Bootstrap: RAxML

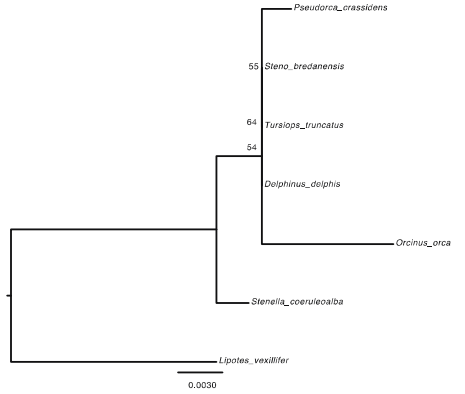

Polycystin (PKD) family receptor for egg jelly (PKDREJ)

PAUP* Parsimony

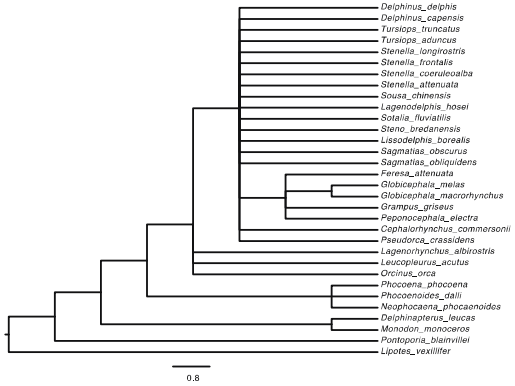

Garli ML

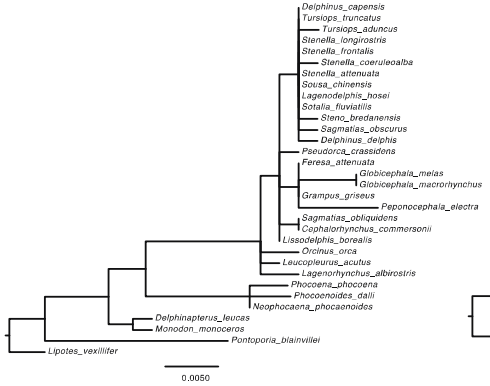

RAxML

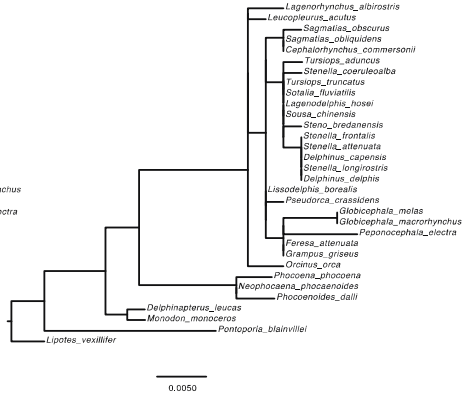

Bootstrap: PAUP* Parsimony

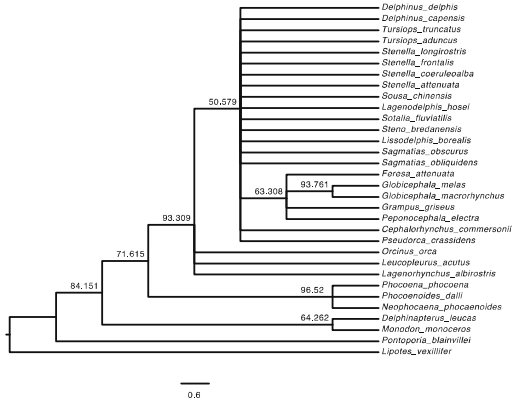

Bootstrap: Garli ML

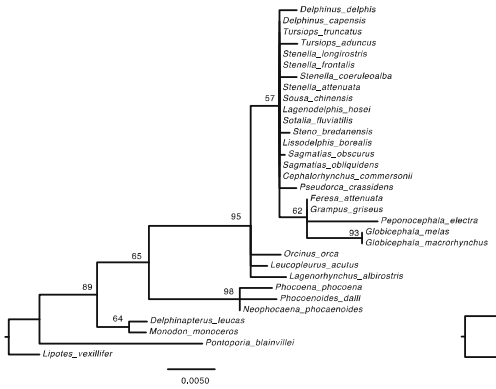

Bootstrap: RAxML

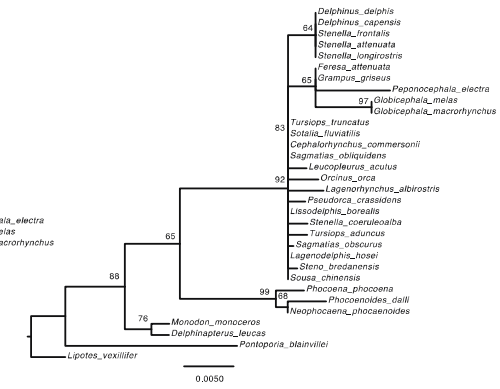

Protamine 1
(PRM1)

PAUP* Parsimony

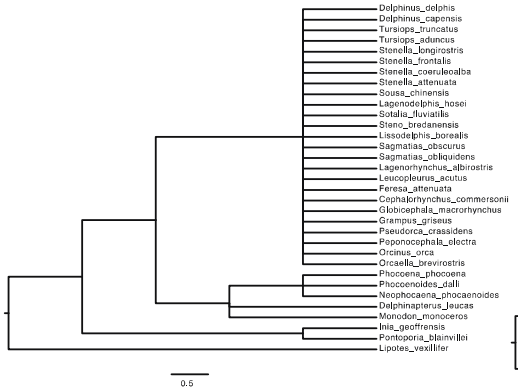

Garli ML

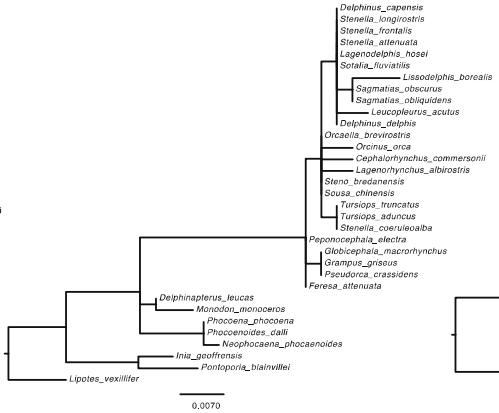

RAxML

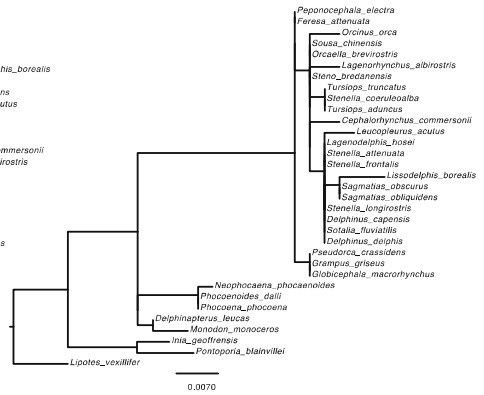

Bootstrap: PAUP* Parsimony

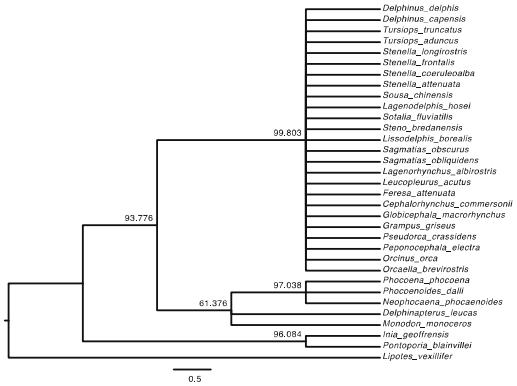

Bootstrap: Garli ML

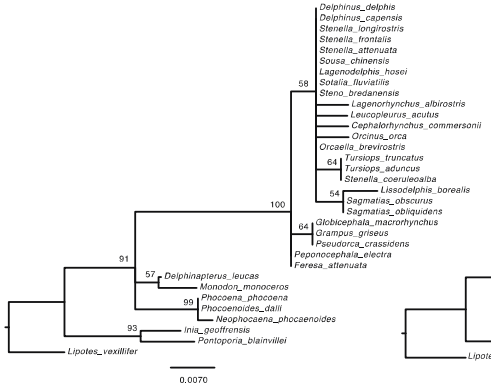

Bootstrap: RAxML

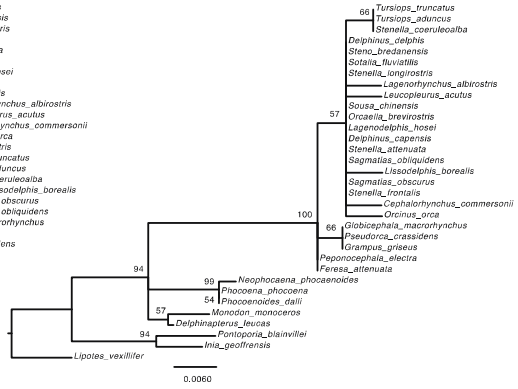

Recombination activating gene 1 (RAG1)

PAUP* Parsimony

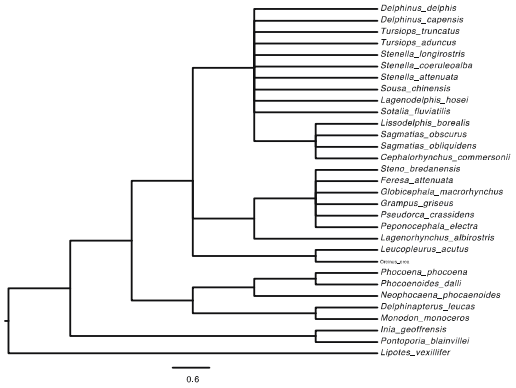

Garli ML

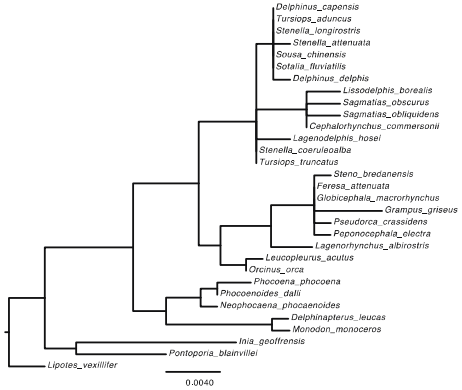

RAxML

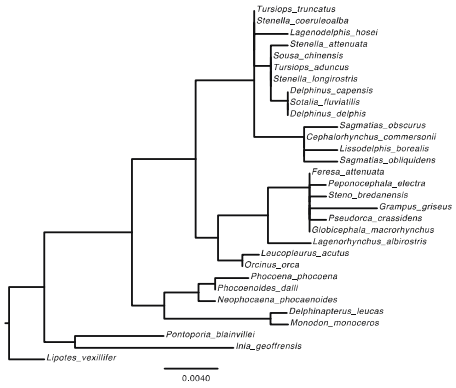

Bootstrap: PAUP* Parsimony

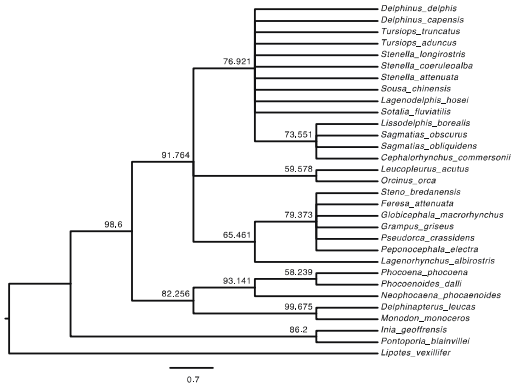

Bootstrap: Garli ML

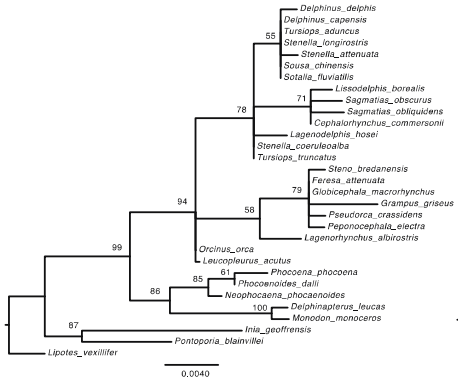

Bootstrap: RAxML

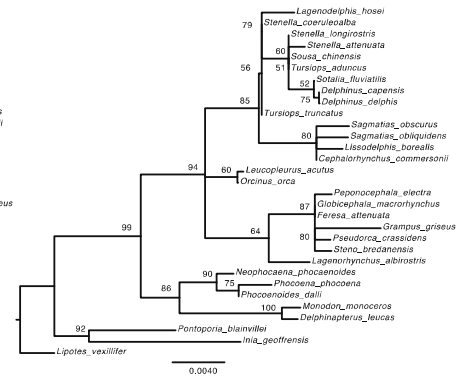

Retinol binding protein 3 (RBP3)

PAUP* Parsimony

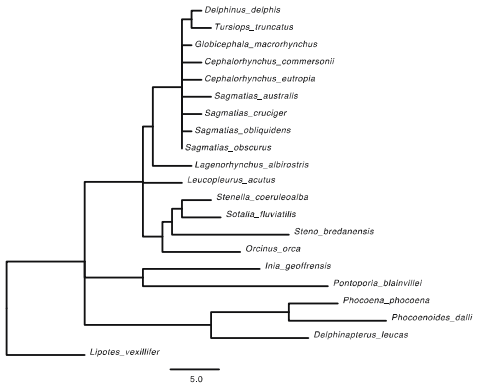

Garli ML

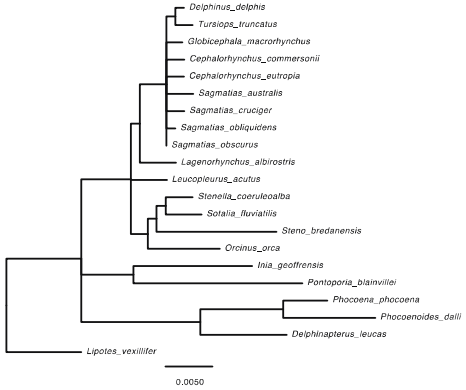

RAxML

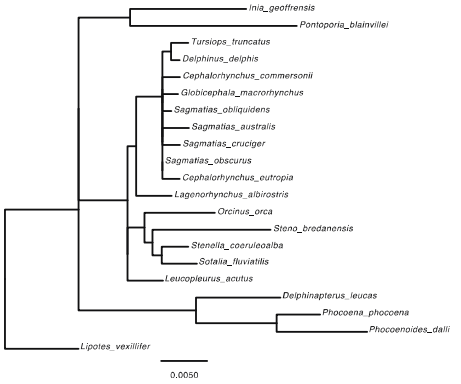

Bootstrap: PAUP* Parsimony

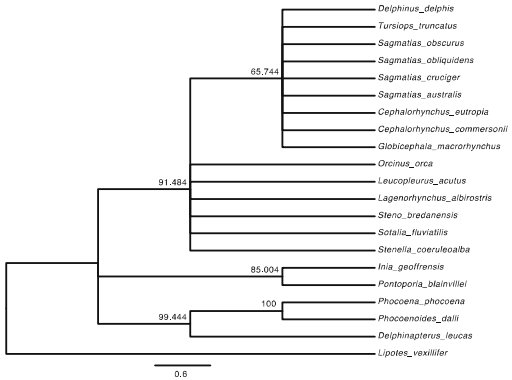

Bootstrap: Garli ML

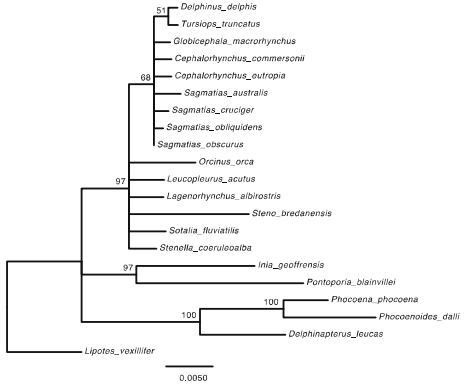

Bootstrap: RAxML

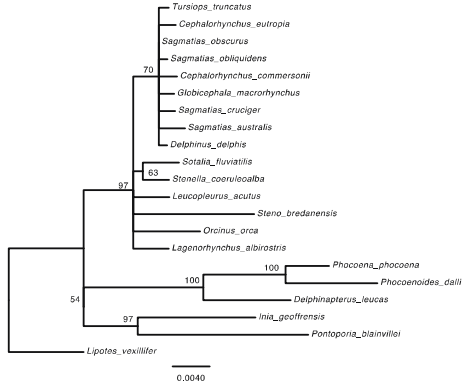

Spectrin beta, non-erythrocytic 1 (SPTBN1)

PAUP* Parsimony

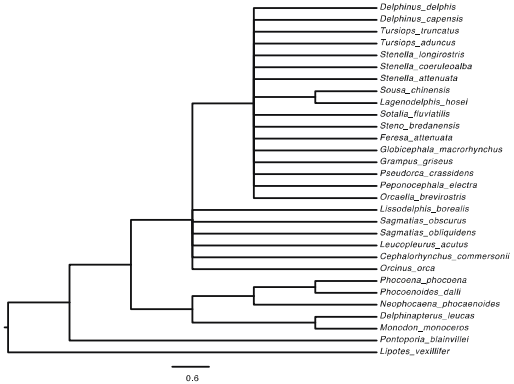

Garli ML

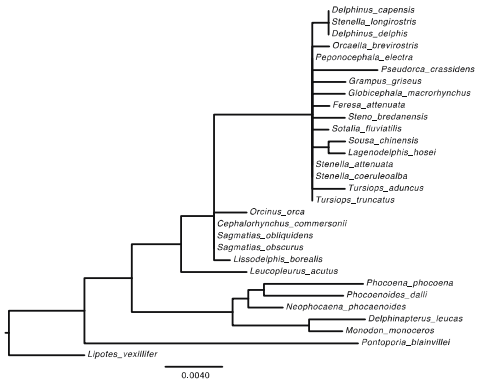

RAxML

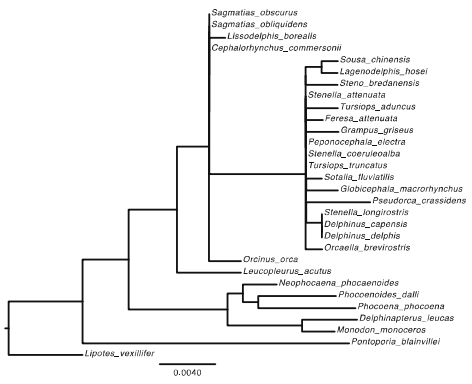

Bootstrap: PAUP* Parsimony

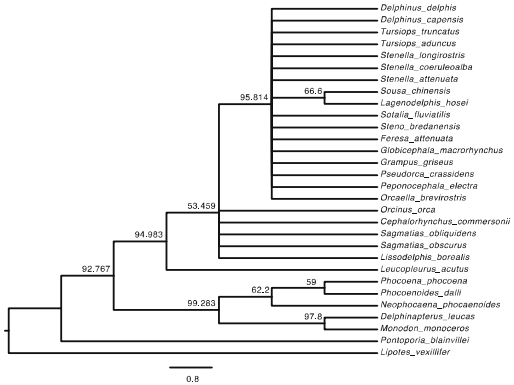

Bootstrap: Garli ML

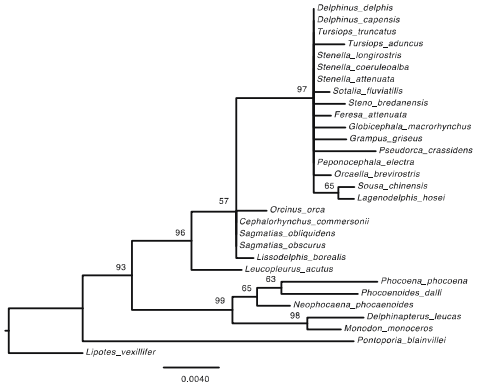

Bootstrap: RAxML

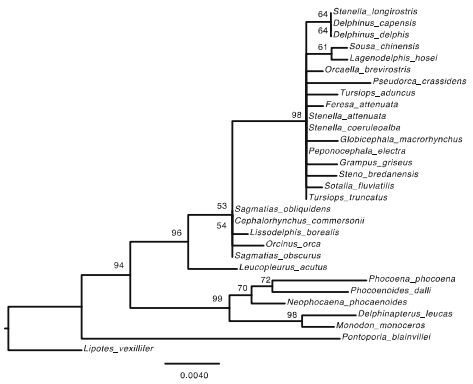

Signal transducer and activator of transcription factor 5A (STAT5A)

PAUP* Parsimony

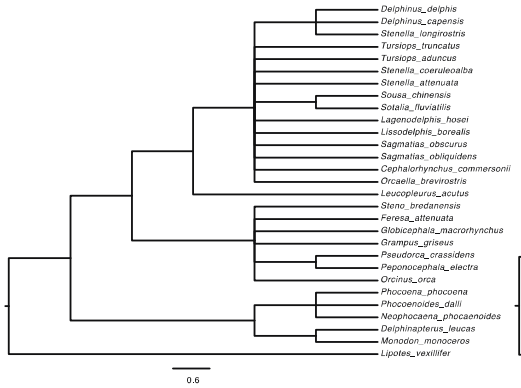

Garli ML

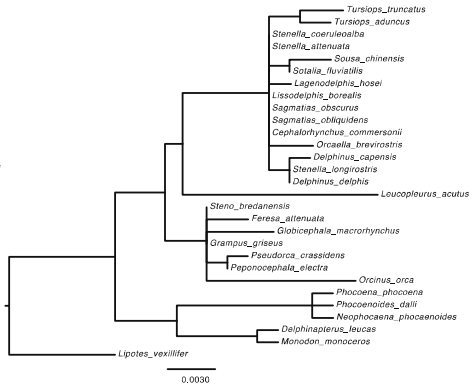

RAxML

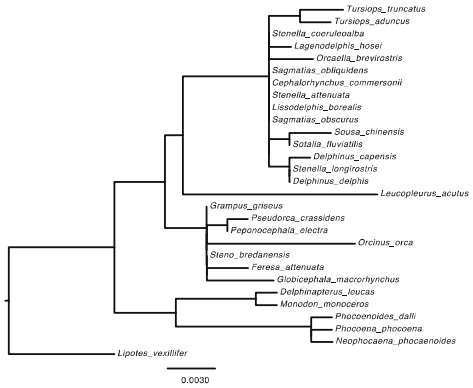

Bootstrap: PAUP* Parsimony

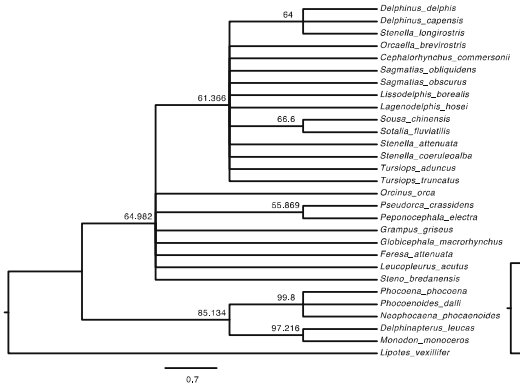

Bootstrap: Garli ML

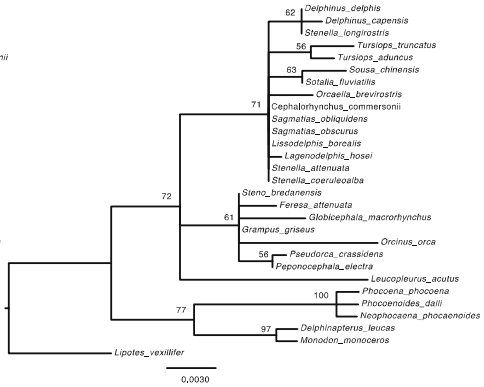

Bootstrap: RAxML

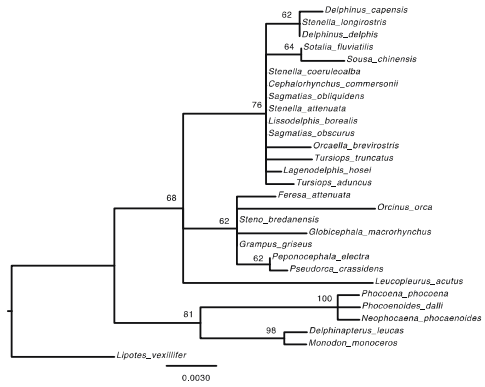

T-box 4
(TBX4)

PAUP* Parsimony

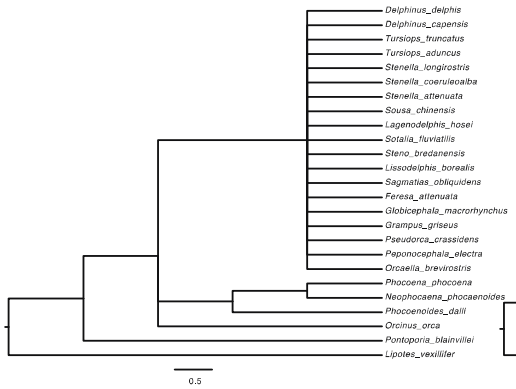

Garli ML

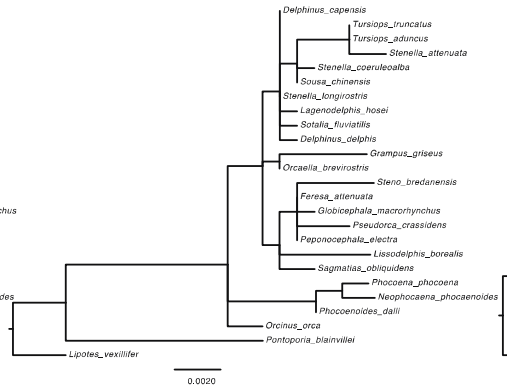

RAxML

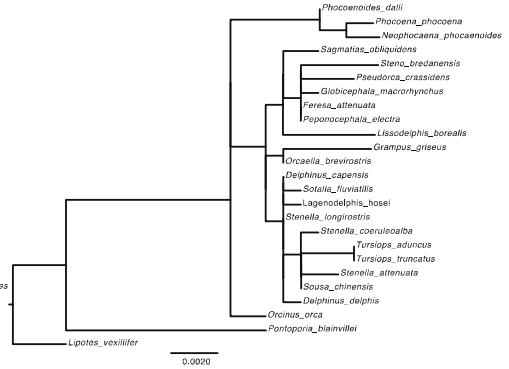

Bootstrap: PAUP* Parsimony

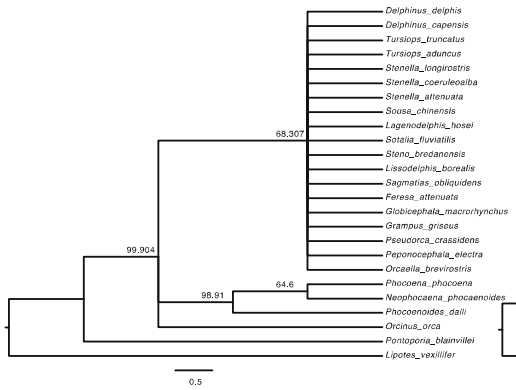

Bootstrap: Garli ML

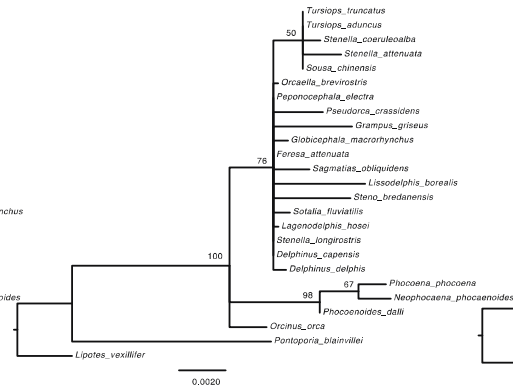

Bootstrap: RAxML

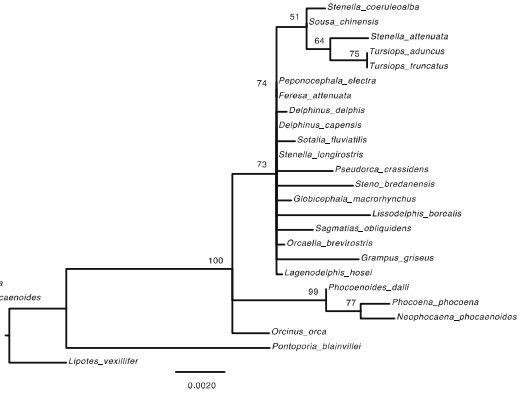

Thyroid stimulating hormone beta (TSHB)

PAUP* Parsimony

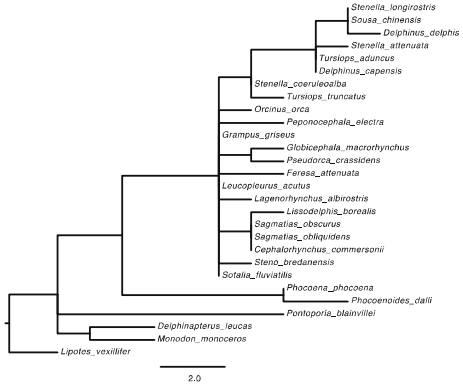

Garli ML

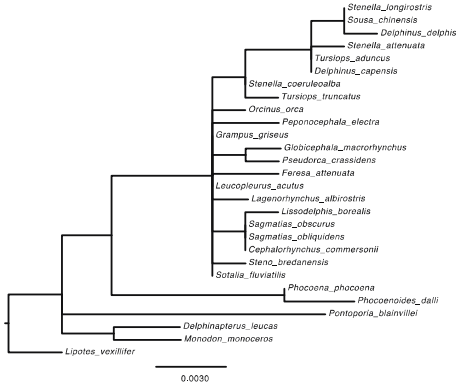

RAxML

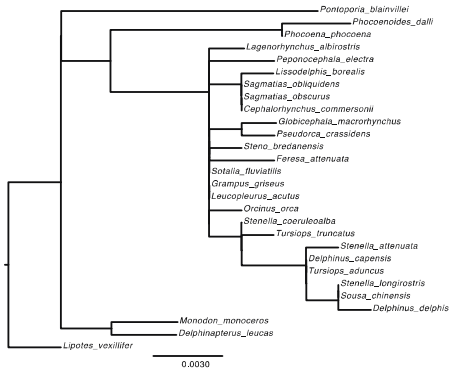

Bootstrap: PAUP* Parsimony

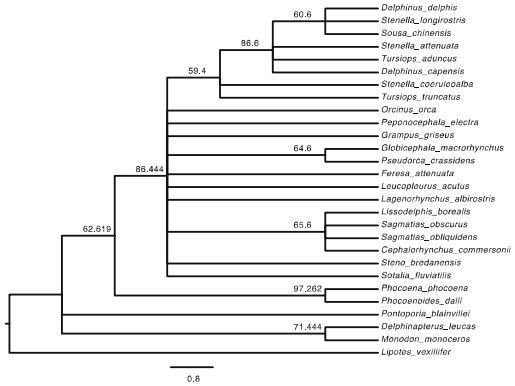

Bootstrap: Garli ML

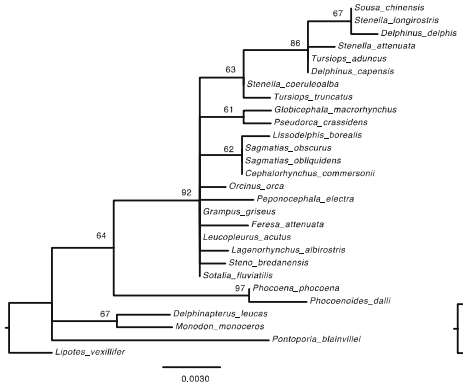

Bootstrap: RAxML

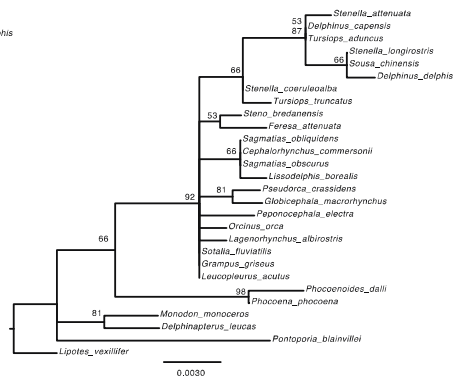

Yintrons
(DBY7, DBY8, SMCY7, UBE1Y)

PAUP* Parsimony

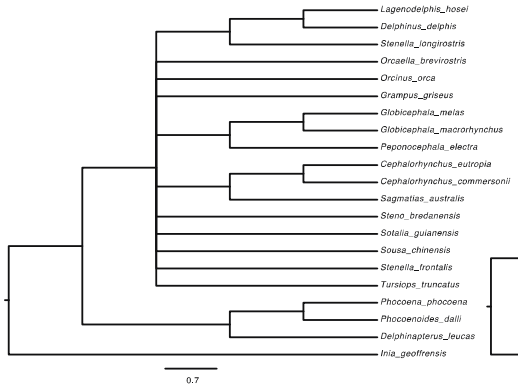

Garli ML

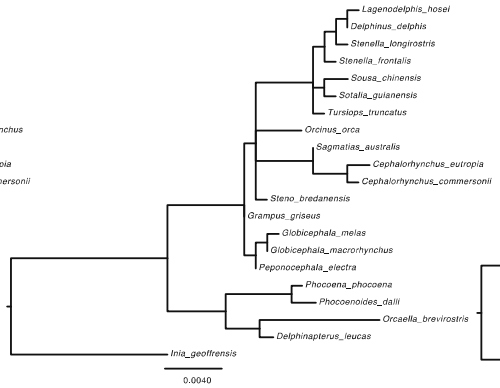

RAxML

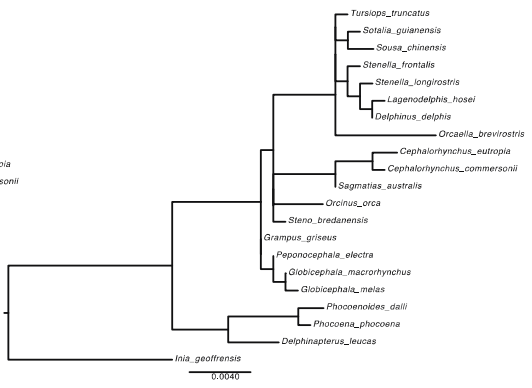

Bootstrap: PAUP* Parsimony

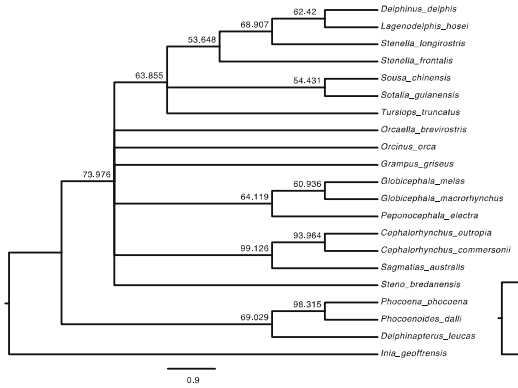

Bootstrap: Garli ML

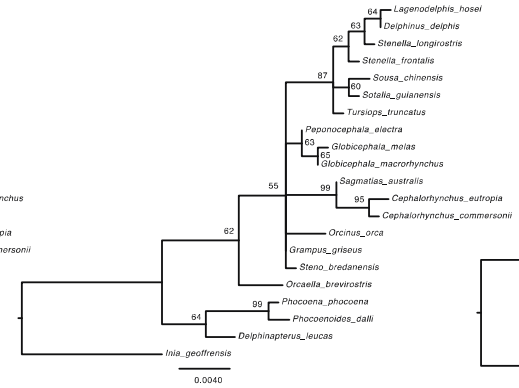

Bootstrap: RAxML